

Mechanisms of Guanylyl Cyclase Gene Regulation by FoxO Transcription Factors

Joseph Carl Galley

University of Pittsburgh, 2021

Submitted to the Graduate Faculty of
School of Medicine in partial fulfillment
of the requirements for the degree of
Doctor of Philosophy

University of Pittsburgh

2021

UNIVERSITY OF PITTSBURGH
SCHOOL OF MEDICINE

This dissertation was presented

by

Joseph Carl Galley

It was defended on

June 23, 2021

and approved by

Patrick J. Pagano, Professor of Medicine, Department of Pharmacology & Chemical Biology

Edwin Jackson, Professor of Medicine, Department of Pharmacology & Chemical Biology

Alessandro Bisello, Associate Professor, Department of Pharmacology & Chemical Biology

Delphine Gomez, Assistant Professor of Medicine, Department of Pathology

Aditi Gurkar, Assistant Professor of Medicine, Division of Geriatric Medicine

Dissertation Director: Adam C. Straub, Ph.D., Associate Professor of Medicine, Department of
Pharmacology & Chemical Biology

Copyright © by Joseph Carl Galley

2021

Mechanisms of Guanylyl Cyclase Gene Regulation by FoxO Transcription Factors

Joseph Carl Galley, PhD

University of Pittsburgh, 2021

Nitric oxide (NO) is a known vasodilator molecule produced in the vascular endothelium which freely diffuses to the smooth muscle cells (SMC) due to its small, non-polar nature. Once in the SMC, NO binds its cognate receptor, soluble guanylyl cyclase (sGC) to catalyze formation of cGMP to cause dilation. This process maintains healthy blood pressure and hemodynamic function. Therapeutic strategies have sought to target this pathway by elevating available NO treatment, stimulation of NO-sensitive sGC, or activation of NO-insensitive sGC. Despite successes of several sGC modulator clinical trials, little study had been devoted to transcription mechanisms responsible for sGC gene expression in SMC. We thus sought to identify transcriptional regulators of sGC in SMC tissue.

We identified several predicted Forkhead box subclass O (FoxO) protein binding sites on sGC promoters. We then inhibited the FoxO proteins in aortic SMC and observed significant loss of sGC gene and protein expression as well as cGMP production. Treated *ex vivo* murine aortas showed loss of sGC expression and loss of NO-dependent vasodilatory function. We next showed that a murine 2-kidney-1-clip (2K1C) model of hypertension causes increased vasodilatory function and expression of sGC in the contralateral renal arteries. Because

angiotensin II (Ang II) causes many of the blood pressure effects in renovascular hypertension, we treated cultured renal SMC with Ang II and observed increased sGC expression through Ang II type 1 receptor (AT1R)-dependent agonism. This increase in sGC expression and downstream function was dependent upon functional FoxO transcriptional activity. We knocked down each FoxO protein in aortic SMC and showed that loss of FoxO1 and FoxO3 increase sGC expression and downstream function, while FoxO4 loss decreased sGC expression and function. We then used sGC β promoter-luciferase vectors to show which regions are necessary for transcriptional function and again show that expression requires FoxO transcription. Finally, we show that FoxO4 binds several predicted locations using chromatin immunoprecipitation of the sGC β promoter. Combined, we are the first to identify the FoxO family as transcriptional regulators of sGC in SMC, opening a new avenue for therapeutic innovation in basic and clinical vascular research.

Table of Contents

| | |
|---|-----------|
| Preface..... | xi |
| Acknowledgements: | xii |
| 1.0 Introduction..... | 1 |
| 1.1 Public Health Burden of Hypertension | 1 |
| 1.2 Function and Regulation of sGC..... | 3 |
| 1.3 Drugs Targeting sGC and Their Clinical Impacts | 7 |
| 1.4 A Brief Overview of the FoxO Transcription Factors | 9 |
| 1.5 The Purpose of This Dissertation | 12 |
| 2.0 Antagonism of Forkhead Box Subclass O Transcription Factors Elicits Loss of Soluble Guanylyl Cyclase Expression | 15 |
| 2.1 Summary: | 15 |
| 2.2 Introduction: | 16 |
| 2.3 Materials and Methods: | 18 |
| 2.4 Results: | 22 |
| 2.5 Discussion: | 25 |
| 3.0 Angiotensin II Augments Renovascular sGC Expression Via an AT₁R - FoxO Transcription Factor Signaling Axis..... | 50 |
| 3.1 Summary: | 50 |
| 3.1.1 Graphical Summary: | 52 |
| 3.2 Introduction: | 53 |
| 3.3 Methods: | 54 |

| | |
|--|------------|
| 3.4 Results: | 62 |
| 3.5 Discussion: | 66 |
| 4.0 FoxO4 Regulates sGCβ Transcription in Vascular Smooth Muscle..... | 86 |
| 4.1 Summary: | 86 |
| 4.2 Introduction: | 87 |
| 4.3 Methods: | 89 |
| 4.4 Results: | 97 |
| 4.5 Discussion:..... | 100 |
| 5.0 Conclusions and Future Directions | 110 |
| 5.1 Conclusions of Our Work | 110 |
| 5.2 What are Some of the Additional Non-Transcriptional Mechanisms of sGC? | 111 |
| 5.3 What Are the Implications of sGC Activator/Modulator Treatment on RAAS Inhibited Patients?..... | 115 |
| 5.4 What are the Implications for Renal Transplant Patients? | 116 |
| 5.5 Similarities and Differences Between the FoxO Transcription Factors? | 117 |
| Bibliography | 123 |

List of Tables

| | |
|--|-----|
| Table 1: qRT-PCR Primers..... | 37 |
| Table 2: Antibodies..... | 39 |
| Table 3: Map of FoxO Binding on Human GUCY1A3 Region..... | 40 |
| Table 4: Map of FoxO Binding on Human GUCY1B3 Region..... | 45 |
| Table 5: Calculations for vasodilatory responses of renal arteries to ACh and SNP..... | 81 |
| Table 6: Catalogue of primary and secondary antibodies..... | 82 |
| Table 7: Catalogue of PCR primer sequences used..... | 84 |
| Table 8: Primer Sequences for RT-qPCR and ChIP..... | 108 |
| Table 9: Catalog of Antibodies for Western Blot and ChIP..... | 109 |

List of Figures

| | |
|-----------------|-----|
| Figure 1 | 31 |
| Figure 2 | 32 |
| Figure 3 | 33 |
| Figure 4 | 34 |
| Figure 5 | 35 |
| Figure 6 | 36 |
| Figure 7 | 48 |
| Figure 8 | 49 |
| Figure 9 | 72 |
| Figure 10 | 73 |
| Figure 11 | 74 |
| Figure 12 | 75 |
| Figure 13 | 76 |
| Figure 14 | 77 |
| Figure 15 | 78 |
| Figure 16 | 79 |
| Figure 17 | 80 |
| Figure 18 | 102 |
| Figure 19 | 103 |
| Figure 20 | 104 |
| Figure 21 | 105 |

| | |
|-----------------|-----|
| Figure 22 | 106 |
| Figure 23 | 107 |

Preface

Dedication:

I dedicate this work to my late grandfather – Joseph Mascetta – my namesake who ignited the spark in me for a loving drive to pursue a career in scientific research and pedagogy. His invaluable influence on me from a very young age fostered a devotion to learning and exploration of the enigmatic world in which we live.

Acknowledgements:

I am so grateful to have had the chance to pursue my PhD degree at the University of Pittsburgh. The resources, mentoring and scholarship available here have been invaluable to my success.

I would like to begin by extending a huge thank you to my mentor, Adam Straub. You were a tremendous advocate for my work throughout my thesis project and consistently gave me more opportunities to be successful. Thank you for pushing me and for being such an exemplary role model.

I would like to thank the members of my committee, Patrick Pagano, Ed Jackson, Alessandro Bisello, Delphine Gomez, and Aditi Gurkar, for inspiring me both inside and outside of the lab. Your support, guidance and confidence has encouraged me to be a better scientist, for which I will be eternally grateful.

I would like to thank all of my colleagues in the Straub lab. I could not have asked for a better team to work with. Thank you Megan Miller, Scott Hahn, and Subramaniam Sanker; you have always been patient with me and your knowledge helped me enormously in my development as a scientist. To my fellow graduate students, Nolan Carew, Heidi Schmidt, and Oyin Dosunmu-Ogunbi, thank you for your help with experiments, grants, manuscripts and navigating the curricula at Pitt. Thank you to Katherine Wood and Shuai Yuan for your comprehensive analytical aid in my writing and technical skills throughout my PhD; I'm a better writer and scientist today because of you. To Brittany Durgin, you were an invaluable role model as a post-doctoral mentor to me throughout my work, and your comments, guidance, and work ethic have helped me grow tremendously.

To my sisters – Emily and Sara – for helping pass the time and for supporting me as we have grown together throughout our lives. I am very blessed to have grown up with the two of you. Thank you to my friends, who in many ways have helped me grow, mature, and have brought some of the best laughs during this period of my life.

To my mother and father – Lori and John – who nurtured my passion and acted as my foundation during this journey, despite its many trials and tribulations. Thank you for helping me achieve my goals. I love you both.

To my beloved wife and best friend – Abbey – for being my bulwark throughout this journey and for always being there as a trusted voice and a reliable listener. Thank you for helping me remain hopeful and for the love and joy we have shared together every day.

Last, and foremost – to God – during this period my faith has been a guiding light to realize my goals.

1.0 Introduction

The ability to alter the diameter of blood vessels is a tightly regulated process which is affected by a variety of environmental, genetic, and internal factors. Changes in the internal diameter of the blood vessels manifest in altered blood flow dynamics across the affected vascular beds, as the resistance to flow applied by the blood vessel is inversely proportional to the vessel's diameter. In light of this knowledge, alterations which decrease blood vessel diameter will have vital impacts throughout the body, leading to pathological conditions which can cause high blood pressure or other conditions resulting from hypertensive stress.

Relaxation of the vascular smooth muscle is one of the main methods the body has to mitigate pathologies which might restrict blood flow. These regulatory pathways often govern rapid changes to signaling events which control the vascular smooth muscle contractile and relaxation responses. The ability of the vasculature to respond to these stimuli via these many signaling mechanisms constitutes a necessary component for maintaining proper cardiovascular health. These pathways and those that influence them remain one of the most important areas of public health study.

1.1 Public Health Burden of Hypertension

Cardiovascular disease (CVD) represents the most prevalent cause of death in the world with more than 17.9 million global deaths annually,¹ and more than 655,000 CVD-related deaths annually in the U.S.²In addition to deaths, CVD represents a tremendous economic cost across

the globe. In the U.S. alone annual spending on patients was \$109.1 billion in 2012,³ and this figure is projected to increase to more than \$200 billion in direct costs with \$40 billion in indirect costs by the year 2030.⁴ Hypertension affects nearly one out of three adults in the U.S., making it the most preventable risk factor for CVD-related death.⁵⁻¹⁰ Moreover, the global number of those affected by hypertension was estimated to be 1.39 billion people in 2010, representing 31.1% of adults, up from 24% or approximately 918 million in 2000.¹¹⁻¹² This increase is irrespective of the new hypertension classification by the American College of Cardiology/American Heart Association Task Force on Clinical Practice Guidelines 2017,¹³ which reclassified hypertensive patients from systolic blood pressure >140 mmHg or diastolic blood pressure >90 mmHg to systolic blood pressure >130 mmHg or diastolic blood pressure >80 mmHg based upon the findings of randomized clinical trials like the Systolic Blood Pressure Intervention Trial which showed that more aggressive systolic blood pressure target criteria (systolic BP ≤ 120 mmHg from ≤ 140 mmHg) reduces cardiovascular disease and all-cause mortality.¹⁴⁻¹⁷ These new criteria have amplified the number of people estimated as hypertensive from approximately 32% in the U.S. to 45.4%,¹⁸ and this change is even more profound in lower income nations like China where this results in an increase from 23.2% to 46.4%.¹⁹ This increase is consistent with global trends between 2000 and 2010, which showed that adults with ≥ 140 mmHg systolic BP in countries classified by the World Bank to be of low or middle income increased from 23.8% to 31.5%.¹¹ These data suggest that the global health burden of hypertension will continue to be an important area of study, especially as Asia and Africa develop further, shifting much of the public health burden from hunger to undernourishment, obesity, and hypertension.²⁰ The growing population of hypertensive patients across the world highlights the importance of new cardiovascular research techniques to alleviate the large public

health burden, however, many significant questions still remain concerning the proper treatment methods to meet this emergent need.

1.2 Function and Regulation of sGC

Arterial dilation is one of the pivotal aspects of physiology necessary for mitigating high blood pressure. Many of the mechanisms responsible for potentiating these processes require communication between multiple cell types to cause relaxation of the vascular smooth muscle. One such heterocellular pathway involves the cleavage of L-arginine to create nitric oxide (NO) and L-citrulline.²¹⁻²² This production occurs primarily through nitric oxide synthase 3, also known as endothelial nitric oxide synthase (eNOS).²³⁻²⁴ This NO generated in the endothelium freely diffuses to the adjacent smooth muscle cells where it interacts with the heme iron group of its cytosolic receptor, soluble guanylyl cyclase (sGC).²⁵ In order for sGC to have functional catalytic activity, it must form a heterodimeric structure with at least one α and one β subunit in order for the catalytic pocket to form at the C-termini of both subunits. Indeed, seminal studies by Andreas Friebe and his colleagues showed in mice that the loss of the β 1 subunit of sGC indicate a lack of smooth muscle sGC β 1 protein in vascular smooth muscle is sufficient to cause hypertension,²⁶ and a global deletion of sGC β 1 causes not only hypertension but also arrests intestinal peristaltic activity resulting in gut dysmotility and death.²⁷ There are two α subunits and two β subunits capable of comprising sGC protein, though the β 2 isoform has not been shown to be expressed in high amounts.²⁸ Additionally, while some research has shown that it is possible for α 2 β 1 heterodimers to form, α 1 β 1 dimers predominate in most tissues.²⁸

The heme moiety of sGC is held within the heme-nitric oxide/oxygen (H-NOX) region of the β subunit, and NO coordinates with the heme iron, causing the iron atom to be cleaved from the His-105 residue due to the change in distance between the peptide and the metal ion.²⁹ Moreover, binding of an NO molecule elicits conformational changes within the coiled-coil domains of both the α and β subunit of sGC to properly align the catalytic domains of each to form the 5'-guanosine triphosphate (GTP) binding pocket.³⁰⁻³¹ Seminal works by Dennis Stuehr's group showed that heat shock protein 90 (Hsp90) drives the insertion of the heme moiety into the apo-sGC β 1 subunit during cellular development,³² however, they also demonstrated that NO promotes the rapid dissociation of sGC β 1 subunit from Hsp90 to allow the union of sGC α 1 subunit to form enzymatically functional sGC α 1 β 1 heterodimers.³³ Further works have provided supporting data which indicated that the prolonged inhibition of Hsp90 promotes accelerated proteasomal degradation of sGC protein.^{32,34}

Importantly, the heme-iron oxidation state is the key determinant in the binding capability of NO to promote the production of cGMP. The NO-sensitive state requires the iron to be in the Fe²⁺ (Ferrous) oxidation state in order to coordinate this interaction, while the Fe³⁺ (Ferric) oxidation state remains insensitive to NO and incapable of producing downstream cGMP.³⁵ Exogenous compounds such as methylene blue, 1H-[1,2,4]oxadiazolo-[4,3-a]quinoxalin-1-one (ODQ) or ferricyanide (FeCN) are capable of oxidizing the heme iron group of sGC, rendering it insensitive to NO binding.³⁶⁻³⁷ Similarly, endogenous oxidants hydrogen peroxide,³⁸ superoxide,³⁹ and peroxynitrite have been shown to impact the binding of NO to sGC.⁴⁰ Further research by Dr. Adam Straub's group demonstrated that Cyb5R3 is the key enzyme responsible for maintaining ferrous, NO-sensitive heme.⁴¹ They demonstrated that Cyb5R3 interacts directly with sGC protein following treatment with ODQ and that loss or

pharmacological inhibition of Cyb5R3 exacerbates the loss of cGMP production and promotes the loss of sGC protein and dysfunctional vasorelaxation in isolated blood vessels.⁴¹⁻⁴² Furthermore, overexpression of Cyb5R3 rescues cGMP-dependent SMC function following oxidation.^{41,43} These data demonstrate that endogenous heme reduction mechanisms are essential to maintain NO-dependent vasodilation within blood vessels.

Localization of proteins within cellular microdomains also play important roles in the redox environment and efficiency of signal transduction between cell types. Immunoprecipitation studies have shown that multi-protein complexes can form between Hsp90 or Hsp70 and sGC to stabilize the oxidized isoform of the enzyme.⁴⁴⁻⁴⁵ Based on the findings that calveolar invaginations play important roles in cardiovascular diseases,⁴⁶ studies in the heart have suggested that calveolar localization of sGC is critical for maintaining the heme in its NO-sensitive, ferrous iron state.⁴⁷⁻⁴⁸ Moreover, since Cyb5R3 is a membrane-associated protein required for restoration of sGC heme redox state,⁴¹ it is likely that membrane association of sGC following redox stress represents another necessary component of NO-dependent sGC signaling within the vascular wall.

Importantly, the class III family of cyclases have a broad range of structures with only a small homologous domain that links this group of adenylyl, guanylyl, and diguanylate cyclases.⁴⁹ Key redox-sensitive cysteines help to modulate the activity of the sGC heterodimer, with many helping to maintain structural integrity, while others are necessary to support the function of the respective domains. A recent study identified an oxidation-sensitive thiol/disulfide switch mechanism between Cys-489 and Cys-571 of sGC β 1 that can result in disulfide bridge formation due to coordination with Thioredoxin-1 (Trx1) and Protein Disulfide Isomerase (PDI) through mixed disulfide formation.⁵⁰ This marks an important new finding in the field, explaining

seemingly incongruous data showing that treatment with reductants such as dithiothreitol (DTT) or Tris-(2-carboxyethyl)phosphine (TCEP) blunt responsiveness to NO,⁵¹⁻⁵² while isolated sGC enzyme is commonly incubated with DTT and glutathione (GSH) to preserve activity. Because the DTT and GSH mixture can form mixed disulfide intermediates,⁵² this mixture likely mimics the interaction which occurs with Trx1 and PD1 in specific domains of cytosolic sGC.

Another redox-regulatory mechanism which governs sGC function is comprised of Cysteine S-nitrosation. This process provides a necessary negative feedback check on sGC activity, wherein excess NO production leads to inhibitory S-nitrosothiol (SNO) formation.⁵³⁻⁵⁵ Just as this negative feedback regulation via SNO formation slows the production of cGMP, it is essential that this process be reversible. Interestingly, Trx1 not only serves to facilitate the formation of disulfide bonds, but also aids in the denitrosation of Cys residues to restore enzymatic activity.⁵⁶ This study demonstrated that a mixed disulfide bond forms between Cys-73 of Trx1 and Cys-609 of sGC α 1. Furthermore, pharmacological inhibition of Trx1 using 1-chloro-2,4-dinitrobenzene (DNCEB) following nitrosocysteine (CSNO) treatment caused a significant decrease in cGMP production and also showed that overexpression of Trx1 significantly rescued cGMP production after CSNO treatment.⁵⁶ Cys-609 of sGC α 1 has recently been identified as a novel residue for S-nitrosation.⁵⁷ Mutation of the Cys-609 of sGC α 1 showed resistance to CSNO-mediated decreases in cGMP production, however, overexpression of Trx1 was incapable of rescuing deficient cGMP production, suggesting that Trx1-mediated disulfides may play an important role through Cys-609 of sGC α 1.⁵⁶

1.3 Drugs Targeting sGC and Their Clinical Impacts

Two distinct drug mechanisms are capable of modulating the activity of sGC based upon the oxidation state of the iron of the β subunit. The first class, termed sGC stimulators, relies on the NO-sensitive, Fe^{2+} (ferric) iron oxidation state for the production of cGMP and a number of these drugs have been recently approved for the treatment of cardiovascular diseases.⁵⁸⁻⁶⁰ YC-1 demonstrated synergistic increases in sGC activity when combined with the NO donor, sodium nitroprusside (SNP) in ex vivo tissue preparations.⁶² Additionally, this drug demonstrated NO-independent activation when used in conjunction with carbon monoxide (CO) by promoting dose-dependent increases in sGC activity.⁶¹ The authors concluded that because CO showed no dose-dependent increases in sGC activity when used alone, YC-1 likely owes its mechanistic effects to stabilization of an active conformation of the enzyme upon diatomic molecular coordination with the heme iron of sGC β 1.⁶¹ Similarly, studies with sGC stimulators BAY 41-8543 and BAY 41-2272, both of which were designed using the chemical structure of YC-1, both displayed promising effects in the treatment of pulmonary hypertension.⁶³⁻⁶⁵ These molecules demonstrated synergistic effects with NO treatment that showed higher potency to produce cGMP-dependent effects.⁶⁶⁻⁶⁷ BAY 63-2521 (Riociguat) has recently been approved for the treatment of chronic thromboembolic pulmonary hypertension,⁵⁹ and has also shown efficacy for the treatment of pulmonary arterial hypertension,⁶⁰ though despite its promising synergistic effect with NO treatment, may have limited therapeutic capability due to its shorter half-life of 7 hours in healthy individuals and 12 hours in patients.⁶⁸ A Phase III clinical trial using BAY 1021189 (Vericiguat) to treat chronic heart failure in patients with reduced ejection fraction showed lower incidence of mortality due to CVD and decreased hospitalizations due to CVD complications than the placebo.⁵⁸ sGC stimulator drugs represent an encouraging new class of molecules capable of inducing sGC activity, however these drugs require NO-sensitive sGC in order to work.

The second class of sGC modulators, namely sGC activator drugs, are characterized by those capable of inducing sGC activity via NO-independent mechanisms. Mechanistic studies using HMR-1766, also known as Ataciguat, and BAY 58-2667, also known as Cinaciguat, showed increased cGMP production following pre-treatment with a variety of oxidizing agents.⁶⁹ Additionally, both drugs demonstrate a preference for heme-deficient enzyme based upon *in vitro* studies.⁶⁹⁻⁷⁰ In recent Phase II clinical trials for acute decompensated heart failure, Cinaciguat showed effective decreases in cardiac load, however, trials ceased after Phase IIb due to a high incidence of hypotension in those treated with Cinaciguat over the placebo.⁷¹ Interestingly, a new study using BAY 60-2770 showed higher association with purified sGC enzyme by size exclusion chromatography and affinity than Cinaciguat and demonstrated higher sGC activity than Cinaciguat.⁷²⁻⁷³ Because BAY 60-2770 mimics the heme moiety of sGC,⁷³ there may be therapeutic potential to examine its use in a similar manner to the clinical trials using Cinaciguat in the future. A recent study using an *in vivo* mouse model of sickle cell disease (SCD) evaluated the efficacy of sGC modular therapy and the sGC activator, BAY 54-6544, improved pulmonary vasorelaxation in an NO-independent manner.⁷⁴ BAY 54-6544 also reversed pulmonary hypertension, cardiac remodeling and improved endothelial cell function in SCD mice,⁷⁴ suggesting that sGC activator therapy may be an effective novel treatment strategy to alleviate age-related pathologies associated with SCD. With many sGC activator therapies in clinical trials, these compounds reveal a novel approach to treat patients where sGC function is compromised by oxidation or heme degradation. sGC-cGMP signaling within the vasculature is critical to sustain its proper dilatory function.

sGC-cGMP signaling within the vasculature is critical to sustain its proper dilatory function. Redox regulation of sGC enzyme is modulated by a variety of events including heme iron oxidation, sGC membrane localization, coordination of sGC with various proteins to prevent oxidation or facilitate reduction, and modification of reactive Cys residues by S-nitrosation or formation of mixed disulfide bonds. Because many of these studies were performed using artificial systems, further investigation using *in vivo* models will be necessary to demonstrate the

mechanistic effects of these promising *in vitro* findings. Despite these findings, however, some major basic science questions still remain regarding the transcriptional regulation of the sGC enzyme both in cultured SMC and *in vivo*. Prior to our work, few studies had examined the transcriptional regulation of sGC,⁷⁵⁻⁷⁶ let alone within SMC,⁷⁷ the tissue type where it is the most well-known. Furthermore, because there has been a significant amount of clinical progress using sGC stimulators and activators in the past few years, the marriage of the molecular research with the clinical efficacy proffers a novel approach to treat pathogenesis within the vascular wall and identification of the transcriptional regulators of sGC offer additional tools to clinicians to identify more effective treatment strategies for different vascular beds.

1.4 A Brief Overview of the FoxO Transcription Factors

One of the largest families of transcription factors, the forkhead box (Fox) family, is named for the ectopic “fork-shaped” head which developed in *Drosophila* with mutations in the *fh* gene.⁷⁸ Shortly thereafter, another group independently discovered the FoxA1 protein in rats, identifying the first orthologous FoxO expressed in mammals.⁷⁹ These discoveries initiated the study of this novel “forkhead” domain for transcription factors,⁸⁰ a group which has more than 50 members in mammals, comprising an immensely diverse group of genes which are classified into subfamilies FoxA to FoxS by sequence similarity.⁸¹⁻⁸² Because there are many Fox transcription factors, the gene targets regulated by this large family are broad and are involved in a multitude of cell types and regulate myriad pathways.⁸³⁻⁸⁴ These proteins contain a DNA binding domain which have a distinctive set of approximately 100 amino acids that are comprised of three α -helices that are flanked by two flexible loops,⁷⁹ giving the appearance of

butterfly wings by X-ray crystallography experiments.⁸⁵⁻⁸⁹ This structure is the reason why the Fox family of transcription factors are often referred to as the “winged helix” transcription factors.

The subclass O family (FoxO) of transcription factors are classified by their sequence similarity and their inhibition by phosphatidylinositol 3-kinase (PI3K) and protein kinase B (PKB/Akt).⁹⁰⁻⁹⁷ The FoxO proteins and their ancestral orthologs appear to have played significant roles in organisms across the animal kingdom, as orthologs have been identified to have existed more than 500 million years ago.⁹⁸ The most ancient identification of this pathway, found in *C. elegans*, shows that the FoxO ortholog called DAF-16, is regulated by the orthologous insulin pathway in nematodes (via the DAF-2 receptor) in the same manner as mammalian FoxO proteins and inactivation of this pathway can alter the lifespan of the animals by more than 3-fold.⁹⁹⁻¹⁰² Similarly, when overexpressed in *D. melanogaster*, *dFOXO*, which is the fruit fly ortholog of mammalian FoxO transcription factors, extends the lifespan of flies.¹⁰³ Remarkably, mice lacking the insulin receptor in adipose tissue had a 30% longer lifespan than controls.¹⁰⁴ Insulin signaling is the primary regulatory of the FoxO transcription factors in mammals, insects and nematodes, and the stress-response pathways are also preserved between invertebrates and mammals, suggesting an important position for this evolutionarily conserved pathway regulated by this transcription factor family.

In mammals, there are 4 identified FoxO family members, named for the order they were discovered: FoxO1,¹⁰⁵ FoxO3,¹⁰⁶ FoxO4,¹⁰⁷ and FoxO6.¹⁰⁸ FoxO2 is identical to FoxO3 (*FoxO3A* gene, as opposed to the *FoxO3B* pseudogene identified in humans),¹⁰⁹ and FoxO5 is the FoxO3 ortholog found in zebrafish (*Danio rerio*).¹¹⁰ The mammalian FoxO proteins were first identified due to rhabdomyosarcomas and acute myeloid leukemias,¹⁰⁵⁻¹⁰⁸ identifying them

as important regulators of the cell cycle and cell proliferation. These proteins have been identified to play important parts in a multitude of pathways including oxidative stress mitigation,¹¹¹⁻¹¹² cell cycle progression,¹¹³⁻¹¹⁴ aging,¹¹⁵ and glucose metabolism.^{99,116}

Identification of the signaling threshold and contexts in which these different pathways become activated is an important component of ongoing FoxO transcription factor research. For example, some human cancers have been shown to have less functional FoxO3, leading to higher rates of proliferation and worse health outcomes.¹¹⁷⁻¹²⁰ Similarly, expression of constitutively active forms of FoxO proteins inhibit cell growth in tumors in vivo,¹²¹⁻¹²³ and the FoxO genes have shown to interact with key cell growth and apoptotic partners like p53 and SMAD transcription factors.¹²⁴⁻¹²⁸ These studies demonstrate the important role that the FoxO family play in the blocking hyperproliferation and induction of apoptosis.¹²⁴⁻¹²⁸

In addition to the importance of tumor suppression, many of the stimuli which help FoxO genes regulate oxidative stress and metabolism have been linked to the post-translational modifications made to alter subcellular location and DNA-binding affinity.^{95,97,129} De-acetylation of FoxO3 by NAD-dependent deacetylase sirtuin-1 (SIRT1) following hydrogen peroxide showed that the increased SIRT1 interaction with FoxO3 increased gene expression of growth arrest and DNA damage response protein 45 alpha (Gadd45 α), while also demonstrating that inhibition of SIRT1 and class I and II histone deacetylases (HDACs) led to increased expression of the apoptotic marker, Bcl2-like protein 11 (Bim), and elevated cleaved caspase 3.¹²⁹⁻¹³⁰ These data suggest the interesting prospect that differential post-translational modifications not only alter the activity of the FoxO transcription factors, but also control the genetic targets of the FoxO proteins, adding another level of supervisory control over the expression of FoxO transcriptional targets.

While the FoxO transcription factors have long been identified as important regulators of cancer and aging,¹³¹ there is now emergent research that has identified some of the functional contributions in the context of vascular biology. Loss of FoxO1 in pulmonary vasculature has recently been shown to induce SMC hyperplasia and pulmonary hypertension.¹³² Additionally, FoxO1 and FoxO3a in endothelium have been shown to repress the expression of endothelial nitric oxide synthase and post-natal silencing of these two transcription factors has been shown to promote angiogenesis and proliferation of various vascular cell types *in vivo*.¹³²⁻¹³⁴ Constitutive activity of the FoxO transcription factors have been shown to inhibit the growth of several different cell types,¹³⁵⁻¹³⁶ alluding to the fact that FoxO transcription factors are important for preventing hyperproliferation in a multitude of tissues. Increased production of cGMP in smooth muscle has been shown to have similar effects in suppressing cellular proliferation.¹³⁷⁻¹³⁸ These data support the idea that both sGC function and FoxO transcription factor function both contribute to the regulation of smooth muscle quiescence. Finally, recent publications have shown that the different members of the FoxO family have distinct functions from one another in the vasculature despite similar regulatory processes.¹³⁹⁻¹⁴⁰ Our work herein suggests that the FoxO transcription factors are indispensable regulators of vascular function through their regulation of sGC expression.

1.5 The Purpose of This Dissertation

My goal for this dissertation is to inform you, the reader, about our discovery that the FoxO family of transcription factors play a vital role in the gene expression of sGC and the effects caused by changes to FoxO transcriptional activity or expression in SMC. sGC has been

shown to be necessary for survival in knockout mouse models due to lethal vascular malformation and lack of gut motility in early in development.²⁷ Additionally, sGC is fundamental for the maintenance of homeostatic blood pressure, as SMC-specific knockout of sGC β in adult animals leads to development of a severe hypertensive phenotype.²⁶ As has been mentioned, the FoxO transcription factors are major regulators of mammalian aging, and aging is correlated with the loss of both sGC and FoxO expression.¹⁴¹⁻¹⁴⁶ Therefore, it was on these grounds that I sought to identify how this enzyme was regulated at the level of transcription and the effects on downstream signaling when this regulation is disrupted.

Here we explain our original research that is published as well as our data in preparation for peer review underscoring the contributions of the FoxO transcription factors in the regulation of sGC expression in multiple cell and tissue types. Studies in Chapter 2 outline our published results where we showed that loss of FoxO transcriptional activity using an inhibitory drug significantly decreases the mRNA expression of sGC leading to blunted sGC protein expression and downstream signaling both in isolated rat aortic SMC and in FoxO inhibitor-treated murine aortic tissue.¹⁴⁷ Chapter 3 encapsulates our published research which demonstrated in a model of renal hypertension that sGC is elevated and dilatory function in the contralateral renal arteries of these animals are augmented compared to their respective controls. We go on to show that angiotensin II causes an increase in the expression of sGC in renal SMC through a mechanism dependent upon the FoxO transcription factors and that the loss of this activity not only blunts the increase in expression, but also impairs the downstream signaling.¹⁴⁸ Our findings in Chapter 4 show that FoxO4 is the primary FoxO protein responsible for the regulation of sGC in SMC across multiple species. Here we also identify the specific regulatory sites where the FoxO proteins interact with the sGC promoter. In Chapter 5, I discuss many of the questions that still

remain unanswered, the implications of our findings for the field of vascular research and the future research directions that may bear productive results for others henceforth. And finally, I discuss the impact our findings may have for clinical and pharmaceutical research for the treatment of hypertension.

2.0 Antagonism of Forkhead Box Subclass O Transcription Factors Elicits Loss of Soluble Guanylyl Cyclase Expression

Joseph C. Galley,^{1,2} Brittany G. Durgin,¹ Megan P. Miller,¹ Scott A. Hahn,¹ Shuai Yuan,¹ Katherine C. Wood,¹ and Adam C. Straub.^{1,2}

¹Heart, Lung, Blood and Vascular Medicine Institute, University of Pittsburgh, Pittsburgh, Pennsylvania;

²Department of Pharmacology and Chemical Biology, University of Pittsburgh, Pittsburgh, Pennsylvania

Copyright American Society for Pharmacology & Experimental Therapeutics, 2018

2.1 Summary:

Nitric oxide (NO) stimulates soluble guanylyl cyclase (sGC) activity leading to elevated intracellular cyclic guanosine 3', 5'-monophosphate (cGMP) and subsequent vascular smooth muscle relaxation. It is known that downregulation of sGC expression attenuates vascular dilation and contributes to the pathogenesis of cardiovascular disease. However, it is not well understood how sGC transcription is regulated. Here, we demonstrate that pharmacological inhibition of Forkhead Box subclass O (FoxO) transcription factors using the small molecule inhibitor, AS1842856, significantly blunts sGC α and β mRNA expression by more than 90%. These effects are concentration-dependent and concomitant with greater than 90% reduced expression of the known FoxO transcriptional targets, glucose-6-phosphatase (G6Pase) and growth arrest and DNA damage protein 45 α (Gadd45 α). Similarly, sGC α and sGC β protein expression showed a concentration-dependent downregulation. Consistent with the loss of sGC α

and β mRNA and protein expression, pre-treatment of vascular smooth muscle cells (VSMC) with the FoxO inhibitor decreased sGC activity measured by cGMP production following stimulation with an NO donor. To determine if FoxO inhibition resulted in a functional impairment in vascular relaxation, we cultured mouse thoracic aortas with the FoxO inhibitor and conducted *ex vivo* two-pin myography studies. Results show that aortas have significantly blunted sodium nitroprusside (SNP)-induced (NO-dependent) vasorelaxation and a 42% decrease in sGC expression after 48-hour FoxO inhibitor treatment. Taken together, these data are the first to identify that FoxO transcription factor activity is necessary for sGC expression and NO-dependent relaxation.

2.2 Introduction:

Arterial blood vessel dilation is mediated, in part, through production of the endogenous endothelial vasodilator molecule, nitric oxide (NO). NO signals by binding to ferrous heme iron in soluble guanylyl cyclase (sGC) in vascular smooth muscle cells (VSMC) to catalyze the intracellular conversion of guanosine 5'-triphosphate to the second messenger molecule cyclic guanosine 3', 5'-monophosphate (cGMP).¹⁴⁹ Increased cGMP, in turn, activates protein kinase G (PKG) leading to vascular smooth muscle relaxation needed to govern tissue perfusion and blood pressure.¹⁵⁰ Indeed, several prior studies conducted in spontaneous hypertensive rats showed sGC mRNA and protein expression to be downregulated and associated with impaired NO-dependent vasodilation.^{142,151} Moreover, SMC-specific inducible knockout of sGC β in mice results in hypertension, suggesting sGC expression in SMC is critical for modulating vascular tone.²⁶ Genome wide association studies of single nucleotide polymorphisms also identified

genetic variants within the sGC genes *GUCY1A3* and *GUCY1B3* as associated with a high risk for cardiovascular disease.¹⁵²⁻¹⁵⁴ Of translational importance, small molecule sGC modulators have been developed for clinical use to restore disease-associated loss of sGC activity and cGMP production to varying degrees of success.¹⁵⁵⁻¹⁵⁹ For example, Riociguat (BAY 63-2521), a heme-dependent sGC stimulator, has been recently approved for treatment of pulmonary arterial hypertension and chronic thromboembolic pulmonary hypertension.⁵⁹⁻⁶⁰ Additionally, Cinaciguat (BAY 58-2667), a NO-independent sGC activator which increases cGMP when sGC heme is oxidized or resides in the heme-deficient state,³⁵ but further studies were halted with BAY 58-2667 after it showed risk for hypotension in a phase IIb clinical trial for treatment of acute heart failure syndrome.⁷¹ Importantly, the clinical efficacy of these sGC modulators is dependent on adequate sGC protein expression.

While the NO-sGC-cGMP pathway continues to be extensively studied, there are a limited number of studies that have identified the mechanisms regulating sGC transcription. Prior work by *Kloss et al* has shown interacting partners with sGC transcripts, namely human antigen R (HuR), which stabilizes the sGC mRNA,^{143,160} and miR-34c-5p and ARE/poly(U)-binding/degradation factor 1 (AUF1), which destabilize and promote the degradation sGC transcripts.¹⁶¹⁻¹⁶² Furthermore, CCAAT-binding factor deletion significantly blunts production of sGC mRNA expression in a neuroblastoma cell line.⁷⁵ However, beyond these studies our knowledge of the transcription factor(s) responsible for the constitutive expression of sGC, particularly within VSMC, remain elusive.

The Forkhead box subclass O (FoxO) family of transcription factors namely FoxO1, FoxO3 and FoxO4 are the predominant isoforms in VSMC (Salih and Brunet, 2008).¹¹⁵ Recent studies have identified the importance of this family of transcription factors in the vasculature,

including their role in the promotion of angiogenesis,¹³³⁻¹³⁴ inhibition of endothelial NO production,^{133,163} preventing pulmonary hypertension,¹³² and maintenance of pluripotency in a variety of different cell types.^{113-114,140} Additionally, an important observation in the field has established that aging decreases the expression and capacity for FoxO signaling,^{99,103,115,164-165} and has also been shown to decrease the expression of sGC within the vasculature.^{142,166-167}

However, a link connecting the sGC-cGMP and FoxO pathways has yet to be described. Therefore, with the use of *in silico* prediction analysis and a previously characterized FoxO inhibitor compound, AS1842856 (IUPAC name: 5-Amino-7-(cyclohexylamino)-1-ethyl-6-fluoro-4-oxo-1,4-dihydroquinoline-3-carboxylic acid),¹⁶⁸ we sought to determine if the FoxO transcription factor family regulates sGC transcription. Herein, we provide evidence that inhibition of FoxO transcription factors results in significant downregulation of sGC transcript and protein, decreased cGMP production, and impaired NO-induced vasodilation implicating FoxO transcription factors as a major regulator of sGC transcription.

2.3 Materials and Methods:

Cell culture and drug treatment:

Rat aortic smooth muscle cells (RASMC, Lonza) were cultured as previously described.⁴¹ In brief, RASMC were cultured at 37°C in Lonza Smooth Muscle Growth Medium-2 with SmGm-2 SingleQuote supplementation. Cells were passaged using Gibco Trypsin/EDTA up to passage 12. For treatment, FoxO inhibitor, AS1842856 (Cayman, A15871) was dissolved in DMSO at 10 mM stock concentration and diluted in DMSO for further experiments. Control and treatment DMSO concentration was 0.1% of total volume for treatment periods.

qRT-PCR:

RASMCs were cultured in 6-well dishes until confluent and lysed in TRIzol reagent (Thermo Fisher). RNA was isolated from lysates according to the RNA purification protocol from the Direct-zol RNA miniprep plus kit (Zymo). Isolated RNA was reverse transcribed to cDNA using SuperScript III First Strand Synthesis System (Thermo Fisher). Quantitative PCR was performed using PowerUp SyBr Green Master Mix (Thermo Fisher), and 1 μ M target primer (**Table 1**) were mixed and 40 PCR cycles with 95°C melting temperature and 58°C annealing temperature and 72°C extension temperature was performed in QuantStudio 5 Real-Time PCR System (Thermo Fisher).

Western blot:

RASMCs were lysed in ice-cold 1X Cell Lysis Buffer (Cell Signaling) containing 20 mM Tris-HCl (pH 7.5), 150 mM NaCl, 1 mM Na₂EDTA, 1 mM EGTA, 1% Triton, 2.5 mM sodium pyrophosphate, 1 mM beta-glycerophosphate, 1 mM Na₃VO₄, 1 μ g/ml leupeptin supplemented with additional protease and phosphatase inhibitors (Sigma). Protein lysate concentrations were quantified using a standard Bicinchoninic acid kit (Thermo-Fisher). Laemmli buffer was added for final concentration containing 31.5 mM Tris-HCl (pH 6.8), 10% glycerol, 1% SDS, and 0.005% Bromophenol Blue. Lysates were boiled and subjected to electrophoresis on 4-12% BisTris polyacrylamide gels (Life Technologies). Proteins were transferred to nitrocellulose membrane and blocked for 1 hour at room temperature with 1% BSA in PBS. Membranes were rocked overnight with primary antibodies (**Table 2**) diluted in 1% BSA in PBST at 4°C. Membranes were washed and incubated with secondary antibodies from LI-COR (**Table 2**) diluted in 1% BSA in PBST for 1 hour at room temp followed by washing with PBST.

Visualization and analyses were completed utilizing a LI-COR Odyssey Imager and Image Studio Software.

cGMP ELISA:

Confluent RASMCs were cultured in 12-well dishes and pretreated with 10 μ M sildenafil (Sigma) for 45 minutes and then stimulated with the NO-donor, diethylammonium (Z)-1-(N,N-diethylamino)diazen-1-ium-1,2-diolate (DEA NONOate, Cayman), for 15 minutes. Baseline measurements were performed after 45 min treatment with 10 μ M sildenafil. Cell samples were lysed in 125 μ L ice-cold 1X Cell lysis buffer (Cell Signaling) supplemented with protease and phosphatase inhibitors (Sigma). cGMP production was determined via enzyme-linked immunosorbent assay (ELISA assay; Cell Signaling). 10 μ L of sample (approximately 5-10 μ g of protein) was added to each well and diluted with additional lysis buffer, and exact protein concentration of each sample was quantified using a standard BCA protein assay kit (Thermo-Fisher). ELISA assays were performed hereafter according to the manufacturer's protocol.

Immunofluorescence staining:

Twelve-week old C57BL/6J mice (Jackson Laboratories) were sacrificed via CO₂ asphyxiation. Thoracic aortas were excised and placed in 4% paraformaldehyde solution for 24 hours, followed by 24 hours in 30% sucrose in PBS. Tissues were then frozen in optimum cutting temperature compound fixative (OCT, Tissue-Tek) via liquid nitrogen and cryosectioned at 8 μ M thickness with 3 sections/slide using a FSE Cryostat Microtome slicer (Thermo Scientific). Slides were permeabilized with -20°C acetone for 10 minutes, air dried for 10 minutes, washed thrice for 5 minutes each in PBS, and then blocked with PBS + 0.25% Triton-X 100 + 10% horse serum + 1% fish skin gelatin (blocking buffer) for 1 hour. Slides were incubated with rabbit anti-sGC β primary antibody and anti-ACTA2 AlexaFluor 488 conjugated

primary antibody (**Table 2**) diluted in blocking buffer (40 μ L/section) and placed overnight at 4°C in a darkened humidity chamber. Slides were then washed twice for 5 minutes in PBS + 0.1% Tween-20, incubated with donkey anti-rabbit AlexaFluor 594 antibody for 1 hour at room temperature in a darkened humidity chamber (**Table 2**), then washed twice for 5 minutes in PBS + 0.1% Tween-20. Coverslips were then mounted onto microscope slides using Duolink mounting medium containing 4',6-Diamidino-2-Phenylindole, Dihydrochloride (DAPI). Aortas were imaged using an Olympus FluoView 1000 confocal microscope. Fluorescence semi-quantitation was calculated by quantifying the fluorescent signal from each respective channel relative to area of aortic tissue imaged via ImageJ Software.

Treatment of aortic rings and myography:

The following treatment method was performed as previously described.⁴² In brief, isolated murine thoracic aortas were isolated from mice and incubated with 10 μ M FoxO inhibitor for 48 hours in 1 part Lonza Smooth Muscle Growth Medium-2 supplemented with SmGM-2 SingleQuot kit to 9 parts unsupplemented Lonza Smooth Muscle Growth Medium-2. Following treatment, aortas were cut into 2 mm rings before being placed on a two-pin myograph (DMT [Danish Myo Technology]). Aortic rings were then incubated in a physiological salt solution (PSS) for 30 minutes of rest, after which 500 mg tension was applied to the vessels. Vessel viability was tested using potassium physiological salt solution (KPSS) for 15 minutes, followed by a triplicate of PSS washes and a 60-minute resting period. Cumulative concentration responses to phenylephrine (PE 10^{-9} - 10^{-5}) and sodium nitroprusside (SNP, 10^{-9} - 10^{-4}) determined vessel contractility and relaxation responses, respectively. Finally, relaxation percentage was determined by normalizing cumulative SNP relaxation to maximal contraction at 10^{-5} M PE and maximal dilation at 10^{-4} M SNP in Ca^{2+} free PSS.

Statistics:

TransFAC analysis software was used to predict FoxO binding sites on sGC promoter DNA utilizing settings to include the minimum number of false positives (**Fig. 1**). For drug response and time course cell culture experiments, a student's t-test was used to determine significance for **Fig. 5E-5G**, **Fig. 6A**, and **Fig. 7** using GraphPad Prism version 7.03 software, and a one-way ANOVA was used to determine significance for **Fig. 2B-2C**, **2E-2F**, **Fig. 3A-3E**, **Fig. 4A-4B**, **4D-4E**, and **Fig. 8A-8F** using GraphPad Prism version 7.03 software. A two-way analysis of variance (2-way ANOVA) test for **Fig. 6B** was performed for each data point to determine significance using GraphPad Prism version 7.03 software. Calculated p-values represent significant difference from control group and error bar represent standard deviation (s.d.) and symbols for confidence were represented by the following: * p<0.05, ** p<0.01, *** p<0.001, **** p<0.0001.

2.4 Results:

We began our study by analyzing the promoters for both sGC α and β subunits for potential transcription factor binding sites. TRANSFAC analysis software was used to evaluate the human sGC promoter using the GRCh38/hg38 reference genome,¹⁶⁹⁻¹⁷⁰ and 158 and 91 predicted binding sites were identified on the DNA +/-10kbp flanking the sGC α and sGC β transcription start sites, respectively. We discovered an abundance of FoxO family transcription factor binding sites clustered around 47 binding regions for sGC α and 36 binding regions for sGC β . Binding domains for FoxO family proteins in coordination with at least one other transcription factor clustered around 55 regions for sGC α (**Table 3**) and 10 regions for sGC β

(**Table 4**). A fragment of each gene's promoter, 2000 base pairs upstream and 200 base pairs downstream of the transcription start site (TSS) was analyzed and showed 25 FoxO binding sites on the sGC α promoter (**Fig. 1A**) and 15 binding sites on the sGC β promoter (**Fig. 1B**). FoxO binding sites on sGC α clustered around 4 locations, namely 1900, 1800, 1000, and 100 base pairs upstream of the TSS. Likewise, the 2200 base pair sGC β promoter fragment contained 3 clusters of predicted binding sites 1600, 1500 and 1200 base pairs upstream of the TSS.

The enrichment of the FoxO transcription factors based upon *in silico* analyses led us to investigate whether our predictive promoter analysis could be validated. We tested this by treating rat aortic smooth muscle cells (RASMC) with a FoxO inhibitor drug AS1842856, which has been shown to inhibit all three FoxO isoforms expressed in VSMC: FoxO1, FoxO3, and FoxO4.¹⁶⁸ In 48-hour AS1842846 drug (**Fig. 2A**) treatment experiments in RASMC, we observed a stoichiometric loss of sGC α (**Fig. 2B**) and sGC β (**Fig. 2C**) mRNA expression of 90-95% at concentrations of 1 μ M or greater. Over the same treatment period, a loss of 80% in the protein expression of sGC α (**Fig. 2D and E**) and a 74% decrease in sGC β (**Fig. 2D and F**) was observed at concentrations of 1 μ M or greater. Increasing concentrations of AS1842856 were accompanied by no change in FoxO1 mRNA expression (**Fig. 3A**), while an increase in FoxO3 (**Fig. 3B**) and FoxO4 (**Fig. 3C**) mRNA expression was observed. Classical FoxO transcriptional targets, such as growth arrest and DNA damage inducible α (Gadd45 α) and glucose-6-phosphatase (G6Pase) expression exhibited the same degree of decreased gene expression (greater than 90%) at concentrations of 1 μ M or greater (**Fig. 3D and 3E**). These drug experiments show that inhibition of FoxO transcriptional activity was commensurate with a loss of sGC expression, suggesting that the FoxO family plays a regulatory role in sGC gene expression. Additionally, measurement of the gene expression of other cyclic nucleotide

generating-enzymes adenylate cyclase (ADCY) and particulate guanylyl cyclase (pGC) showed that FoxO inhibition did not have a significant dampening effect on their expression. In fact, FoxO inhibition caused increased gene expression of ADCY1 and pGC1 with no significant changes in gene expression of ADCY3 or pGC2 (**Fig. 7**).

Assessment of FoxO temporal activity on sGC expression was then assessed using cultured RASMC treated with 1 μ M FoxO inhibitor. We observed that sGC α (**Fig. 4A and Fig. 8A**) and sGC β (**Fig. 4B and Fig. 8B**) mRNA expression significantly decreased after initial inhibitor administration and continued to decline with increased drug exposure time. Moreover, suppression of sGC mRNA was observed throughout the treatment period, reaching 80-90% reduction by 48 hours (**Fig. 4A and 4B**). As with the drug response experiment, the loss of sGC α and β protein expression over time (**Fig. 4C-4E**) mirrored the observations in mRNA. sGC protein expression was marginally affected during the first few hours after FoxO inhibition, diminished by 32% loss of sGC α and 40% loss of sGC β within 6 hours (**Fig. 8D-F**), while significant losses in gene expression of sGC α (**Fig. 8A**), sGC β (**Fig. 8B**) and G6Pase (**Fig. 8C**) were observed within 3 hours of drug treatment. This trend was also observed in the longer time course experiments, wherein it reached maximal loss of 78% sGC α and 76% sGC β by the end of the 48-hour treatment period (**Fig. 4D and 4E**). Combined, these experiments provide evidence that the loss of sGC expression in cultured RASMC via inhibition of FoxO transcriptional activity occurs rapidly and remains impaired throughout a 48 hour treatment period.

We then assessed the impact of FoxO inhibition on sGC protein expression within isolated blood vessels. Mouse thoracic aortas were isolated and treated with 10 μ M FoxO inhibitor drug for 48 hours and then immunostained for sGC β , smooth muscle alpha actin

(ACTA2), and nuclei (DAPI). A higher concentration compared to culture experiments was necessary for loss of sGC expression, as studies have shown that sGC protein is highly stable *in vivo* (Groneberg et al., 2010). We chose to treat *ex vivo* tissue to circumvent the extensive mechanisms to stabilize sGC protein *in vivo*. FoxO inhibitor treatment decreased sGC β protein expression by 48% (**Fig. 5A-A'**, and **5E**), but had no significant effect on the expression of smooth muscle alpha actin (ACTA2) (**Fig. 5B-B'** and **5F**), or on the density of nuclei staining (DAPI) within these isolated blood vessels (**Fig. 5C-C'** and **5G**). Taken together, these data show that inhibition of FoxO activity in *ex vivo* tissue significantly lowers sGC expression, consistent with our previous studies in RASMCs (**Fig 5D-5D'**).

Next, the extent to which FoxO inhibition impacts sGC signaling function was examined by measuring RASMC cGMP production and isolated aorta vessel relaxation. Cultured RASMC experiments showed that after 1 μ M FoxO inhibitor treatment for 48-hours, cGMP production was reduced 85-90% after stimulation with 0.5 to 1 μ M of NO-donor DEA-NONOate (**Fig. 6A**). Similarly, *ex vivo* vessel myography studies on isolated murine aortas treated with 10 μ M FoxO inhibitor for 48 hours had impaired vasodilation in response to concentrations of the NO donor sodium nitroprusside (SNP) greater than 100 nM (**Fig. 6B**). Collectively, these data suggest that the loss of sGC expression following FoxO inhibition results in a corresponding loss of NO-dependent, sGC-mediated cGMP production and vasoreactivity.

2.5 Discussion:

sGC is crucial for NO-dependent relaxation to maintain cardiovascular health. To date, few studies have investigated the transcriptional regulation of sGC, and none have identified the

transcription factors responsible for the constitutive expression of sGC within the vasculature. Prior work showed the CCAAT binding factor regulates sGC gene expression within a neuroblastoma cell line.⁷⁵ However, no such regulation of sGC was observed in VSMC, which prompted us to search for other transcription factors capable of initiating sGC transcription. One candidate family, the Forkhead box subclass O (FoxO) family of transcription factors, is known to regulate the development of new blood vessels and has been implicated in the prevention of pulmonary arterial hypertension.^{132,134,171} Our predictive analysis of the human *GUCY1A3* and *GUCY1B3* promoters show that a plethora of potential FoxO binding sites are found along the upstream genetic regions of both sGC subunits. These findings inspired further exploration of the impact of FoxO proteins on the expression and downstream function of sGC.

In this study, we inhibited FoxO transcriptional activity using a pan-FoxO inhibitor (AS1842856) and observed significant decreases in the gene expression of sGC and well-established targets of FoxO proteins. The decrease in sGC mRNA transcription demonstrated a stoichiometric decrease in both sGC α and sGC β gene expression. This inhibition rapidly attenuated sGC gene expression and signifies that the decrease in expression of one gene matched the expression of the other. Proportionate expression of sGC α and sGC β protein expression is necessary for optimal enzymatic activity of the obligate heterodimeric protein. Therefore, a symmetrical decrease in both sGC α and sGC β mRNA and protein suggests dual α and β regulation by FoxO transcriptional activity. Alternatively, it is possible that mechanisms which destabilize or stabilize sGC mRNA have the capability to alter sGC expression. For example, increases in the mRNA destabilizer, ARE/poly(U)-binding/degradation factor 1 (AUF1), or loss of an sGC mRNA chaperone, human antigen R (HuR), could contribute to the

observed loss of sGC mRNA,^{143,160-161} but exploration of these hypotheses requires further investigation.

In a similar manner to the observations in sGC mRNA expression, FoxO inhibitor treatment decreased sGC α and β protein expression in cultured RASMC commensurate with the swift concentration-dependent loss of sGC mRNA expression. Moreover, FoxO inhibition in mouse aortas caused a loss of sGC β protein expression and vascular reactivity. This likely suggests that the loss of protein expression and downstream activity occurs as a direct result of the loss of sGC mRNA, and not through post-translational regulatory mechanisms. Signaling molecules identified to have effects on sGC protein expression, such as transforming growth factor β (TGF β) in the developing lung, have decreased the expression of sGC α_1 protein, however, no change was observed on the expression of sGC mRNA in response to hypoxia-induced TGF β expression.¹⁷² Furthermore, the chaperone-dependent E3-ligase protein, C terminus of heat shock cognate 70-interacting protein (CHIP), which is responsible for degradation of sGC protein, also targets the FoxO proteins for proteasomal degradation,¹⁷³⁻¹⁷⁴ Previous studies also indicated that the half-life of sGC β in cultured cells due to CHIP breakdown is roughly 7 hours,¹⁷³ which was consistent with the observed rate of sGC protein loss after our FoxO inhibition experiments and acted as the reasoning for longer drug treatment to observe a loss of protein expression and functional responses in the vasculature. As a result, an effect of FoxO inhibitor treatment alone on CHIP activity would presumably affect both sGC and the FoxO proteins while mRNA expression would not be directly affected. In response to the effects on sGC mRNA expression, the observed loss of sGC protein expression comes due to the lack of sGC transcript production. Additionally, FoxO inhibition caused a 90% reduction of cGMP production by sGC which presumably led to the observed increase in gene expression of

pGC1 as a compensatory mechanism. Despite this increase in pGC1 gene expression, the predominant method of cGMP production in smooth muscle is derived from sGC,²⁶ thus it is unclear whether this compensatory increase would rescue lost function due to impaired NO-dependent cGMP signaling. This effect on sGC protein expression both in culture and *ex vivo* tissue manifests in a loss of cGMP production and subsequent blunting of NO-dependent vasodilation.

We hypothesize that multiple FoxO proteins play a role in the physiological transcription of sGC mRNA due to partial redundancy of the transcription factors, as well as a non-selective effect of the inhibitor drug on all FoxO family members. While we cannot rule out off-target effects of the FoxO inhibitor, our data thus far do not suggest an off-target effect is responsible for the regulation of sGC that we observe. Based upon our pharmacological data and that of Nagashima and colleagues when characterizing this FoxO inhibitor drug, disparate effects on transcriptional activity each of the FoxO proteins are observed after treatment.¹⁶⁸ Pharmacodynamic studies indicate that FoxO1 is 70% inhibited, FoxO4 is 20% inhibited, and FoxO3 is 3% inhibited at a treatment concentration of 100 nM.¹⁶⁸ A recent study also used several *in silico* modeling methods to predict a -6.3 kcal/mol binding energy of AS1842856 to FoxO1 and identified 10 amino acids in the transactivation domain which constitute drug-protein hydrogen bonding and hydrophobic interactions.¹⁷⁵ These studies suggest that AS1842856 is specific for the transactivation domain of FoxO1 which governs the activity of the transcription factor after binding the target DNA sequences. Additionally, the lower affinity for AS1842856 to elicit FoxO3 and FoxO4 inhibition likely explain the necessity for higher drug concentration to induce the loss of sGC transcription both in cultured cells and isolated tissue. Our experiments also showed that FoxO3 and FoxO4 mRNA expression are elevated in response to drug

treatment. These differential effects of the inhibitor drug on each of the isoforms suggest a complicated mechanism with multiple contributing factors in the compensatory expression of FoxO3 and FoxO4. Promoter analyses also showed that the FoxO transcription factors share affinity for the same conserved “TTGTTTAC” DNA motifs, which is supported by previous research.¹⁷⁶⁻¹⁷⁸ This detail may indicate that loss of one transcription factor alone may not be sufficient to achieve the observed knock down of sGC expression in this study. Further investigation is required to elucidate the contributions of each FoxO protein on the transcription of sGC.

Many therapies available today, which include nitrovasodilator compounds that increase the bioavailability of NO,¹⁴⁹ and drugs that target sGC directly,^{59-60,65,71,155} both promote second messenger cGMP signaling to improve cardiovascular health. Deficits in sGC transcription can eliminate the protein target of current therapeutic drugs, rendering many of them ineffective. Discovery of FoxO transcription factors as key regulators of the NO-sGC-cGMP signaling pathway within VSMC also presents a potential contraindication that should be monitored when considering FoxO inhibitor drugs such as AS1842856. Anomalies in blood pressure and other cardiovascular characteristics will be important biomarkers in future drug development studies involving the FoxO proteins. Taken together, the identification of the key transcription factors responsible for production of sGC mRNA is a vital component to our understanding how cardiovascular homeostasis is regulated.

In summary, our study is the first to identify a family of transcription factors, namely the FoxO family, capable of regulating sGC expression in vascular smooth muscle. This reveals a pivotal new role for the FoxO transcription factors in modulating vascular tone and our next studies will investigate the specific role of each FoxO transcription factor in the regulation of

sGC transcription. The discovery of the FoxO family as transcriptional regulators for sGC not only provides an alternative therapeutic approach for blood pressure control, but also reveals a potentially novel mechanism that may impact sGC – related cardiovascular diseases.

Author Contributions:

Participated in research design: Galley, Miller, Durgin, Yuan, and Straub.

Conducted experiments: Galley, Miller, and Hahn.

Contributed new reagents or analytic tools: Galley, Miller, and Hahn.

Performed data analysis: Galley, Miller, and Hahn.

Wrote or contributed to the writing of the manuscript: Galley, Wood, Durgin, Yuan, and Straub.

Acknowledgements:

We would like to acknowledge the Center for Biological Imaging at the University of Pittsburgh for its support and confocal microscope usage. We acknowledge the contributions of Subramaniam Sanker, Nolan Carew, Heidi Schmidt, Rohan Shah, and Jacob Jerome for their aid in critical analysis of the manuscript.

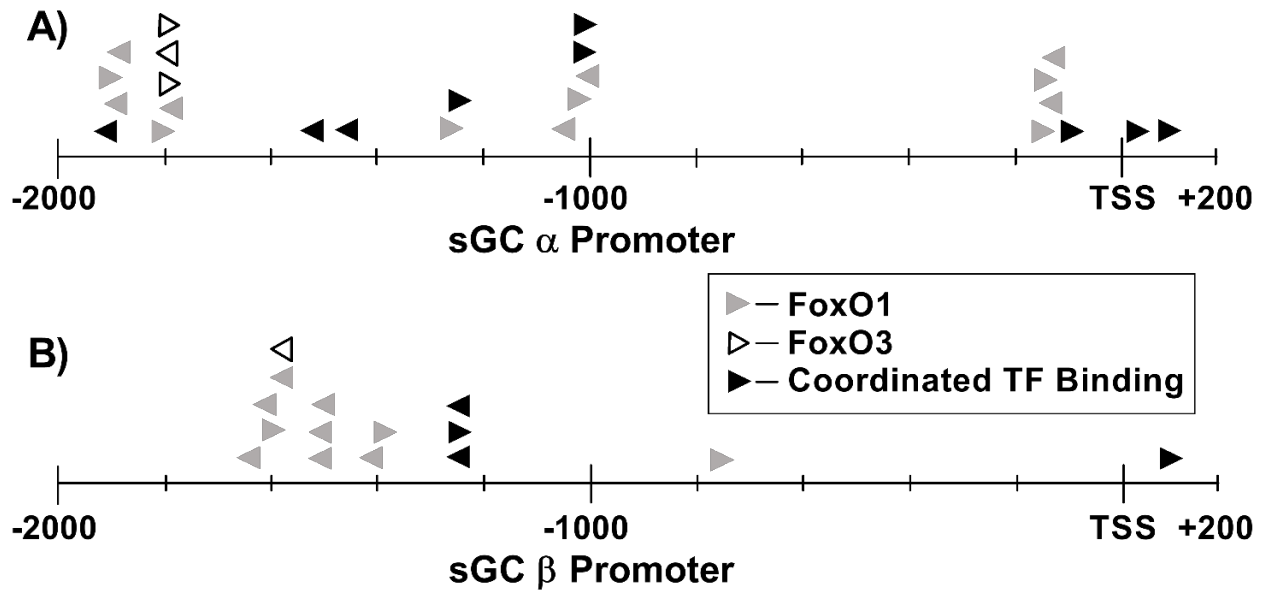


Figure 1

In silico analysis of human sGC promoter.

Transcription factor binding site analysis of human A) sGC α and B) sGC β promoter sequence show predicted FoxO transcription factor binding sites for 2200 bp promoter fragments flanking the sGC transcription start sites. Numbers indicate distance from transcription start site (TSS). Arrows facing right indicate binding sites on the positive (+) DNA strand; Arrows facing left indicate binding sites on the negative (-) DNA strand.

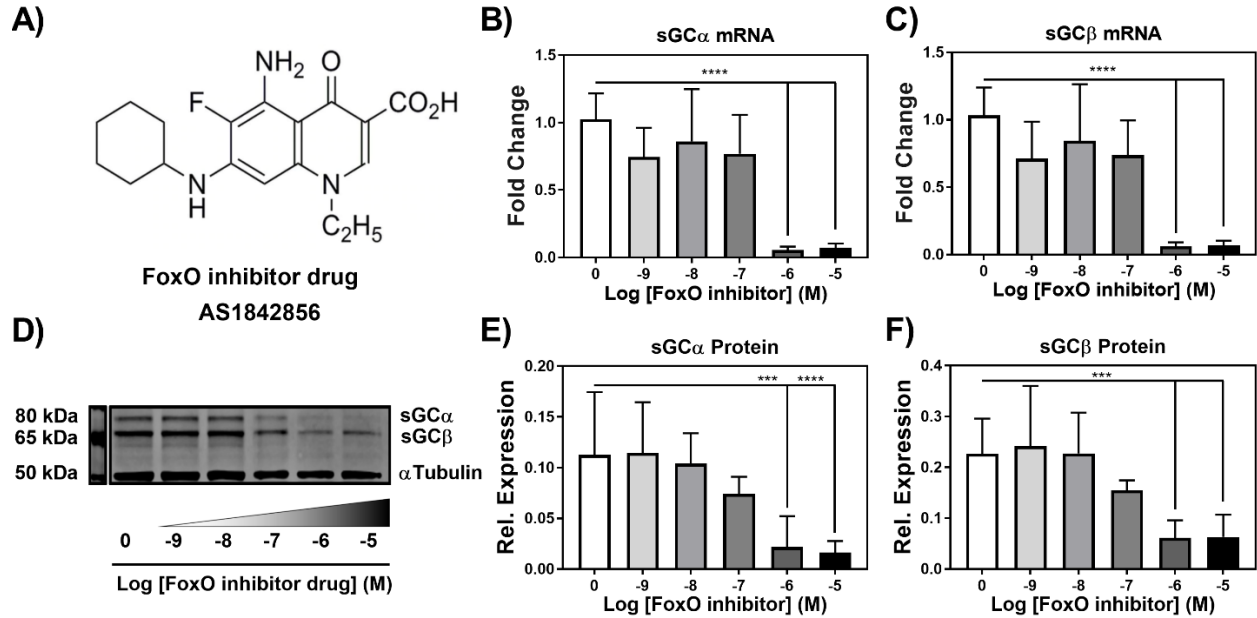


Figure 2

Treatment of RASMC with FoxO inhibitor drug, AS1842856 shows concentration-dependent decrease in sGC mRNA and protein expression.

AS1842856 FoxO inhibitor A) drug structure and effect on B) sGC α mRNA expression or C) sGC β mRNA expression following 48-hour drug treatment. D) Western blot and quantification of 48-hour treatment with FoxO inhibitor on E) sGC α protein expression and F) sGC β protein expression. n=3 for all samples. One-way ANOVA test was used for determination of significance. * p<0.05, ** p<0.01, *** p<0.001, **** p<0.0001. Error bars represent s.d.

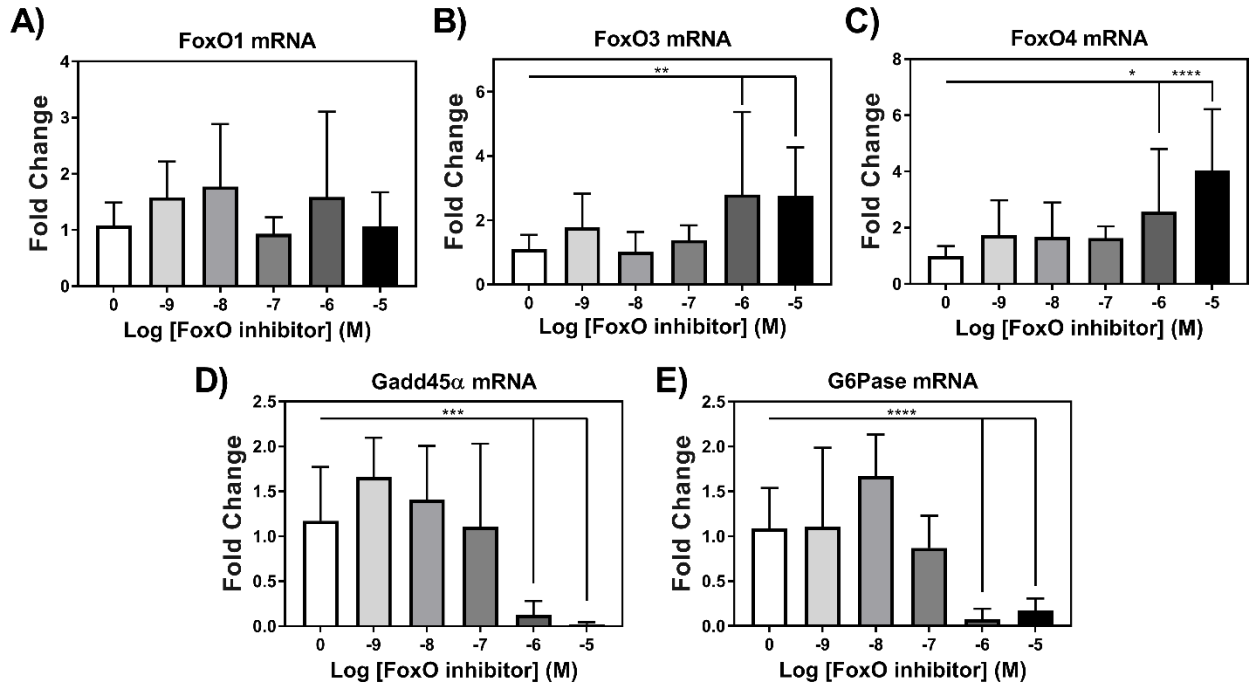


Figure 3

Treatment of RASMC with FoxO inhibitor drug, AS1842856 shows concentration-dependent decrease in canonical FoxO targets with compensatory increase in FoxO3 and FoxO4 mRNA expression.

qRT-PCR from RASMC treated with FoxO inhibitor. Response for 48-hour FoxO inhibitor treatment measuring A) FoxO1, B) FoxO3, C) FoxO4, D) Gadd45 α , or E) G6Pase mRNA expression. n=3 for all samples. One-way ANOVA test was used for determination of significance. * p<0.05, ** p<0.01, *** p<0.001, **** p<0.0001. Error bars represent s.d.

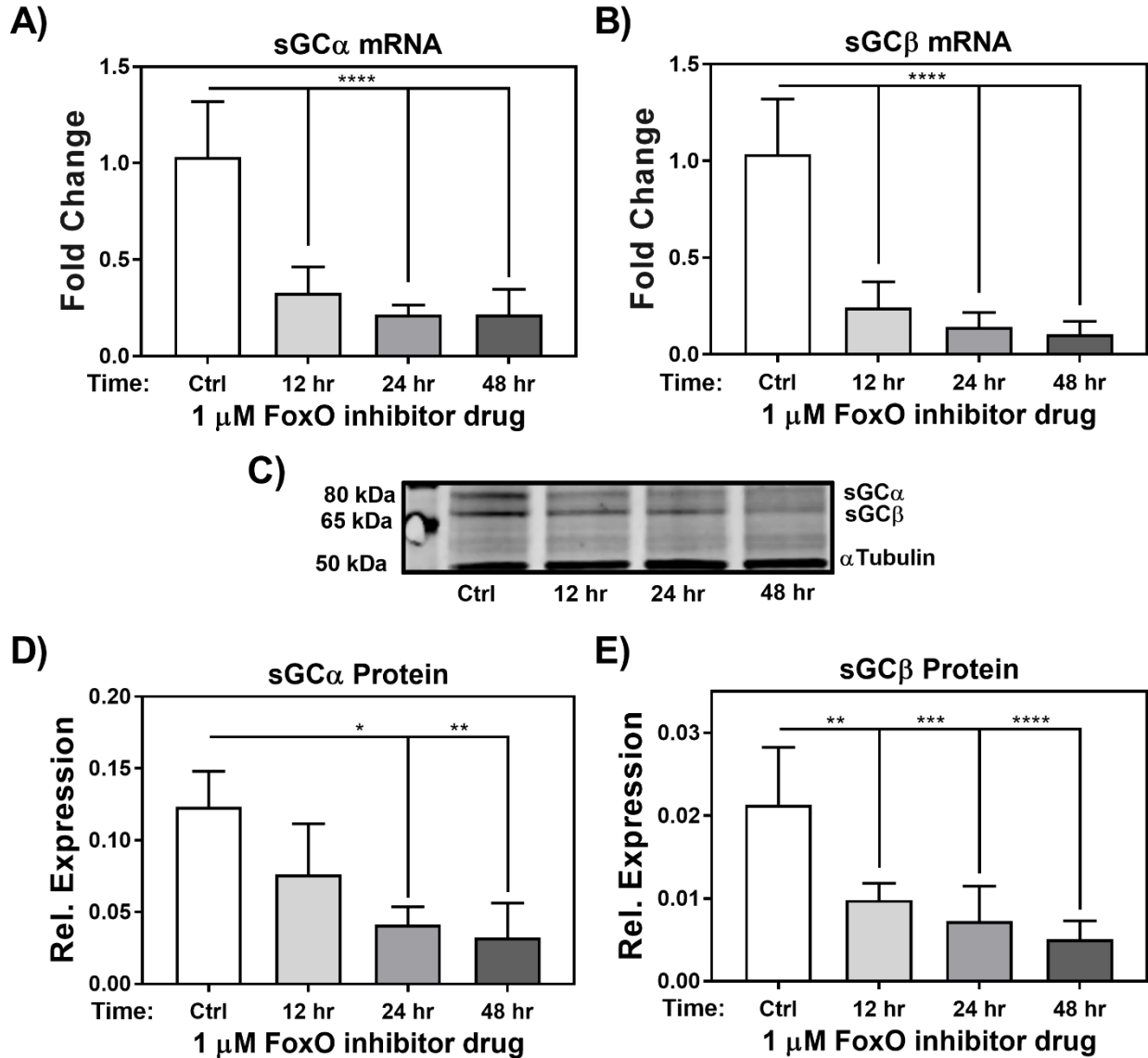


Figure 4

Treatment of RASMNC with FoxO inhibitor drug, AS1842856 shows decrease in sGC mRNA and protein expression occurs rapidly.

qRT-PCR of 1 μ M FoxO inhibitor treatment for 12, 24, and 48 hours on A) sGC α mRNA expression or B) sGC β mRNA expression. C) Western blot and quantification of 1 μ M FoxO inhibitor treatment for 12, 24, and 48 hours on D) sGC α protein expression and E) sGC β protein expression. n=3 for all samples. One-way ANOVA test was used for determination of significance. * p<0.05, ** p<0.01, *** p<0.001, **** p<0.0001. Error bars represent s.d.

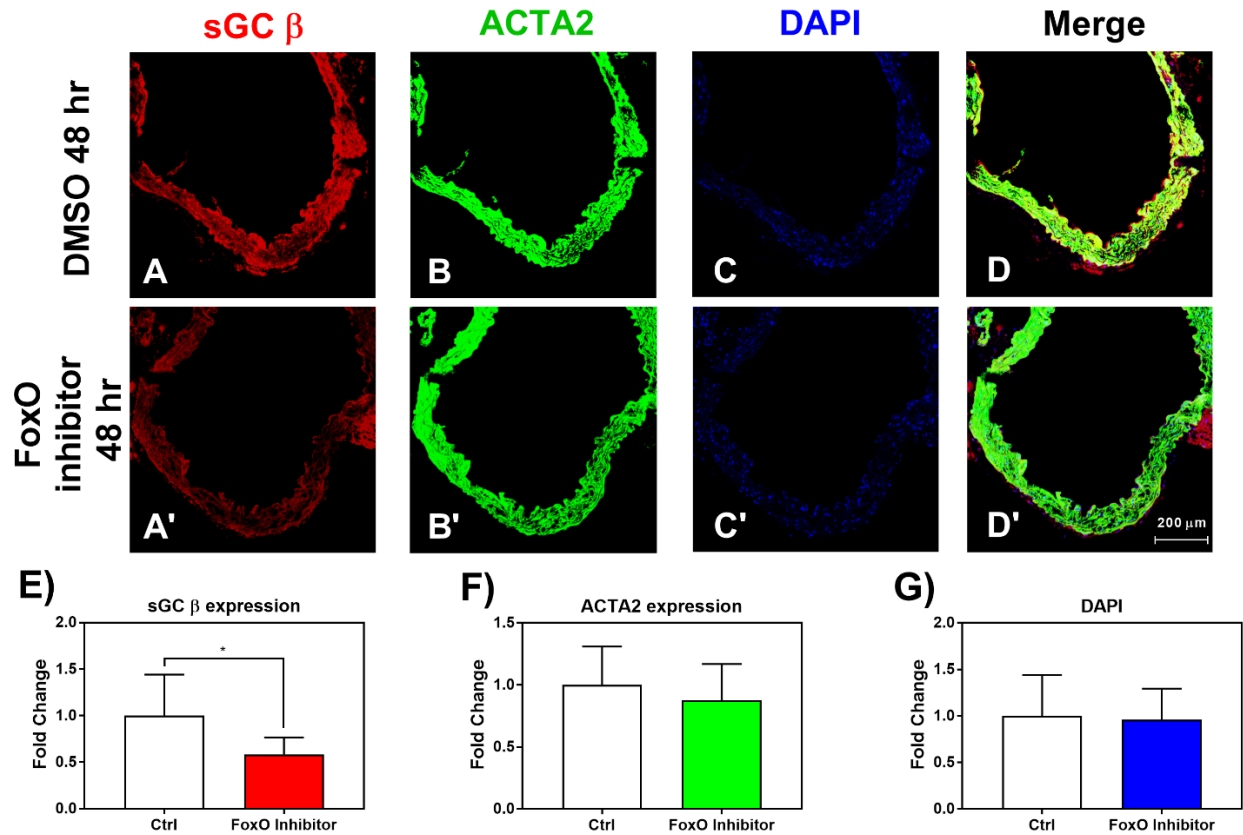


Figure 5

sGC expression in *ex-vivo* murine aortas treated with FoxO inhibitor is decreased.

Representative staining for *ex vivo* murine aortas treated with 10 μM FoxO inhibitor for 48 hours showing A and A') sGC β protein, B and B') Smooth muscle α-actin (ACTA2), C and C') DAPI, and D and D') merged channels. Quantification of immunostaining for E) sGC β protein, F) ACTA2 protein, or G) DAPI staining. n=3 animals. Student's unpaired t-test was used for determination of significance. * p<0.05. Error bars represent s.d.

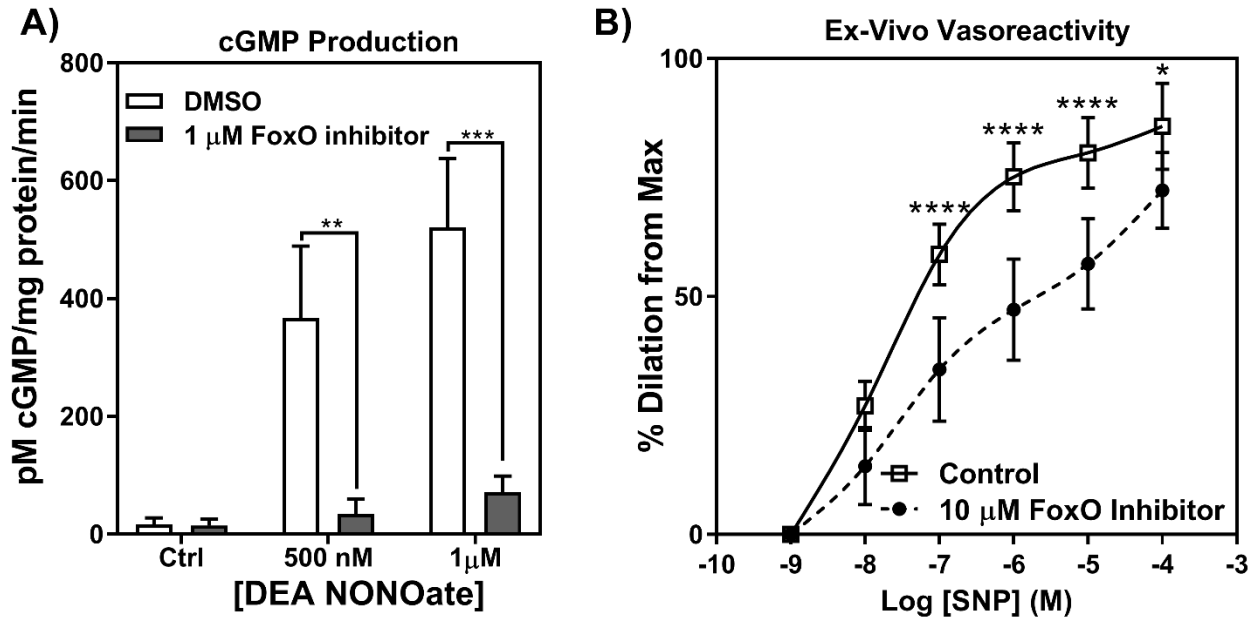


Figure 6

NO-dependent signaling in RASMC and murine aortas is blunted after treatment with AS1842856.

A) cGMP produced by cultured RASMC treated with AS1842856 and stimulated with NO donor DEA NONOate, n=4. Student's unpaired t-test was used for determination of significance. B) *Ex vivo* murine aortic vessels treated with 10 μ M FoxO inhibitor or DMSO for 48 hours and dilated using the NO donor, sodium nitroprusside (SNP), n=5. Two-way ANOVA was used to determine significance. * p<0.05, ** p<0.01, *** p<0.001, **** p<0.0001. Error bars represent s.d.

Table 1: qRT-PCR Primers

| Primer | Sequence |
|-----------------------------|---------------------------------|
| Rat sGC α Forward | CTC CCG TGA CCG CAT CAT |
| Rat sGC α Reverse | CCG GTG TTG ATG TTG ACT GA |
| Rat sGC β Forward | AAT TAC GGT CCC GAG GTG TG |
| Rat sGC β Reverse | GCA GCA GCC ACC AAG TCA TA |
| Rat FoxO1 Forward | CAC CTT GCT ATT CGT TTG C |
| Rat FoxO1 Reverse | CTG TCC TGA AGT GTC TGC |
| Rat FoxO3 Forward | CGG CTC ACT TTG TCC CAG AT |
| Rat FoxO3 Reverse | TCT TGC CAG TCC CTT CGT TC |
| Rat FoxO4 Forward | AGG CTC CTA CAC TTC TGT TAC TGG |
| Rat FoxO4 Reverse | CTT CAG TAG GAG ATG CAA GCA CAG |
| Rat Gadd45 α Forward | GCA GAG CAG AAG ATC GAA AG |
| Rat Gadd45 α Reverse | AAC AGA AAG CAC GAA TGA GG |
| Rat G6Pase Forward | GGC TCA CTT TCC CCA TCA GG |
| Rat G6Pase Reverse | ATC CAA GTC CGA AAC CAA ACA G |
| Mammalian 18S Forward | ACG GAC AGG ATT GAC AGA TTG |
| Mammalian 18S Reverse | TTA GCA TGC CAG AGT CTC GTT |
| Rat ADCY1 Forward | GTC GGA TGG ATA GCA CTG GG |
| Rat ADCY1 Reverse | TTG ACG CTG ACT TTG CCT CT |
| Rat ADCY3 Forward | AGC TCT GAG CGT GGC TAT TC |
| Rat ADCY3 Reverse | AGG CAG CTT CAT CCC ACA TC |
| Rat GUCY2A Forward | ACT CCT GGG GCA AGC G |

Table 1 Continued

| | |
|--------------------|-----------------------------|
| Rat GUCY2A Reverse | AAA TTG GGA GCG TCC GAG AG |
| Rat GUCY2B Forward | TCT CCT CGA CCA CCA AGG AT |
| Rat GUCY2B Reverse | GAT AAG GCA GGG GGA TTG TGT |

Table 1 Abbreviations:

sGC - soluble guanylate cyclase, FoxO1 - forkhead box transcription factor class O1, FoxO3 - forkhead box class O3, FoxO4 - forkhead box class O4, Gadd45 α - growth arrest and DNA damage 45 α , G6Pase - glucose-6-phosphatase, 18S - 18S small ribosomal subunit, ADCY1 – adenylate cyclase 1, ADCY3 – adenylate cyclase 3, GUCY2A – guanylyl cyclase receptor 2A (aka [atrial] natriuretic peptide receptor 1), and GUCY2B – guanylyl cyclase receptor 2B (aka [brain] natriuretic peptide receptor 2).

Table 2: Antibodies

| Antibody | Species | Application | Concentration | Company | Cat. Number |
|--|----------------|--------------------|----------------------|-------------------------------|--------------------|
| sGC β | rabbit | WB, IHC | 1:1000, 1:250 | Cayman | 160897 |
| sGC α | rabbit | WB | 1:500 | Sigma | G4280 |
| α -tubulin | mouse | WB | 1:10000 | Sigma | T6074 |
| Rabbit Alexafluor 594 | donkey | IHC | 1:250 | Life Technologies | A21207 |
| Goat Alexafluor 647 | donkey | IHC | 1:250 | Life Technologies | A21447 |
| Rat Alexafluor 647 | donkey | IHC | 1:250 | Jackson Immuno Research | 712-605-153 |
| ACTA2 conjugated Alexafluor 488 | mouse | IHC | 1:250 | Sigma | F3777 |

Table 2 Legend:

sGC denotes soluble guanylate cyclase, ACTA2 denotes smooth muscle α -actin, WB denotes western blot, and IHC denotes immunohistochemistry.

Table 3: Map of FoxO Binding on Human GUCY1A3 Region

GUCY1A3 Promoter FoxO Binding (Table 3 Continued)

| Transcription Factor(s) | Location start from TSS | Location end from TS | Length (bp) | DNA Strand |
|-------------------------|-------------------------|----------------------|-------------|------------|
| FoxO1:PDEF | -9815 | -9803 | 13 | + |
| GCMa:FoxO1 | -9588 | -9575 | 14 | + |
| FoxO1 | -9177 | -9172 | 6 | - |
| FoxO1 | -9162 | -9149 | 14 | + |
| FoxO1 | -9162 | -9149 | 14 | - |
| FoxO1 | -9142 | -9137 | 6 | - |
| FoxO1 | -8915 | -8910 | 6 | - |
| FoxO1 | -8792 | -8787 | 6 | - |
| ERF:FoxO1 | -8530 | -8517 | 14 | - |
| FoxO1:Elf-1 | -8508 | -8495 | 14 | - |
| FoxO1:HoxA10 | -8458 | -8445 | 14 | - |
| FoxO1:Elf-1 | -8429 | -8416 | 14 | - |
| FoxO1 | -8345 | -8332 | 14 | - |
| FoxO1:Elf-1 | -8336 | -8323 | 14 | - |
| FoxO1 | -8209 | -8204 | 6 | - |
| FoxO1 | -7857 | -7844 | 14 | + |
| FoxO1 | -7854 | -7849 | 6 | - |
| FoxO1 | -7730 | -7725 | 6 | - |
| FoxO3 | -7479 | -7468 | 12 | + |
| FoxO1 | -7164 | -7151 | 14 | - |
| FoxO3 | -7164 | -7151 | 14 | + |
| FoxO1:HoxA10 | -7164 | -7151 | 14 | + |
| FoxO3 | -7164 | -7151 | 14 | - |
| FoxO1:PDEF | -7066 | -7054 | 13 | - |
| FoxO1:HoxA10 | -6659 | -6646 | 14 | - |
| FoxO1:HoxA10 | -6643 | -6630 | 14 | - |
| FoxO4 | -6545 | -6535 | 11 | - |
| FoxO3 | -6545 | -6534 | 12 | - |
| FoxO4 | -6545 | -6532 | 14 | + |
| FoxO3 | -6545 | -6532 | 14 | + |
| FoxO1 | -6545 | -6532 | 14 | + |
| FoxO1 | -6544 | -6534 | 11 | + |
| FoxO1 | -6542 | -6537 | 6 | - |
| FoxO3 | -6542 | -6535 | 8 | - |
| FoxO1 | -6542 | -6535 | 8 | - |
| FoxO6 | -6541 | -6535 | 7 | - |
| FoxO3 | -6541 | -6535 | 7 | - |
| GCMa:FoxO1 | -5953 | -5940 | 14 | + |
| GCMa:FoxO1 | -5749 | -5736 | 14 | - |

GUCY1A3 Promoter FoxO Binding (Table 3 Continued)

| Transcription Factor(s) | Location start from TSS | Location end from TS | Length (bp) | DNA Strand |
|-------------------------|-------------------------|----------------------|-------------|------------|
| FoxO1 | -5522 | -5517 | 6 | - |
| FoxO1 | -5362 | -5355 | 8 | - |
| FoxO1 | -5360 | -5355 | 6 | + |
| FoxO1:Elf-1 | -5352 | -5339 | 14 | + |
| FoxO1:Elf-1 | -5092 | -5079 | 14 | - |
| GCMa:FoxO1 | -5059 | -5046 | 14 | - |
| FoxO1:HoxA10 | -5036 | -5023 | 14 | + |
| FoxO1 | -4995 | -4990 | 6 | - |
| FoxO1:Elf-1 | -4680 | -4667 | 14 | - |
| FoxO1 | -3416 | -3411 | 6 | - |
| FoxO1:ETV7 | -2794 | -2774 | 21 | - |
| FoxO1 | -2587 | -2582 | 6 | + |
| FoxO1 | -2450 | -2445 | 6 | + |
| FoxO1:Elf-1 | -2135 | -2122 | 14 | - |
| FoxO1:HoxA10 | -1941 | -1928 | 14 | - |
| FoxO1 | -1905 | -1898 | 8 | - |
| FoxO1 | -1905 | -1897 | 9 | + |
| FoxO1 | -1903 | -1898 | 6 | + |
| FoxO1 | -1812 | -1799 | 14 | + |
| FoxO3 | -1807 | -1794 | 14 | + |
| FoxO3 | -1807 | -1794 | 14 | + |
| FoxO1 | -1807 | -1794 | 14 | + |
| FoxO3 | -1807 | -1794 | 14 | - |
| FoxO1 | -1807 | -1794 | 14 | - |
| FoxO1:PDEF | -1549 | -1537 | 13 | - |
| GCMa:FoxO1 | -1497 | -1484 | 14 | - |
| FoxO1 | -1277 | -1272 | 6 | + |
| GCMa:FoxO1 | -1253 | -1240 | 14 | + |
| FoxO1 | -1078 | -1073 | 6 | - |
| FoxO1 | -1000 | -993 | 8 | - |
| FoxO1:HoxA10 | -1000 | -987 | 14 | + |
| FoxO1:ETV7 | -1000 | -980 | 21 | + |
| FoxO1 | -998 | -993 | 6 | + |
| FoxO1 | -124 | -111 | 14 | + |
| FoxO1 | -113 | -105 | 9 | - |
| FoxO1 | -112 | -107 | 6 | - |
| FoxO1 | -112 | -105 | 8 | + |
| FoxO1:ETV7 | -81 | -61 | 21 | - |
| FoxO1:ETV7 | 38 | 58 | 21 | + |
| FoxO1:Elf-1 | 96 | 109 | 14 | - |

GUCY1A3 Promoter FoxO Binding (Table 3 Continued)

| Transcription Factor(s) | Location start from TSS | Location end from TS | Length (bp) | DNA Strand |
|-------------------------|-------------------------|----------------------|-------------|------------|
| FoxO1:Elf-1 | 326 | 339 | 14 | + |
| E2F-3:FoxO6 | 643 | 659 | 17 | + |
| FoxO1:PDEF | 667 | 679 | 13 | - |
| FoxO1:ETV7 | 1222 | 1242 | 21 | + |
| E2F-3:FoxO6 | 1313 | 1329 | 17 | - |
| FoxO1:Elf-1 | 1363 | 1376 | 14 | - |
| FoxO1:ETV7 | 1854 | 1874 | 21 | - |
| FoxO1:Elk-1 | 1861 | 1874 | 14 | - |
| FoxO1:Net | 1861 | 1874 | 14 | - |
| ERF:FoxO1 | 1861 | 1874 | 14 | - |
| GCMa:FoxO1 | 1870 | 1883 | 14 | + |
| FoxO1 | 2157 | 2162 | 6 | + |
| FoxO1:ETV7 | 2263 | 2283 | 21 | + |
| FoxO1 | 2339 | 2344 | 6 | + |
| FoxO1:HoxA10 | 2720 | 2733 | 14 | + |
| FoxO1 | 2804 | 2810 | 7 | - |
| FoxO1 | 2804 | 2811 | 8 | + |
| FoxO1 | 2805 | 2810 | 6 | + |
| FoxO1 | 2918 | 2923 | 6 | + |
| FoxO1:ETV7 | 3193 | 3213 | 21 | + |
| FoxO1 | 3473 | 3486 | 14 | + |
| FoxO1 | 3473 | 3486 | 14 | - |
| FoxO3 | 3473 | 3486 | 14 | - |
| FoxO1 | 3501 | 3514 | 14 | - |
| FoxO3 | 3537 | 3548 | 12 | + |
| FoxO1 | 3538 | 3545 | 8 | - |
| FoxO1 | 3538 | 3546 | 9 | + |
| FoxO1 | 3540 | 3545 | 6 | + |
| FoxO1 | 3618 | 3623 | 6 | - |
| FoxO1 | 4036 | 4041 | 6 | + |
| FoxO1 | 4052 | 4057 | 6 | + |
| FoxO1:Elk-1 | 4135 | 4148 | 14 | + |
| FoxO1:Net | 4135 | 4148 | 14 | + |
| E2F-3:FoxO6 | 4145 | 4161 | 17 | + |
| FoxO1:HoxA10 | 4391 | 4404 | 14 | - |
| FoxO4 | 4424 | 4434 | 11 | - |
| FoxO3 | 4424 | 4435 | 12 | - |
| FoxO1 | 4426 | 4435 | 10 | - |
| FoxO1 | 4427 | 4432 | 6 | - |
| FoxO1:Elk-1 | 4650 | 4663 | 14 | - |

GUCY1A3 Promoter FoxO Binding (Table 3 Continued)

| Transcription Factor(s) | Location start from TSS | Location end from TS | Length (bp) | DNA Strand |
|-------------------------|-------------------------|----------------------|-------------|------------|
| ERF:FoxO1 | 4650 | 4663 | 14 | - |
| FoxO1:Net | 4650 | 4663 | 14 | - |
| GCMa:FoxO1 | 4830 | 4843 | 14 | - |
| FoxO1:PDEF | 4888 | 4900 | 13 | + |
| FoxO1 | 4923 | 4929 | 7 | - |
| FoxO1:Elf-1 | 5104 | 5117 | 14 | - |
| FoxO1:Elf-1 | 5183 | 5196 | 14 | - |
| FoxO1:PDEF | 5563 | 5575 | 13 | + |
| FoxO1:HoxA10 | 5574 | 5587 | 14 | + |
| FoxO1 | 5853 | 5860 | 8 | - |
| FoxO1 | 5853 | 5861 | 9 | + |
| FoxO1 | 5855 | 5860 | 6 | + |
| FoxO1 | 6070 | 6076 | 7 | - |
| FoxO1 | 6267 | 6272 | 6 | - |
| FoxO1 | 6291 | 6296 | 6 | + |
| FoxO1 | 6296 | 6301 | 6 | + |
| FoxO1:Net | 6313 | 6326 | 14 | - |
| ERF:FoxO1 | 6313 | 6326 | 14 | - |
| FoxO1:ETV7 | 6423 | 6443 | 21 | + |
| FoxO1:ETV7 | 6428 | 6448 | 21 | - |
| E2F-3:FoxO6 | 6581 | 6598 | 18 | + |
| FoxO1 | 6802 | 6807 | 6 | + |
| FoxO1:PDEF | 6809 | 6821 | 13 | + |
| FoxO1:HoxA10 | 7167 | 7180 | 14 | - |
| E2F-3:FoxO6 | 7512 | 7528 | 17 | - |
| FoxO1 | 7668 | 7673 | 6 | + |
| FoxO1 | 7676 | 7681 | 6 | + |
| FoxO1 | 7745 | 7758 | 14 | + |
| E2F-3:FoxO6 | 8396 | 8412 | 17 | - |
| GCMa:FoxO1 | 8670 | 8683 | 14 | + |
| FoxO1 | 8754 | 8767 | 14 | - |
| FoxO1 | 8754 | 8767 | 14 | - |
| FoxO3 | 8754 | 8767 | 14 | + |
| FoxO1 | 8790 | 8795 | 6 | + |
| FoxO1 | 8969 | 8974 | 6 | - |
| FoxO1:HoxA10 | 9382 | 9395 | 14 | - |
| FoxO1:Elf-1 | 9454 | 9467 | 14 | + |
| FoxO1:Elf-1 | 9542 | 9555 | 14 | + |

Table 3 Legend

E2F-3 denotes E2F transcription factor 3, Elf-1 denotes erythroblast transformation-specific-like factor 1, Elk1 denotes erythroblast transformation-specific-like gene 1, ERF denotes erythroblast transformation-specific domain-containing factor, Erm denotes erythroblast transformation-specific related molecule, ETV7 denotes erythroblast transformation variant 7, FoxO1 denotes forkhead box class O1, FoxO3 denotes forkhead box class O3, FoxO4 denotes forkhead box class O4, FoxO6 denotes forkhead box class O6, GCMa denotes glial cell missing motif, HoxA10 denotes homeobox protein A10, Net denotes erythroblast containing transformation-specific repressor protein, and PDEF denotes prostate-derived erythrocyte transformation-specific factor.

Table 4: Map of FoxO Binding on Human GUCY1B3 Region

GUCY1B3 Promoter FoxO Binding (Table 4 Continued)

| Transcription Factor(s) | Location start from TSS | Location end from TSS | Length (bp) | DNA Strand |
|-------------------------|-------------------------|-----------------------|-------------|------------|
| FoxO1 | -9807 | -9802 | 6 | - |
| FoxO1 | -9807 | -9800 | 8 | + |
| FoxO1 | -8902 | -8897 | 6 | + |
| Erm:FoxO1 | -7513 | -7501 | 13 | + |
| FoxO1:PEA3 | -7513 | -7500 | 14 | + |
| FoxO1 | -6347 | -6339 | 9 | - |
| FoxO1 | -6346 | -6341 | 6 | - |
| FoxO1 | -6346 | -6339 | 8 | + |
| FoxO1 | -6340 | -6335 | 6 | - |
| FoxO1 | -6197 | -6192 | 6 | - |
| FoxO1 | -5912 | -5899 | 14 | - |
| FoxO3 | -5910 | -5903 | 8 | + |
| FoxO1 | -5910 | -5900 | 11 | - |
| FoxO6 | -5909 | -5903 | 7 | + |
| FoxO4 | -5909 | -5903 | 7 | + |
| FoxO3 | -5909 | -5902 | 8 | + |
| FoxO1 | -5909 | -5902 | 8 | + |
| FoxO1 | -5659 | -5654 | 6 | + |
| FoxO1:HoxA10 | -5330 | -5323 | 8 | - |
| FoxO1 | -5330 | -5317 | 14 | + |
| FoxO1:PEA3 | -5328 | -5323 | 6 | + |
| FoxO1 | -5135 | -5122 | 14 | + |
| FoxO1 | -5066 | -5058 | 9 | - |
| FoxO1 | -5065 | -5060 | 6 | - |
| FoxO1 | -5065 | -5058 | 8 | + |
| FoxO1:HoxB13 | -4726 | -4710 | 17 | + |
| FoxO3 | -4536 | -4525 | 12 | + |
| FoxO1 | -4533 | -4528 | 6 | + |
| FoxO3 | -4305 | -4294 | 12 | - |
| FoxO1 | -4302 | -4297 | 6 | - |
| FoxO3 | -4246 | -4235 | 12 | - |
| FoxO1 | -4244 | -4235 | 10 | - |
| FoxO1 | -4243 | -4238 | 6 | - |
| FoxO1 | -3617 | -3612 | 6 | + |
| FoxO1 | -2878 | -2873 | 6 | + |
| FoxO1 | -2763 | -2756 | 8 | - |
| FoxO1 | -2761 | -2756 | 6 | + |
| FoxO1 | -1347 | -1342 | 6 | - |
| FoxO3 | -1276 | -1265 | 12 | - |

GUCY1B3 Promoter FoxO Binding (Table 4 Continued)

| Transcription Factor(s) | Location start from TSS | Location end from TSS | Length (bp) | DNA Strand |
|-------------------------|-------------------------|-----------------------|-------------|------------|
| FoxO1 | -1273 | -1268 | 6 | - |
| FoxO1 | -1266 | -1261 | 6 | + |
| FoxO1 | -1187 | -1182 | 6 | - |
| FoxO1 | -1182 | -1177 | 6 | - |
| FoxO1 | -1178 | -1173 | 6 | - |
| FoxO1 | -1100 | -1095 | 6 | - |
| FoxO1:HoxA10 | -945 | -932 | 14 | + |
| ERF:FoxO1 | -923 | -910 | 14 | - |
| FoxO1:PEA3 | -923 | -910 | 14 | - |
| FoxO1:ETV1 | 466 | 477 | 12 | + |
| FoxO1:ETV1 | 1416 | 1427 | 12 | + |
| FoxO1 | 2087 | 2092 | 6 | + |
| FoxO1 | 2241 | 2246 | 6 | - |
| FoxO4 | 3467 | 3477 | 11 | - |
| FoxO3 | 3467 | 3478 | 12 | - |
| FoxO3 | 3467 | 3480 | 14 | + |
| FoxO3 | 3468 | 3480 | 13 | - |
| FoxO1 | 3469 | 3478 | 10 | - |
| FoxO1 | 3470 | 3475 | 6 | - |
| FoxO1 | 3696 | 3701 | 6 | + |
| FoxO1 | 4677 | 4682 | 6 | + |
| FoxO1 | 4681 | 4686 | 6 | + |
| FoxO1 | 5432 | 5440 | 9 | - |
| FoxO1 | 5433 | 5438 | 6 | - |
| FoxO1 | 5433 | 5440 | 8 | + |
| FoxO1 | 5907 | 5912 | 6 | - |
| FoxO1 | 5960 | 5965 | 6 | + |
| FoxO1 | 5964 | 5969 | 6 | + |
| FoxO1 | 6469 | 6474 | 6 | + |
| FoxO1:HoxA10 | 7151 | 7164 | 14 | + |
| FoxO3 | 7303 | 7314 | 12 | - |
| FoxO3 | 7303 | 7316 | 14 | + |
| FoxO3 | 7304 | 7316 | 13 | - |
| FoxO1 | 7305 | 7314 | 10 | - |
| FoxO1 | 7306 | 7311 | 6 | - |
| FoxO1 | 7708 | 7721 | 14 | - |
| FoxO3 | 7710 | 7717 | 8 | + |
| FoxO1 | 7710 | 7720 | 11 | - |
| FoxO4 | 7711 | 7717 | 7 | + |
| FoxO6 | 7711 | 7717 | 7 | + |

GUCY1B3 Promoter FoxO Binding (Table 4 Continued)

| Transcription Factor(s) | Location start from TSS | Location end from TSS | Length (bp) | DNA Strand |
|-------------------------|-------------------------|-----------------------|-------------|------------|
| FoxO1 | 7711 | 7718 | 8 | + |
| FoxO1 | 9377 | 9382 | 6 | - |
| FoxO1 | 9428 | 9441 | 14 | + |
| FoxO1 | 9429 | 9439 | 11 | + |
| FoxO1 | 9431 | 9437 | 7 | - |
| FoxO6 | 9432 | 9438 | 7 | - |
| FoxO3 | 9432 | 9439 | 8 | - |
| FoxO1:HoxA10 | 9861 | 9874 | 14 | - |
| FoxO3 | 9864 | 9875 | 12 | - |
| FoxO1 | 9866 | 9875 | 10 | - |
| FoxO1 | 9867 | 9872 | 6 | - |
| FoxO1 | 9915 | 9920 | 6 | - |

Table 4 Legend:

ERF denotes erythroblast transformation-specific domain-containing factor, Erm denotes erythroblast transformation-specific related molecule, ETV1 denotes erythroblast transformation variant 1, FoxO1 denotes forkhead box class O1, FoxO3 denotes forkhead box class O3, FoxO4 denotes forkhead box class O4, FoxO6 denotes forkhead box class O6, HoxA10 denotes homeobox protein A10, HoxB13 denotes homeobox protein B13, and PEA3 denotes erythrocyte transformation-like factor PEA3.

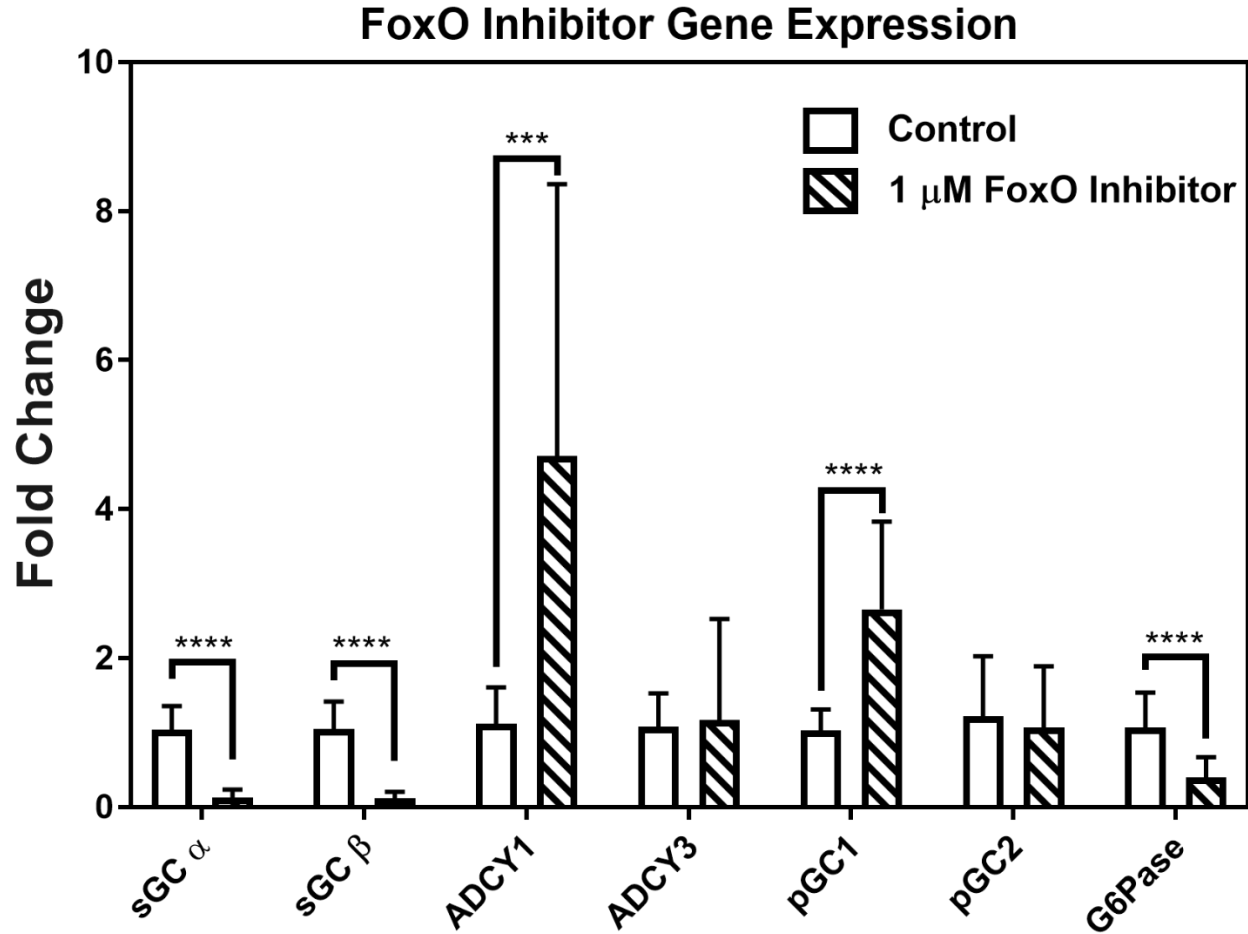


Figure 7

Treatment of RASMC with FoxO inhibitor drug, AS1842856 shows changes in gene expression with decrease in sGC mRNA.

qRT-PCR of 1 μ M FoxO inhibitor treatment measuring the gene expression of cyclic nucleotide producers or classical FoxO target, G6Pase. n=3 for all samples. Student's unpaired t-test was used for determination of significance. * p<0.05, ** p<0.01, *** p<0.001, **** p<0.0001. Error bars represent s.d.

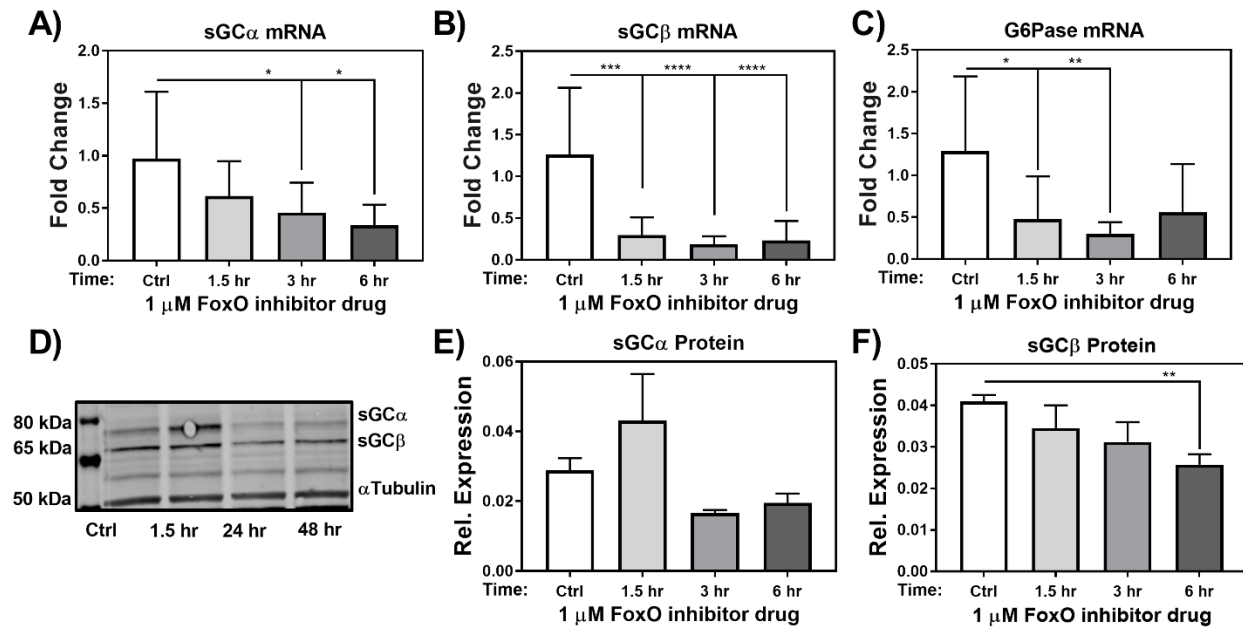


Figure 8

Treatment of RASMC with FoxO inhibitor drug, AS1842856 shows rapid decrease in sGC mRNA followed by loss of protein expression.

qRT-PCR of 1 μ M FoxO inhibitor treatment for 1.5, 3, and 6 hours on A) sGC α mRNA expression or B) sGC β mRNA expression. C) Western blot and quantification of 1 μ M FoxO inhibitor treatment for 1.5, 3, and 6 hours on D) sGC α protein expression and E) sGC β protein expression. n=3 for all samples. One-way analysis of variance test was used for determination of significance. * p<0.05, ** p<0.01, *** p<0.001, **** p<0.0001. Error bars represent s.d.

3.0 Angiotensin II Augments Renovascular sGC Expression Via an AT₁R - FoxO Transcription Factor Signaling Axis

Joseph C. Galley, B.A.,^{1,2} Scott A. Hahn, M.S.,¹ Megan P. Miller, B.S.,¹ Brittany G. Durgin, Ph.D.,¹ Edwin K. Jackson Ph.D.,² Sean D. Stocker, Ph.D.³ and Adam C. Straub, Ph.D.^{1,2}

¹Heart, Lung, Blood and Vascular Medicine Institute, University of Pittsburgh, Pittsburgh, Pennsylvania;

²Department of Pharmacology and Chemical Biology, University of Pittsburgh, Pittsburgh, Pennsylvania;

³Department of Medicine, Renal-Electrolyte Division, University of Pittsburgh, Pittsburgh, Pennsylvania

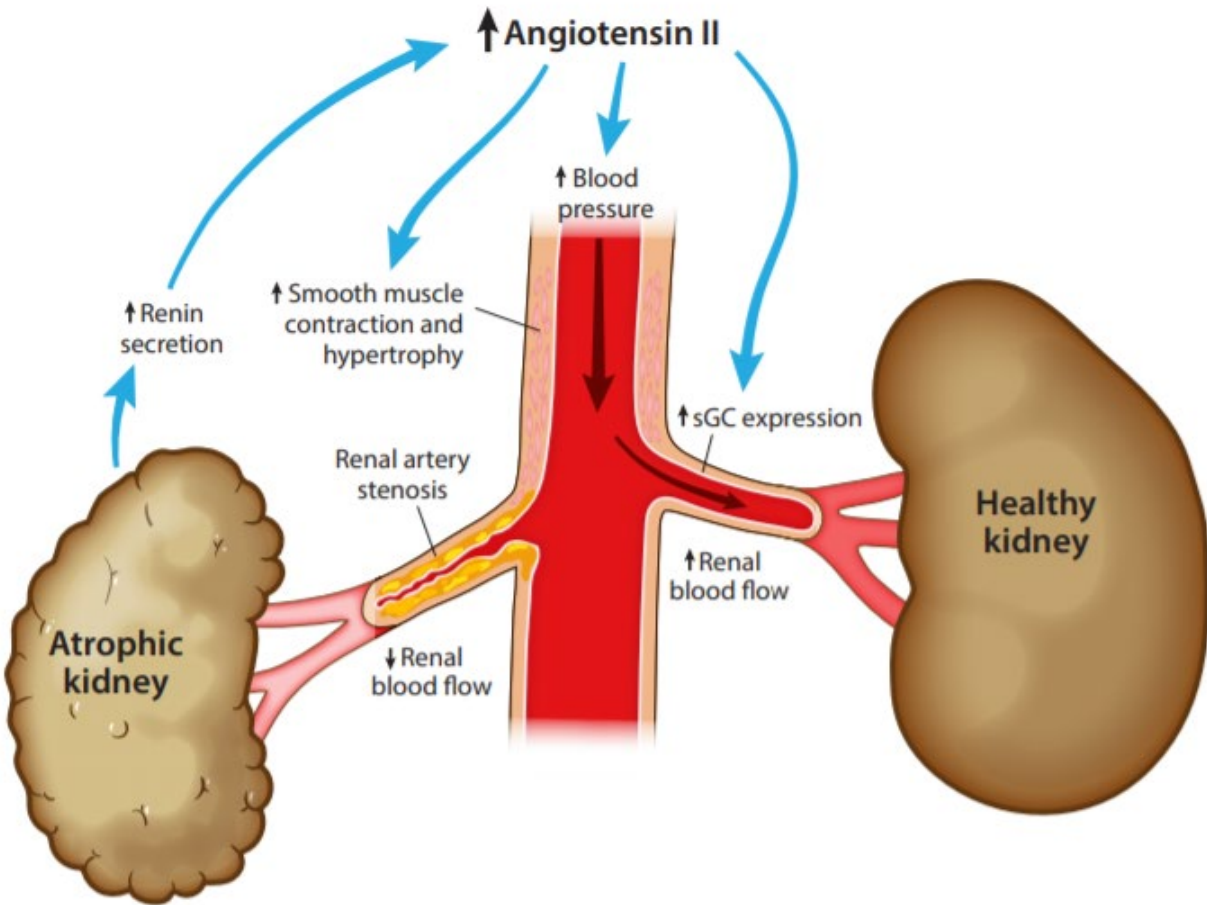
Copyright British Journal of Pharmacology, 2021

3.1 Summary:

Background and Purpose: Reduced renal blood flow triggers activation of the renin-angiotensin-aldosterone system (RAAS) leading to renovascular hypertension. Renal vascular smooth muscle expression of the nitric oxide (NO) receptor, soluble guanylyl cyclase (sGC), modulates the vasodilatory response needed to control renal vascular tone and blood flow. Here, we tested if angiotensin II (Ang II) impacts sGC expression via an Ang II type 1 receptor (AT₁R)-forkhead box subclass O (FoxO) transcription factor dependent mechanism.

Experimental Approach: Using a murine two-kidney-one-clip (2K1C) renovascular hypertension model, we measured renal artery vasodilatory function and sGC expression. Additionally, we conducted cell culture studies using rat renal pre-glomerular smooth muscle

cells (RPGSMCs) to test the *in vitro* mechanistic effects of Ang II treatment on sGC expression and downstream function. **Key Results:** Contralateral, unclipped renal arteries in 2K1C mice showed increased NO-dependent vasorelaxation compared to sham control mice. Immunofluorescence studies revealed increased sGC protein expression in 2K1C contralateral renal arteries over sham controls. RPGSMCs treated with Ang II caused a significant upregulation of sGC mRNA and protein expression as well as downstream sGC-dependent signaling. Ang II signaling effects on sGC expression occurred through an AT₁R and FoxO transcription factor-dependent mechanism at both the mRNA and protein expression levels. **Conclusion and Implications:** Renal artery smooth muscle, *in vivo* and *in vitro*, upregulate expression of sGC following RAAS activity. In both cases, upregulation of sGC leads to elevated downstream cGMP signaling, suggesting a previously unrecognized protective mechanism to improve renal blood flow in the uninjured contralateral renal artery.



3.1.1 Graphical Summary:

Renal artery stenosis causes elevated circulating Angiotensin II. This, in turn, leads to contraction and hypertrophy of smooth muscle and elevated blood pressure. Additionally, soluble guanylyl cyclase (sGC) expression and cGMP in the non-stenotic renal artery increases allowing for increased blood flow to the healthy kidney.

3.2 Introduction:

Renovascular hypertensive patients constitute 24.2% of all patients with drug resistant hypertension,¹⁷⁹ a condition characterized by uncontrolled hypertension despite treatment with three or more adequately dosed anti-hypertensive therapies.¹⁸⁰ While the prevalence in the general population is low (1-2%),¹⁸¹ renovascular hypertension is more common in elderly patients over age 65 (6.8%) and is present in nearly 40% of individuals with established peripheral or coronary artery disease.¹⁸²⁻¹⁸³ Approximately 90% of renovascular hypertension stems from atherosclerotic renal artery stenosis (ARAS).¹⁸⁴⁻¹⁸⁵ ARAS leads to obstruction of renal artery blood flow, resulting in renin-angiotensin-aldosterone-system (RAAS) activation and subsequent elevation of circulating blood plasma angiotensin II (Ang II).¹⁸⁶ In response, the non-stenosed renal artery is subjected to increased blood flow leading to augmented sodium and water excretion by the kidney. This process, known as pressure natriuresis, helps to mitigate increased fluid retention, volume overload, and systemic blood pressure.¹⁸⁷

A main contributor to pressure natriuresis is endothelial-derived nitric oxide (NO), which has been shown to play a critical role in the dilation of the renal vasculature.¹⁸⁸⁻¹⁹¹ NO diffuses to vascular smooth muscle cells (VSMCs) where it binds its cognate receptor, soluble guanylyl cyclase (sGC), which produces cGMP to elicit vasorelaxation.^{23,149,192} Of clinical importance, sGC modulating compounds, which enhance cGMP production, have been approved for treatment of pathologies such as pulmonary arterial hypertension, chronic thromboembolic pulmonary hypertension, and heart failure with reduced ejection fraction,⁵⁸⁻⁶⁰ and many are currently under investigation for treatment of renal and cardiovascular diseases.¹⁹³ In addition, we have recently shown that basal sGC expression is regulated by the forkhead box subclass O (FoxO) transcription factors in aortic VSMCs.¹⁴⁷

Based on this evidence, we hypothesized that renal artery smooth muscle responds to elevated RAAS signaling with amplified sGC-mediated production of cGMP. In this study, we used a two-kidney-one-clip (2K1C) hypertension model, wherein blood flow to one renal artery is reduced,¹⁸⁶ as a model of RAAS activation and renal hypertension. We find that renal smooth muscle responds to increased levels of Ang II by increasing the expression of sGC. This increased sGC expression occurs in an Ang II type 1 receptor (AT₁R) and FoxO transcription factor-dependent manner. Consequently, this results in enhanced downstream cGMP signaling and increased smooth muscle relaxation. These studies are the first to show that exposure of renal smooth muscle to elevated Ang II results in a protective mechanism whereby sGC expression is increased, leading to elevated cGMP production and vasorelaxation.

3.3 Methods:

Statement on Ethical Use of Animals:

Rodent models were used in this study, as they have physiological mechanisms similar to the mechanisms of human blood pressure control. Mechanistic studies to understand the changes in multi-organ signaling and physiology were then studied in more detail at the molecular level in cell culture studies. These two main approaches complement one another and reduce the number of animals used. All animals were used in ethical compliance with the University of Pittsburgh's Institutional Animal Care and Use Committee (Protocol #IS00016317 and IS00015180). For all experiments, *a priori* power analyses were performed to determine the number of animals necessary to determine whether differences observed were significant. For *ex*

vivo procedures, blinding occurred post tissue harvesting and kidney removal so that the identity of clip vs. sham groups were unknown for myography to avoid bias.

2K1C Renal Stenosis Model:

Renovascular hypertension through a 2K1C model was produced as described previously.¹⁹⁴⁻¹⁹⁵ C57B6/J male mice (Jackson Laboratories) were fed a 0.1% NaCl diet (D17020) for 1 week prior to 2K1C surgery and thereafter. Mice were anesthetized with 2-3% isoflurane in 100% O₂. Through a retroperitoneal incision, the right renal artery was carefully isolated from the renal nerve. A 0.5-millimeter polytetrafluoroethylene catheter (ID: 0.008 X OD: 0.014; Braintree Scientific, SUBL140) was cut longitudinally and placed around the renal artery, distal to the adrenal artery. The catheter was then secured in place with two 10-0 sutures to attenuate blood flow and induce renal stenosis. The mice that received this procedure are the renal clip group of mice. For sham control procedures, renal arteries were isolated from the renal nerve, but a catheter was not placed. Post-surgery, animals were treated by subcutaneous injection of 0.03 mg/kg buprenorphine twice/day for 48 hours (Henry Schein Inc.) and 2 mg/kg enrofloxacin (Norbrook Laboratories) as previously published. Mice were then sacrificed 19-21 days following renal clip or sham surgery. Vascular reactivity for the aorta and mesenteric arteries using these mice was reported previously.¹⁹⁵ The renal arteries from these same animals are analyzed herein. A separate, second cohort of animals using this model (n=6 for each group) were used for immunohistochemical analyses in this study.

Animal harvesting for immunohistochemical analysis:

Male C57BL6/J mice with or without renal stenosis were sacrificed via CO₂ asphyxiation followed by cervical dislocation. The artery contralateral to renal clip (left renal artery) was excised and placed in 4% paraformaldehyde in PBS for 24 hours then placed in 100% ethanol for

processing.¹⁵² Tissues were embedded in paraffin and sectioned at 8 micron thickness. Immunohistochemical analysis was performed as previously described.⁴³ Tissue sections were deparaffinized with xylenes and rehydrated by sequentially decreased concentrations of ethanol (100%-70%) followed by deionized distilled water. Heat-mediated antigen retrieval was then performed using citric acid-buffer (Vector Laboratories, H-3300) for 20 minutes, then sections cooled for 30 minutes at 4°C. Sections were then blocked in 10% horse serum (Sigma H1138) in PBS (MilliporeSigma, H1270) at room temperature for 1 hour. For Figure 10, primary antibodies (See Table 6) for sGC β (Abcam, ab154841, 1:100) and von Willebrand Factor (vWF; Abcam, ab11713, 1:250) were incubated on sections in PBS containing 10% horse serum overnight at 4°C in a humidity chamber. One section per slide was stained with rabbit (Vector Laboratories, I-1000) IgG control to match the corresponding sGC β antibody concentration. Tissue sections were washed thrice for 5 minutes with PBS. For Figure 15, incubation for sGC α (Cayman, 160895, 1:80) and corresponding IgG control were performed on tissue sections in 10% horse serum in PBS overnight at 4°C in a humidity chamber. Tissue sections were then washed thrice for 5 minutes in PBS and then incubated for 1 hour at room temperature using PBS containing 10% horse serum and vWF primary antibody. These samples were washed thrice again in PBS for 5 minutes before the next steps. For all tissues used in Figure 10 and Figure 15, sections were then incubated in PBS containing 10% horse serum with smooth muscle α -actin (ACTA2) primary antibody pre-conjugated to FITC fluorophore (MilliporeSigma, F3777 clone 1A4, 1:500), 4',6-diamidino-2-phenylindole (DAPI, D3571, Thermo Fisher Scientific, 1:100) and secondary antibodies (See Table 6) donkey anti-rabbit AlexaFluor 594 (Invitrogen, A-21207, 1:250) and donkey anti-sheep AlexaFluor 647 (Invitrogen, A-21447, 1:250) for 1 hour at room temperature in a humidity chamber. Tissue sections were then washed thrice in PBS for 5

minutes before being mounted on coverslips using Prolong Gold Antifade mounting medium with DAPI reagent (Invitrogen, P36931). Immunohistochemistry staining of renal arteries were imaged using a Nikon A1 Confocal Laser Microscope at the University of Pittsburgh Center for Biological Imaging. Images were taken with 40X objective magnification with 1024 x 1024 pixel resolution. Increments for Z-stacks of 1 μm were applied for stained and IgG controls. In ImageJ, a region of interest was drawn around ACTA2+ areas representing the smooth muscle cell tunica media then superimposed on sGC β images for quantification of medial smooth muscle sGC α and sGC β expression per medial area.

Treatment of Renal Artery Rings and Myography:

The following treatment method was performed as previously described.⁴³ In brief, murine renal arteries were rapidly cleaned, excised and placed in room temperature physiological salt solution (PSS) which contains: 119 mM NaCl, 4.7 mM KCl, 1.17mM MgSO₄, 1.18 mM KH₂PO₄, 5.5 mM D-glucose, 25 mM NaHCO₃, 0.027 mM EDTA, and 2.5 mM CaCl₂. Arteries were cut into 2-millimeter rings, then placed on a small vessel wire myograph (DMT 620M) filled with PSS (pH 7.4 when bubbled with 95% O₂ 5% CO₂ at 37°). Following a 30 minute rest, arteries were gradually stretched to a tension corresponding to a transmural pressure of 80mmHg. Arteries were then constricted with a dose response of phenylephrine (50nM-50mM). Blood vessels that failed to constrict in response to phenylephrine were excluded from the experiments on the grounds that they could not produce any contractile response. Rings were washed 3 times with PSS and allowed to rest for 30 minutes. A final wash was performed, and arteries were rested for an additional 10 minutes. Following the final 10 minute rest period, arteries were constricted with a single dose of phenylephrine (1 mM) wherein all vessels reached at least 50% of maximal contraction. After reaching a plateau, increasing concentrations of

acetylcholine (ACh; 10 nM - 1 μ M, Sigma, MA6625) or sodium nitroprusside (SNP; 10 nM - 10 μ M, Sigma, 71778) were administered to assess endothelium-dependent and NO-dependent relaxation, respectively. Subsequently, 100 μ M SNP in Ca^{2+} -free PSS was added to the vessels to determine their maximal dilatory responses. The percentage relaxation reported represents the data normalized to the difference between maximal dilation and maximal constriction. For the cohort of animals where renal arteries were treated with ACh vasodilator, n=7 animals for sham surgery and n=8 animals for 2K1C (renal clip) surgery. For the cohort of animals where renal arteries were treated with SNP vasodilator, n=5 animals for sham surgery and n=8 animals for 2K1C (renal clip) surgery.

Cell culture, drug, and peptide treatments:

Renal pre-glomerular smooth muscle cells (RPGSMCs) were isolated from Wistar-Kyoto rats as previously described,¹⁹⁶ cultured at 37°C in SmGm-2 fully supplemented growth medium (Lonza, CC-3181) containing 5% FBS and SmGm-2 SingleQuot (Lonza, CC-3182) reagents and passaged using 1X trypsin-EDTA (Gibco, 10779413) dissolved in 1X PBS. RPGSMCs were used between passages 2-7 for all experiments, after which they were discarded. Cells were cultured to approximately 90% confluency (approximately 48-72 hours) prior to any drug treatment. During drug treatments, RPGSMCs were washed twice with 1X PBS and cultured in serum and growth factor starved Dulbecco's Modified Eagle Medium/Ham's F12 (DMEM/F12, Sigma, D6421) media containing: 100 U/mL penicillin/streptomycin (Gibco, 15140-122), 1.6 mM L-glutamine (Gibco, 25030-081), 200 μ M L-ascorbic acid (Sigma, 50-81-7), 5 μ g/mL apo-transferrin (Sigma, 11096-37-0), and 6.25 ng/mL sodium-selenite (Sigma, 10102-18-8). Losartan (Cayman, 124750-99-8), PD123319 (Sigma, 136676-91-0), and AS18428456 FoxO inhibitor (Cayman, A15871) were dissolved in dimethyl sulfoxide (DMSO, D8418), while Angiotensin II

(Ang II, Sigma, A9525) peptide was dissolved in sterile deionized distilled water for stock solutions prior to treatment. Treatment concentrations were 100 nM Losartan, 100 nM PD123319, 1 μ M AS1842856, and 1 μ M Ang II. Control treatments involved 0.1% DMSO treatment for 48 hours prior to harvesting. For NO stimulation experiments, cells were pretreated with 10 μ M sildenafil citrate (Sigma, PZ0003) for 45 minutes to inhibit cGMP-specific phosphodiesterase 5 activity, and then stimulated with the NO-donor, diethylammonium (Z)-1-(N,N-diethylamino)diazen-1-ium-1,2-diolate (DEA-NONOate, Cayman, 82100) for 15 minutes.

qRT-PCR:

RPGSMCs were cultured in 6-well culture plates until approximately 90% confluent before being washed and switched to serum and growth factor starved media. Cells were then subjected to 48-hour drug and/or peptide treatment before lysis in TRIzol reagent (ThermoFisher, 15596026). The Direct-zol RNA miniprep plus (Zymo, R2051) manufacturer's protocol was used to isolate RNA from cells. For cDNA synthesis, the SuperScript IV First Strand Synthesis (ThermoFisher, 18091050) kit manufacturer's protocol was used. For quantitative real time PCR analysis, the PowerUp SYBR Green Master Mix (ThermoFisher, A25742) and 1 μ M target primer (Table 7) were mixed according to manufacturer's protocol with settings for 40 PCR cycles, 95°C melting temperature, 58°C annealing temperature, and 72°C extension temperature set on a QuantStudio 5 Real-Time 384-well PCR System (ThermoFisher A28140) for amplification. The $\Delta\text{-}\Delta\text{-ct}$ value fold change in expression was used in order to control for cell number and RNA quality with values normalized to an 18S housekeeping gene transcript.

Western blot:

RPGSMCs were cultured in 12-well culture dishes until approximately 90% confluent before being switched to serum and growth factor starved media for 48 hours. Cells were then washed with PBS and 1X Cell Lysis Buffer (Cell Signaling, 9803) containing: (pH 7.5) 20 mM Tris-HCl, 1 mM Na₂EDTA, 1 mM EGTA, 1% Triton, 1 mM β-glycerophosphate, 1 mM Na₃VO₄, 1 μg/mL leupeptin, 2.5 mM sodium pyrophosphate, and additional 1X protease (MilliporeSigma, P8340) and phosphatase inhibitors (MilliporeSigma, P5726) at 4°C. A bicinchoninic acid kit (ThermoFisher, 23225) was used according to the manufacturer's protocol to quantify lysate protein concentration and approximately 15 μg of protein was used for each western blot lane. Lysates were boiled at 100°C for 10 minutes and Laemmli buffer was added such that final lysates contained: (pH 6.8) 31.5 mM Tris-HCl, 10% glycerol, 1% SDS, 2.5% β-mercaptoethanol and 0.005% Bromophenol Blue before being loaded onto 4-12% gradient BisTris polyacrylamide gels (Invitrogen Life Technologies, NP0335BOX). Proteins were transferred from polyacrylamide gels to nitrocellulose membranes (LiCor, 926-31092) and blocked for approximately 30 minutes at room temperature with 1% bovine serum albumin (BSA) in PBS. Membranes were incubated in primary antibody (Table 6) solution containing 1% BSA in PBS with 0.1% Tween 20 overnight at 4°C. Blots were then washed with 1X PBS with 0.05% Tween 20. Membranes were then incubated for one hour at room temperature in secondary antibody solutions containing 1:1 LiCor Intercept Buffer (LiCor, 927-70001): 1X PBS with 0.2% Tween 20 and corresponding secondary antibodies (Table 6). An Odyssey CLx Imager (LiCor, 9140) was used for fluorescence visualization and semi-quantitative analysis was performed using Image Studio software.

Immunocytochemical analysis of hypertrophy:

RPGSMCs were cultured on a single 24 x 50 millimeter cover glass (VWR, 16004-322) to approximately 90% confluency and then serum starved for 48 hours in the DMEM/F12 starvation media described above. Media was then gently aspirated by hand and the cover glass washed with PBS containing 0.1% Triton X-100 for 5 minutes. Cells were then fixed in 4% paraformaldehyde in PBS for 30 minutes at room temperature and then gently washed twice with PBS containing 0.1% Triton X-100. RPGSMCs blocking was carried out in PBS with 10% horse serum for 1 hour at room temperature. Primary antibody incubation for rabbit-sGC β (Cayman, 160897, 1:200) antibody (See Table 6) was carried out in PBS with 10% horse serum overnight at 4°C in a humidified chamber. Cells were then gently washed thrice with PBS for 5 minutes each time before being incubated in donkey anti-rabbit (AlexaFluor, A21207, 1:250) secondary antibody (See Table 6) for 1 hour at room temperature in PBS containing 10% horse serum. PBS was used to wash cells twice for 5 minutes and AlexaFluor 488-conjugated phalloidin (ThermoFisher, A12379, 1:100) in PBS with 10% horse serum was added for 20 minutes to stain for filamentous (F)-actin. Cells were gently washed twice for 5 minutes in PBS before applying Prolong Gold Antifade mounting medium with DAPI reagent (Invitrogen, P36931) with coverslips applied to stained cells. Immunocytochemistry images of RPGSMCs were taken using a Leica DM1000 microscope at 40X objective with 2X zoom applied and cell area was quantified using ImageJ software.

Statistics:

Statistical analyses were performed using Graphpad Prism Software 8.0d. For wire myography, two-way analysis of variance (ANOVA) and an unpaired two-tailed *t*-test for each

treatment concentration. This allowed for determination of significance between groups overall and at specific treatment concentrations. For Figure 9, listed (numerical) P -values represent significance by two-way ANOVA test, while * is indicative of a $P < 0.05$ by unpaired two-tailed t -test to assess differences between groups at each vasodilator concentration. Data normality was assessed via Shapiro-Wilk test. The P -values reported for the qPCR, Western blot, immunostaining analysis, and calculated EC_{50} and E_{max} values were assessed using an unpaired two-tailed t -test for data that was normally distributed, an unpaired two-tailed t -test with Welch's correction to account for data normally distributed but with unequal variance, or Mann-Whitney U -test was applied when data was non-normal and/or bimodally distributed. Symbols were consistent throughout wherein * denotes $P < 0.05$.

3.4 Results:

To determine the effects of RAAS activation on the renal vasculature, we used a two-kidney-one-clip (2K1C) model (Figure 9A), which involves placing a surgical cuff around a single renal artery which clips the artery to restrict blood flow and induce unilateral renal stenosis. To assess the vasoreactivity responses of the 2K1C unclipped contralateral renal arteries compared to their sham counterparts, wire myography was performed on the renal arteries contralateral to the surgical procedures of clipped and sham animals to compare the two groups. We observed that the 2K1C contralateral arteries contracted significantly less to 1 mM phenylephrine (PE) than their sham counterparts (Figure 9B). We also observed an increase in endothelium-dependent vasodilation in response to 10^{-7} M acetylcholine (ACh) treatment (Figure 9C). A significant difference in NO-dependent vasodilation in response to the NO-donor, sodium

nitroprusside (SNP), was observed between sham and clip groups with significant increases in vasorelaxation in the clip groups following 10^{-7} M and 10^{-6} M SNP treatment (Figure 9D). E_{\max} and EC_{50} values for ACh and SNP responses for sham control and renal clip groups are listed in Table 5. Together, the findings of the responses to both ACh and SNP indicate an improvement in the vasorelaxation responses of the contralateral arteries from 2K1C animals over sham controls.

We then quantified renal artery protein expression to explore the causes of the increased NO-sensitivity of 2K1C contralateral renal arteries (Figure 10A-E; Figure 15A-F). No significant changes in vessel nuclei staining (Figure 10A,F; Figure 15A,F), smooth muscle α -actin (ACTA2; Figure 10B,G; Figure 15B,G), or the endothelial marker, Von Willebrand Factor (vWF; Figure 10D,I; Figure 15D,I) expression were observed. We did, however, observe a significant increase in sGC β protein expression (Figure 10C,H) and sGC α protein expression (Figure 15C,H) in the contralateral arteries of 2K1C animals over controls. In addition, no changes were observed in medial area (Figure 10J; Figure 15J). These data indicate the increases in sGC expression in contralateral renal arteries compared to sham controls likely drive the increased NO-sensitive vasodilation response.

Next, we sought to determine what drives sGC expression changes in renal artery smooth muscle. It is well established that reduced renal blood flow increases angiotensin II (Ang II) in models of 2K1C.¹⁹⁷⁻¹⁹⁸ Therefore, we treated rat renal pre-glomerular smooth muscle cells (RPGSMCs) with vehicle or 10^{-6} M Ang II to test if Ang II increased sGC expression (Figure 11A-D). Ang II treatment led to no differences in cell number (Figure 11A,E) but increased filamentous (F)-actin expression (Figure 11B, F), and cell area (Figure 11D,H) indicating RPGSMC are hypertrophic (Stephenson, et al., 1998). Additionally, Ang-II resulted in a 1.7 fold

increase in sGC β protein expression via immunofluorescence (Figure 11B,F). We also observed an increase in sGC α by 1.9-fold (Figure 16A,C) and a 4-fold increase in sGC β protein expression via western blot analyses (Figure 11I, J). To test if increased sGC expression impacted cGMP production and PKG activity, RPGSMCs were treated with Ang II or vehicle and then subjected to treatment with the NO donor, DEA-NONOate, for 15 minutes prior to harvest to induce sGC-mediated cGMP production. Quantification of vasodilator stimulated protein (VASP) phosphorylated at the serine 239 position, a surrogate indicator of cGMP-dependent protein kinase activity,¹⁹⁹ showed an 8-fold increase in VASP serine 239 phosphorylation (pVASP) in Ang II-treated cells stimulated with DEA-NONOate compared to vehicle controls (Figure 11I,K). Taken together, these data show that Ang II *in vitro* augments sGC expression and cGMP signaling, indicating that elevated RAAS activity increases sGC expression and downstream signaling *in vivo*.

We next tested whether the angiotensin II type 1 (AT₁R) or type 2 receptor (AT₂R) was responsible for increasing sGC levels. Consistent with increased sGC protein expression, we found that Ang II treatment also caused a 3.6-fold increase in sGC α mRNA (Figure 12A) and a 4.4-fold increase in sGC β mRNA (Figure 12B). RPGSMCs co-treated Ang II and Losartan, an AT₁R antagonist,²⁰⁰ showed inhibition of Ang II – induced increases in sGC α mRNA (Figure 12A), sGC β mRNA (Figure 12B), sGC α protein expression (Figure 16A,C) and sGC β protein expression (Figure 12C, D). Conversely, RPGSMCs co-treated with Ang II and AT₂R antagonist, PD123319,²⁰¹ showed no significant impact on the Ang II-induced increases in sGC α mRNA (Figure 12A), sGC β mRNA (Figure 12B), sGC α protein expression (Figure 16A,C) or sGC β protein expression (Figure 12C, D). Combined, these data indicate that the Ang II mediated increase in sGC expression occurs through activation of AT₁R.

Recently, we published evidence that the FoxO family of transcription factors regulate the mRNA expression of sGC in aortic smooth muscle cells.¹⁴⁷ To determine whether the FoxO family of transcription factors can also influence the function of renal smooth muscle, we treated RPGSMCs with 10^{-6} M of the FoxO transcription factor inhibitor, AS1842856 (Nagashima, et al., 2010), alone and in conjunction with Ang II. When AS1842856 was administered alone to RPGSMCs, a significant reduction in sGC α mRNA (Figure 13A), sGC β mRNA (Figure 13B), and sGC β protein expression (Figure 13C,D) was observed. When co-administered with Ang II, AS1842856 was significantly reduced compared to Ang II treatment, but produced no significantly different effect on either sGC α mRNA (Figure 13A), sGC β mRNA (Figure 13B), sGC α protein expression (Figure 16A,C) or sGC β protein expression (Figure 13C,D) when compared to controls. Treatment with AS1842856 also significantly blunted the expression of the downstream FoxO protein target, glucose-6-phosphatase (G6Pase), indicating that FoxO protein activity is potently suppressed (Figure 17A). Additionally, this experiment showed that Ang II, Losartan and PD123319 had no significant effect on the expression of G6Pase. This suggests that Ang II-mediated changes do not universally impact FoxO activity (Figure 17A). These data indicate the FoxO transcription factors are necessary for the Ang II-mediated sGC expression increases in renal smooth muscle.

Next, we tested how cGMP production in RPGSMCs was influenced by Ang II receptor antagonists and FoxO inhibitors in the absence and presence of NO-stimulation with DEA-NONOate. In the absence of DEA-NONOate-stimulation, the vehicle-treated cells showed no significant differences in cGMP production or VASP phosphorylation were observed between the control, Ang II, AS1842856, Ang II + AS1842856, Ang II + Losartan, or Ang II + PD123319 treatment groups (Figure 14A-C). Similar to the observed effect in sGC expression, Ang II and

PD123319 co-treatment followed by DEA-NONOate stimulation produced significant increases in downstream sGC function via cGMP production (Figure 14A) and VASP phosphorylation (Figure 14B,C) compared to solely DEA-NONOate-stimulated controls. Treatment with AS1842856 or Ang II + Losartan followed by DEA-NONOate stimulation caused a decrease in cGMP production (Figure 14A) and showed no significant differences in VASP phosphorylation (Figure 14B,C) or total VASP expression (Figure 10B, D) compared to control cells stimulated solely with DEA-NONOate. We also examined the expression of PDE5 and PKG1 and found that there were no significant changes in mRNA expression, suggesting that the changes in cGMP production and downstream signaling are due solely to changes in sGC expression (Figure 17B,C). Combined, these data show that PD123319 has no significant effect on Ang II-mediated sGC signaling and that the blunting effects of Losartan or AS1842856 on the Ang II-mediated sGC expression also inhibited downstream cGMP signaling following NO-dependent stimulation.

3.5 Discussion:

Renal artery stenosis remains a pervasive cause of secondary hypertension and a condition significantly correlated with high morbidity and mortality.²⁰²⁻²⁰⁵ NO plays an important role in maintaining renal blood flow and glomerular filtration rate following single renal artery stenosis.^{189-190,206} In addition, there is emerging pre-clinical evidence that sGC stimulator drugs which have had notable anti-fibrotic effects, in conjunction with RAAS blockade confer resistance to end stage renal disease and chronic kidney disease.²⁰⁷⁻²⁰⁸ Such therapies have demonstrated an ability to elevate blood flow and/or improve cardiac outcomes as a result of

decreased vascular tone and decreased blood pressure.^{65,156,209} Our previous study, in accordance with previous 2K1C models, showed that our 2K1C renal artery stenosis model causes increased blood pressure without altering body weight or plasma electrolyte concentrations.¹⁹⁴⁻¹⁹⁵ Here we provide the first evidence that sGC expression increases in the vascular smooth muscle of the renal artery contralateral to stenosis to preserve renal blood flow in the 2K1C model.

In this study, we observed a significantly increased vasodilation in the contralateral renal arteries of 2K1C animals. Interestingly, vasodilatory function of the aorta and mesenteric arteries was not different between these sham versus 2K1C mice.¹⁹⁵ This increased vasodilation of the contralateral renal artery was likely due to the significant increase in sGC expression observed in unobstructed renal artery smooth muscle from 2K1C animals compared to their sham controls. We also observed an increase vasodilation of renal clip animals over the sham controls when treated with 10^{-7} M ACh, suggesting some contribution of the endothelium in this response. However, as indicated by the SNP results, the response of the smooth muscle appears to be the predominant change in the renal vasculature. This response may indicate that NO-dependent signaling, which has been established to be a pivotal player in promoting regulation of renovascular homeostasis of blood pressure and fluid retention,^{188,191} is enhanced in the contralateral (non-stenotic) renal arteries compared with other vascular beds following elevated RAAS activity. Others have noticed the significance of endothelial-derived NO, specifically in the context of the 2K1C model, showing that inhibition of endothelial NO signaling exacerbates the high blood pressure and reduced renal blood flow of the 2K1C model.^{55,210} Additionally, this pressor response occurs irrespective to RAAS blockade, suggesting that while the regulation of these two pathways remain distinct, the interaction between them has vital implications.²¹⁰ Moreover, studies of the 2K1C model suggest that Losartan-mediated RAAS blockade following

NO-inhibition further diminishes blood flow to the contralateral renal artery instead of the expected increase in renal blood flow following RAAS inhibition.²¹¹ Our study builds upon this data, suggesting that the reason for the worsening of the phenotype when blocking Ang II signaling is due to an inability of the renal smooth muscle to mobilize a compensatory increase in sGC expression.

In the 2K1C model, it is possible that there are multiple factors which contribute to the changes observed in sGC expression, including RAAS signaling peptides such as Ang II. Therefore, we treated isolated renal pre-glomerular smooth muscle cells (RPGSMCs) with Ang II, to test the response of the renal vasculature to RAAS activation. Following treatment of cultured (RPGSMCs) with Ang II for 48 hours, the increase observed in sGC mRNA and protein expression suggests that RPGSMCs respond differently from aortic smooth muscle. Aortic smooth muscle and endothelial cells exhibit decreased functional NO signaling with excess Ang II exposure, via pathological overproduction of reactive oxygen species (ROS).²¹²⁻²¹³ Moreover, aortic sGC protein expression decreases with Ang II,²¹⁴⁻²¹⁵ and Ang II impairs aortic smooth muscle sGC function.²¹⁵⁻²¹⁶ Furthermore, sGC activator therapy has been shown to rescue heart function in patients with acute decompensated heart failure, many of whom were on RAAS pathway drugs to treat their heart failure, hypertension and other vasculopathies.²¹⁷ However, the trial was halted because the dosage used for this study resulted in hypotension in patients. It may be possible that other signaling molecules like catecholamines, prostacyclins, and others may contribute to the physiological responses we observe following 2K1C, however, further research is needed to test these possibilities. Our studies are the first to show that treatment with Ang II in conjunction with NO-stimulation caused elevated cGMP signaling in RPGSMCs, as indicated by increased cGMP production and VASP phosphorylation. This indicates uniquely enhanced renal

smooth muscle sGC-cGMP signaling following Ang II treatment in renal vascular smooth muscle.

Remarkably, other known responses to Ang II treatment were noted in RPGSMCs, such as elevated F-actin expression and increased cell size. These patterns have been observed in aortic smooth muscle both *in vivo* following infusion with Ang II and *in vitro* following Ang II treatment in culture.²¹⁸⁻²¹⁹ This suggests that while the increases in sGC expression responses are unique to renal smooth muscle, the hypertrophic responses to Ang II conform to the patterns that have been observed by others.

Specifically, our data shows that the AT₁R, but not the AT₂R, is responsible for the elevated expression of sGC observed in renal smooth muscle in response to Ang II. Indeed, co-treatment with Losartan and Ang II was sufficient to reverse all of the Ang II-induced phenotypes we observed in RPGSMCs. In contrast, Ang II co-treatment with PD123319 did not impact any of the phenotypes facilitated by Ang II treatment alone. This response may be due to the high density of AT₁Rs that have been observed in the adventitia of the renal vasculature,^{213,220} and the increased constriction of renal vasculature and, to a smaller extent, gut vasculature following acute Ang II infusion.²²¹ Curiously, this contrasts with the role for the AT₂R in cardiac function, which has been shown to improve outcomes following treatment with AT₂R-specific agonists following myocardial infarction.²²² Our findings suggest that the observed effect on sGC expression and function are largely independent of AT₂R activation. It is also possible that truncation products such as angiotensin 1-7 or angiotensin IV may also play role, albeit minor, in this phenomenon.²²³⁻²²⁴ Taken together, the data herein suggest that renal smooth muscle responds uniquely to Ang II via the AT₁R to promote increased sGC expression

and sGC-cGMP induced vasodilation while maintaining the canonical hypertrophic responses associated with elevated Ang II exposure.

Consistent with our previous work in aortic SMCs,¹⁴⁷ Ang II studies in RPGSMCs showed that inhibition of the forkhead box subclass O (FoxO) transcription factors significantly impair sGC expression. This finding indicates FoxO regulation of sGC expression likely applies to multiple branches of the vascular tree. The FoxO protein(s) responsible for sGC expression regulation are not yet known and the specific role of the FoxO transcription factors in the development and pathology of renal artery stenosis requires further study to assess their diverse functions in vascular physiology. It is nevertheless clear that the Ang II-mediated increases in sGC function cannot occur without functional FoxO transcription factor activity. Ang II can activate Akt,²²⁵ and Akt-mediated phosphorylation is a common regulatory mechanism known to modulate FoxO transcriptional activity.^{90-91,226} In addition, Ang II has been shown to cause increases in ROS, and oxidative stress is known to impact FoxO transcription factor activity through acetylation/deacetylation.²²⁷⁻²³⁰ These findings suggest that there could be an indirect regulatory mechanism between the AT₁R and FoxO transcription factors. Future research in this area should investigate the potential mechanistic links between agonism of the AT₁R and activation of the FoxO transcription factors. Moreover, our research has shown that oxidation or loss of sGC heme iron leads to NO insensitivity, making the protein more responsive to sGC-activating compounds which target oxidized or heme-deficient sGC to produce cGMP.^{41,43} Investigation of Ang II-mediated ROS production may reveal a novel therapeutic target for sGC activating drugs under conditions where high RAAS activity promotes oxidative stress.

Collectively, we show for the first time that in response to elevated RAAS activity, renal smooth muscle responds through an AT₁R and FoxO transcription factor-dependent mechanism

to increase sGC expression and cGMP signaling. These responses likely constitute a compensatory response to allow for maintenance of homeostatic blood volume and electrolyte balance to counteract Ang II-dependent increases in systemic blood pressure, and a means of preserving homeostatic fluid volume and electrolyte balance. These findings will have important clinical implications for the use of NO, FoxO transcription factor activating compounds, or sGC modulators for therapeutic treatment of renal hypertension. Our data suggest that these methods may offer a targeted approach to improve renal blood flow in RAAS-mediated renal stenosis. Combined, this study marks an important discovery of how the renal vasculature responds uniquely to elevated circulating plasma Ang II, advancing our understanding of renal vascular hypertension and the regulation of cGMP signaling within the renal vascular wall.

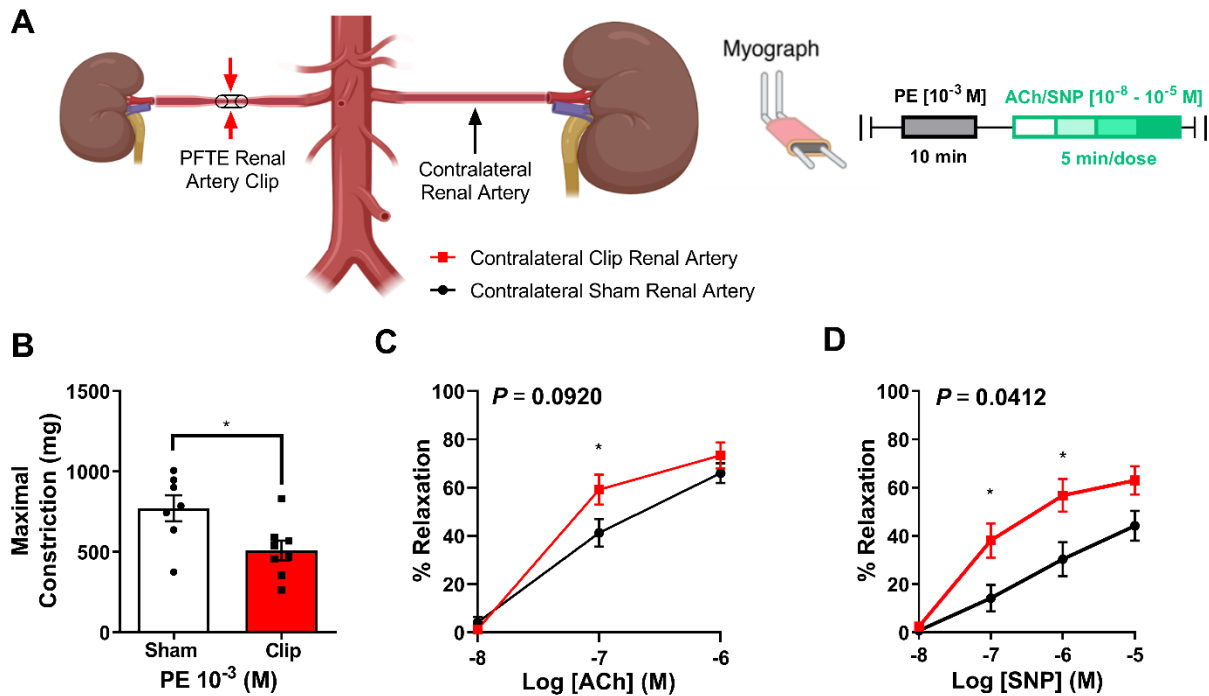


Figure 9

2K1C mouse model contralateral renal arteries have improved vasodilation compared to sham controls.

A) Schematic of 2K1C renovascular hypertension model and experimental design showing wire myography protocol. Black circles represent sham animals while red bars and squares represent contralateral renal arteries from 2K1C (clip) animals. B) Maximal constriction of sham (white bars) or clip (red bars) animal contralateral renal arteries following treatment with 10^{-3} M phenylephrine (PE). The * indicates $P < 0.05$ by unpaired two-tailed *t*-test. C) Vasodilatory responses to acetylcholine (ACh; 10^{-8} - 10^{-6} M) in isolated contralateral renal arteries from mice subjected to 2K1C (n=8) or sham (n=7) surgery. D) Vasodilatory responses to sodium nitroprusside (SNP; 10^{-8} - 10^{-5} M) in isolated contralateral renal arteries from mice subjected to 2K1C (n=8) or sham surgeries (n=5). Numerical *P*-values represent statistical differences between contralateral renal artery response curves from 2K1C versus sham animals by two-way ANOVA with the * indicative of $P < 0.05$ by unpaired two-tailed *t*-test at individual doses between groups. Error bars are \pm SEM.

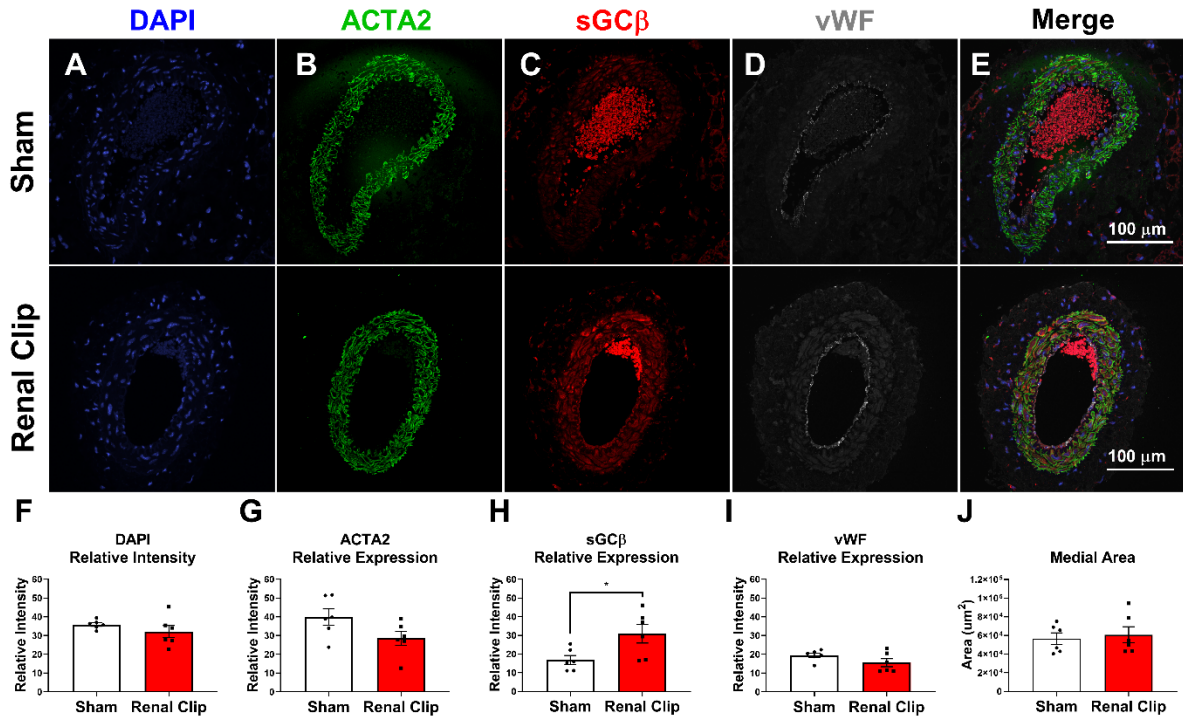


Figure 10

Immunohistochemistry of contralateral renal arteries from 2K1C (renal clip) animals show an increase in sGCβ expression over sham controls.

Immunofluorescent staining of representative maximum intensity projection images and quantification of sham control (n=6, white bars) or renal clip (n=6, red bars) animals for **A,F** DAPI (nuclei, blue), **B,G** ACTA2 (vascular smooth muscle, green), **C,H** sGCβ (red) and **D, I** vWF (endothelium, grey). **E**) Merge image from all channels. **J**) Quantification of medial area (μm²). The * indicates a *P* < 0.05 statistically significant differences between renal clip and sham groups by unpaired two-tailed *t*-test. Error bars are ± SEM.

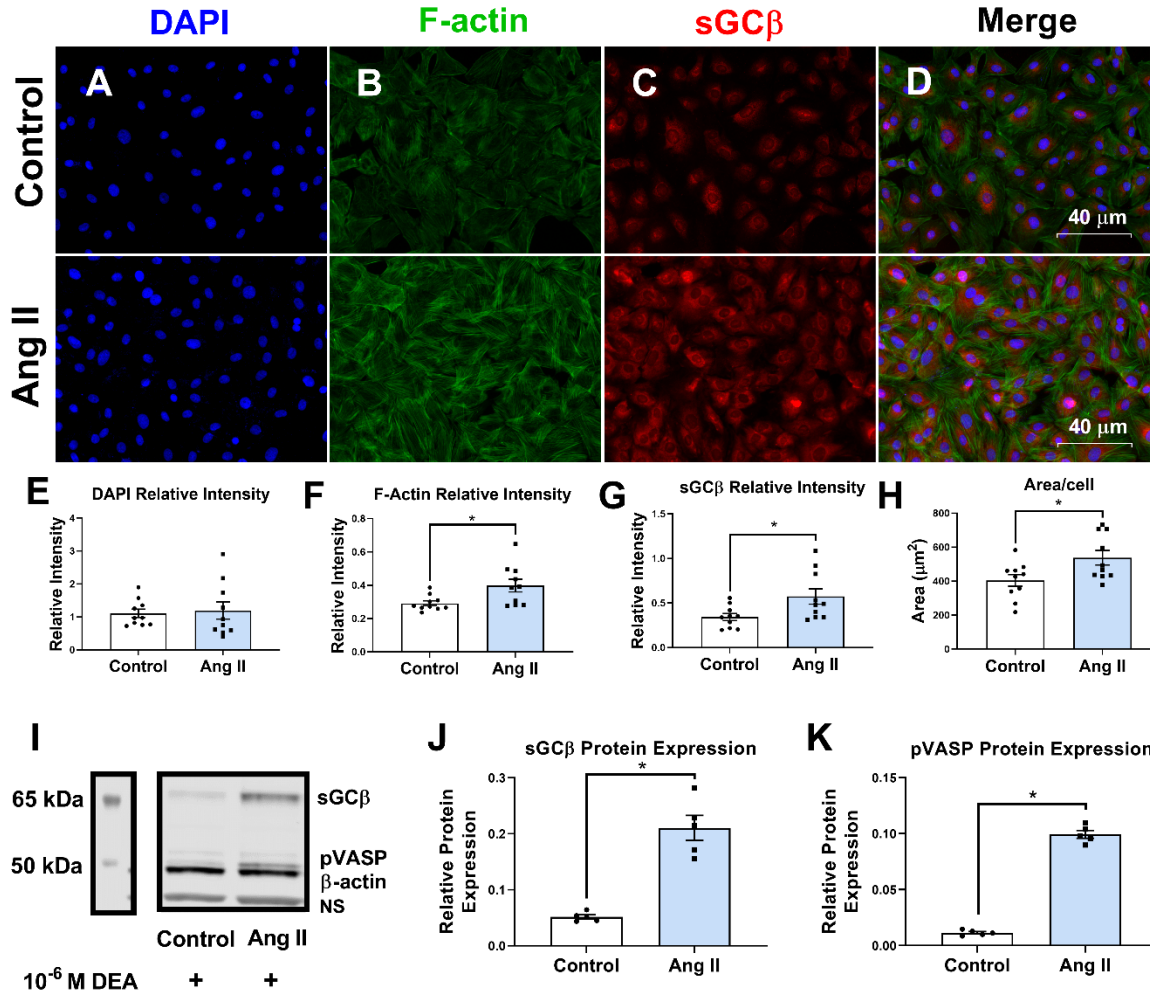


Figure 11

Immunocytochemistry of Ang II treated renal pre-glomerular smooth muscle cells show an increase in F-actin, sGC protein expression, and VASP phosphorylation compared to control-treated cells.

Immunocytochemistry staining and quantification resulting from control (n=10, white) or Ang II (10⁻⁶ M, n=10, light blue) treatment for **A, E**) DAPI (blue, nuclei), **B, F**) F-actin (green), **C, G**) sGCβ (red), **D**) Merged image of channels, or **H**) area/cell analyzed. **I-K**) Image and quantification of sGCβ band density/β-actin density, phosphorylated serine 239 vasodilator stimulated protein (pVASP) band density/β-actin density from Western blot for control (n=5 samples, white) or Ang II (10⁻⁶ M, n=5 samples, light blue)-treated RPGSMCs following DEA-NONOate treatment (10⁻⁶ M). NS denotes a non-specific band. The * indicates a *P* < 0.05 statistically significant difference between control and Ang II-treated cells by unpaired two-tailed *t*-test. Error bars are ± SEM.

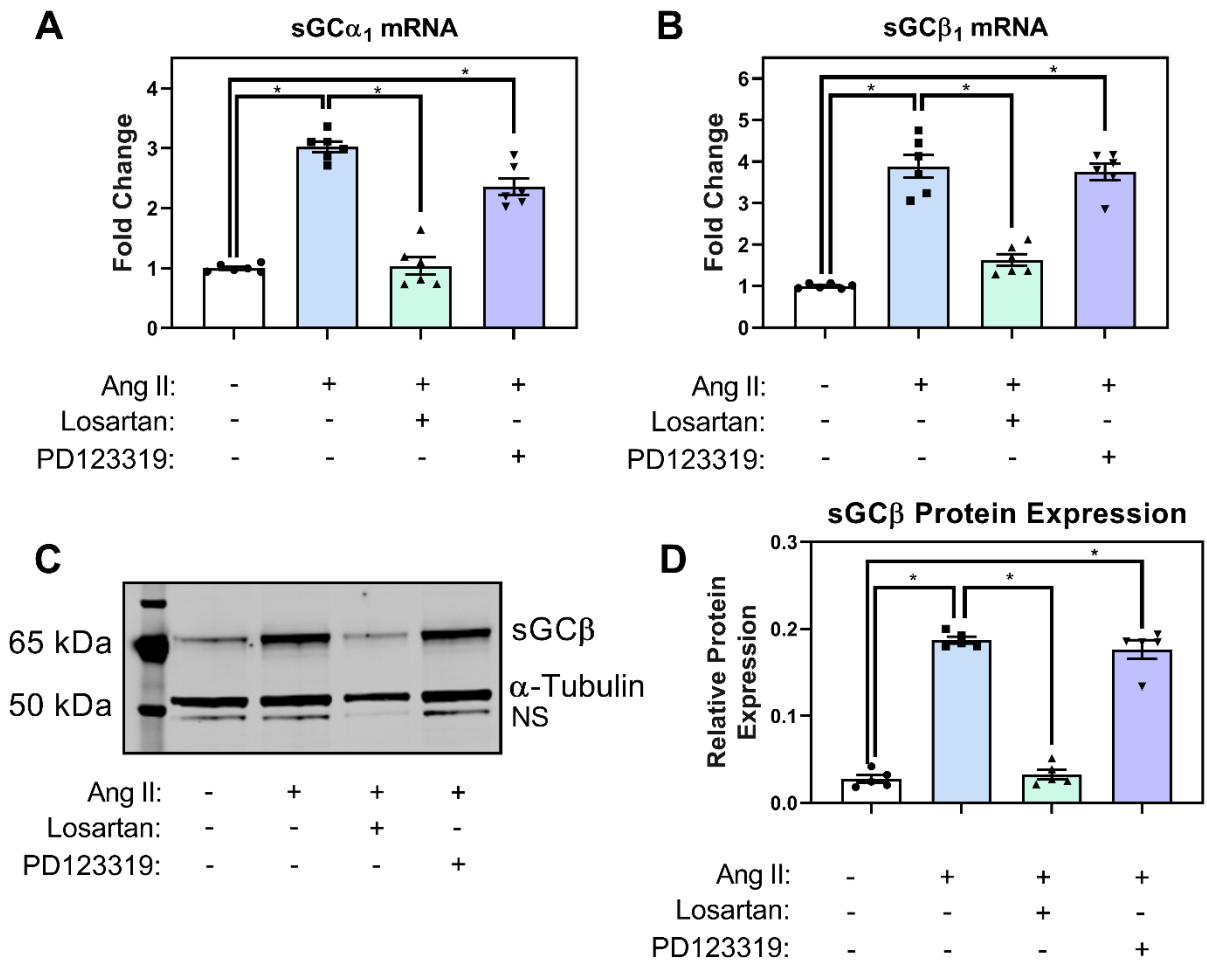


Figure 12

Losartan, but not PD123319, prevents Ang II-mediated increase of sGC expression in renal smooth muscle cells.

RPGSMCs were subjected to treatment with control (DMSO), Ang II (10^{-6} M), Losartan (10^{-7} M), and/or PD123319 (10^{-7} M). **A**) sGC α_1 mRNA (n=6 samples per group), **B**) sGC β_1 mRNA (n=6 samples per group) and **C**, **D**) sGC β protein expression (n=5 samples per group) was quantified relative to α -tubulin expression. NS denotes a non-specific band. The * indicates a $P < 0.05$ significant statistical difference between identified sample groups by unpaired two-tailed *t*-test. Error bars are \pm SEM.

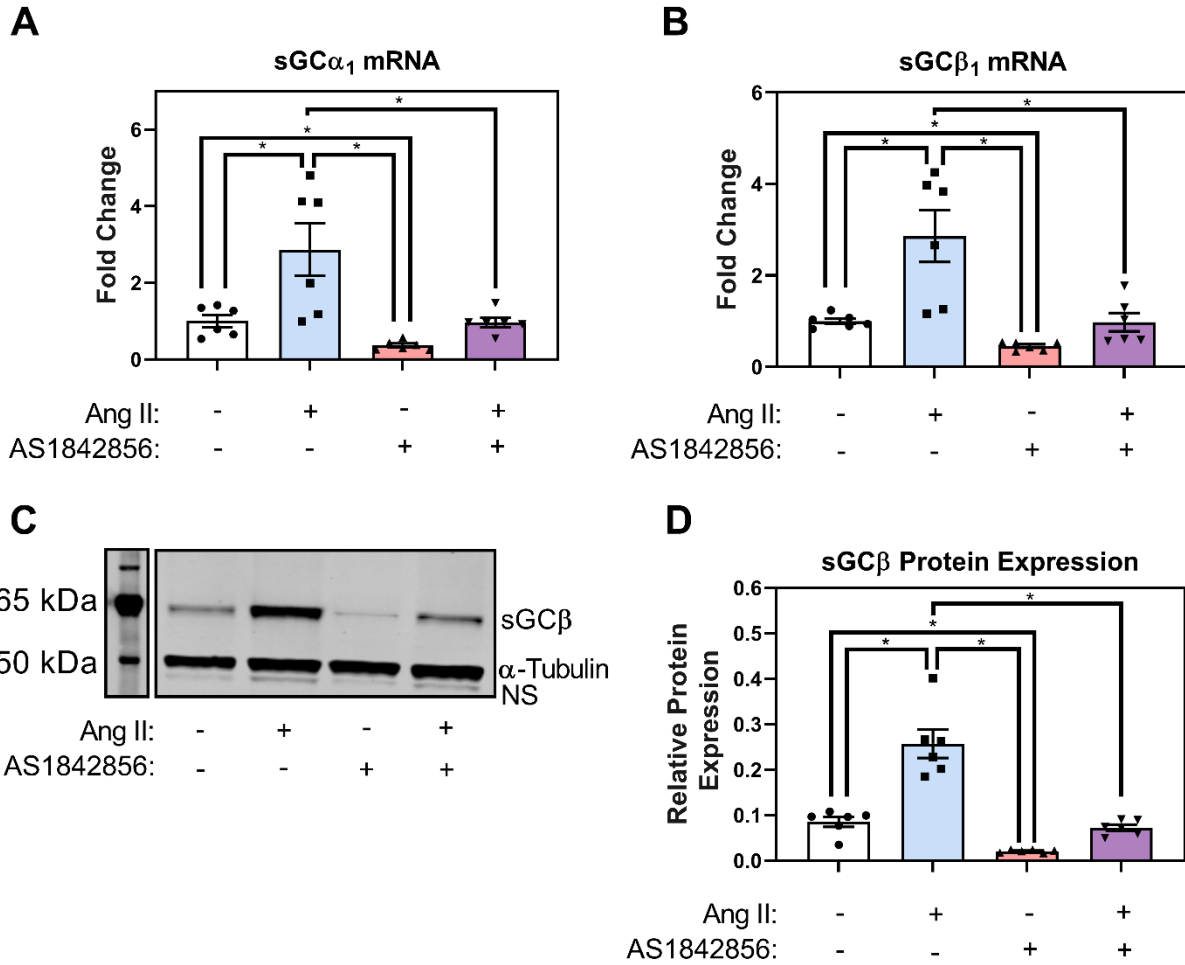


Figure 13

AS1842856 treatment causes a decrease in sGC expression and blunts Ang II-mediated increases in sGC expression in renal smooth muscle cells.

RPGSMCs were treated with control (DMSO), Ang II (10^{-6} M), and/or AS1842856 (10^{-6} M) and expression of **A**) sGC α_1 mRNA (n=6 samples per group), **B**) sGC β_1 mRNA (n=6 samples per group) and **C**, **D**) sGC β protein expression (n=5 samples per group) quantified relative to α -tubulin protein expression. NS denotes a non-specific band. The * indicates a $P < 0.05$ statistically significant difference between identified sample groups by unpaired two tailed t -test or Mann-Whitney U -test. Error bars are \pm SEM.

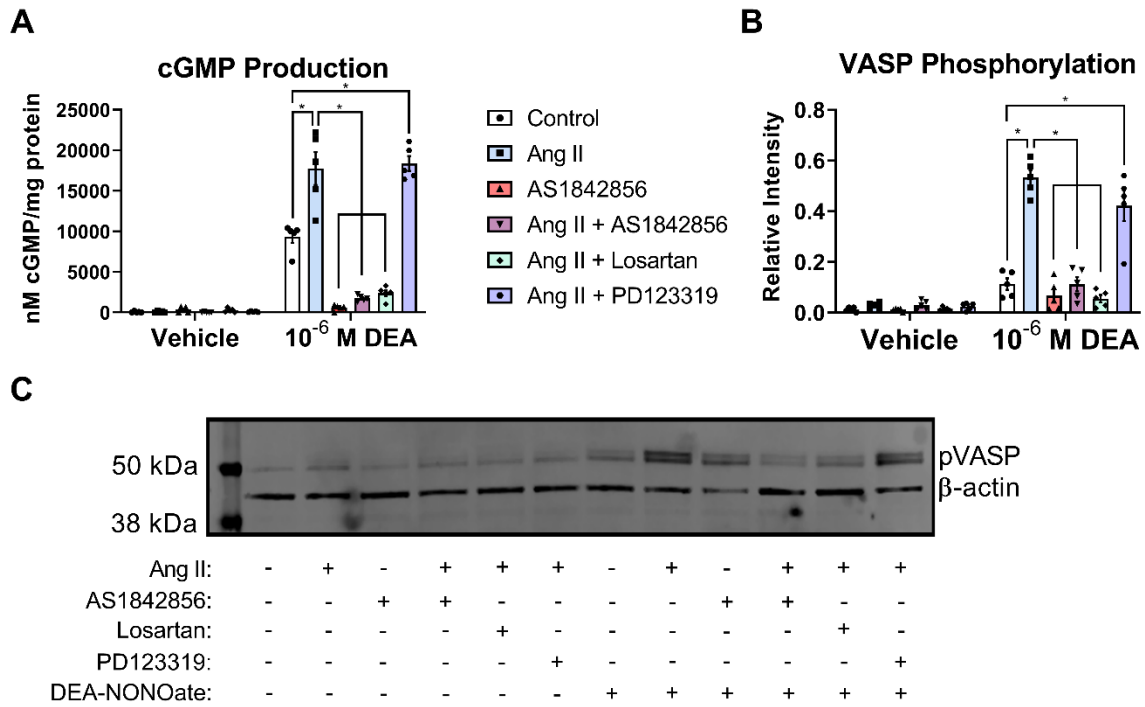


Figure 14

Losartan or AS1842856 blunt Ang II-mediated increases in downstream cGMP signaling in renal smooth muscle cells following NO-stimulation.

A) Quantification of cGMP production by ELISA following treatment of RPGSMCs with control, Ang II (10^{-6} M), AS1842856 (10^{-6} M), Losartan (10^{-7} M), PD123319 (10^{-7} M) and then stimulated with vehicle or DEA-NONOate for 15 minutes (10^{-6} M). **B, C)** Quantification and representative western blot of phosphorylated serine 239 VASP (pVASP) protein following the same treatment as in **A** ($n=5$ samples per group). The * indicates a $P < 0.05$ statistically significant differences between identified sample groups by unpaired two-tailed t -test. Error bars are \pm SEM.

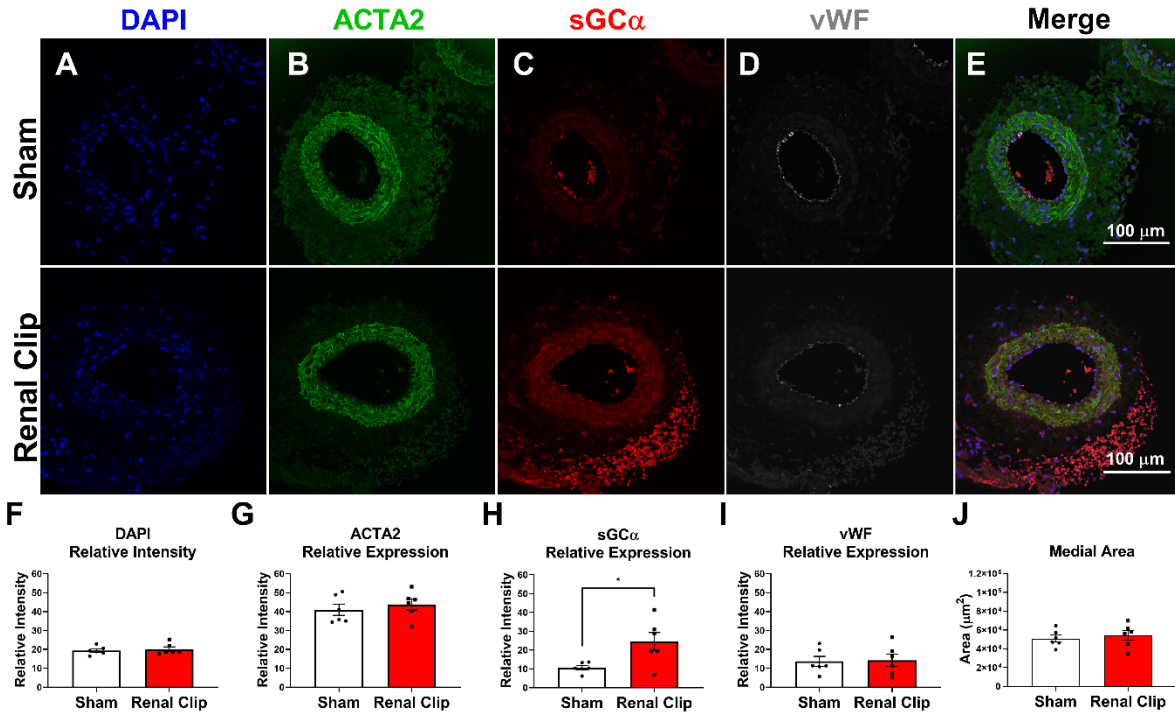


Figure 15

Immunohistochemistry of contralateral renal arteries from 2K1C (renal clip) animals show an increase in sGCα expression over sham controls.

Immunofluorescent staining of representative images and quantification of sham control (n=6, white bars) or renal clip (n=6, red bars) contralateral arteries for **A, F**) DAPI (nuclei, blue) **B, G**) ACTA2 (vascular smooth muscle, green), **C, H**) sGCα (red), and **D, I**) vWF (endothelium, grey). **E**) Merge image of maximum intensity projections from all channels. **J**) Quantification of medial area (μm²). The * indicates a *P* < 0.05 statistically significant difference between renal clip and sham by unpaired two-tailed *t*-test. Error bars are ± SEM.

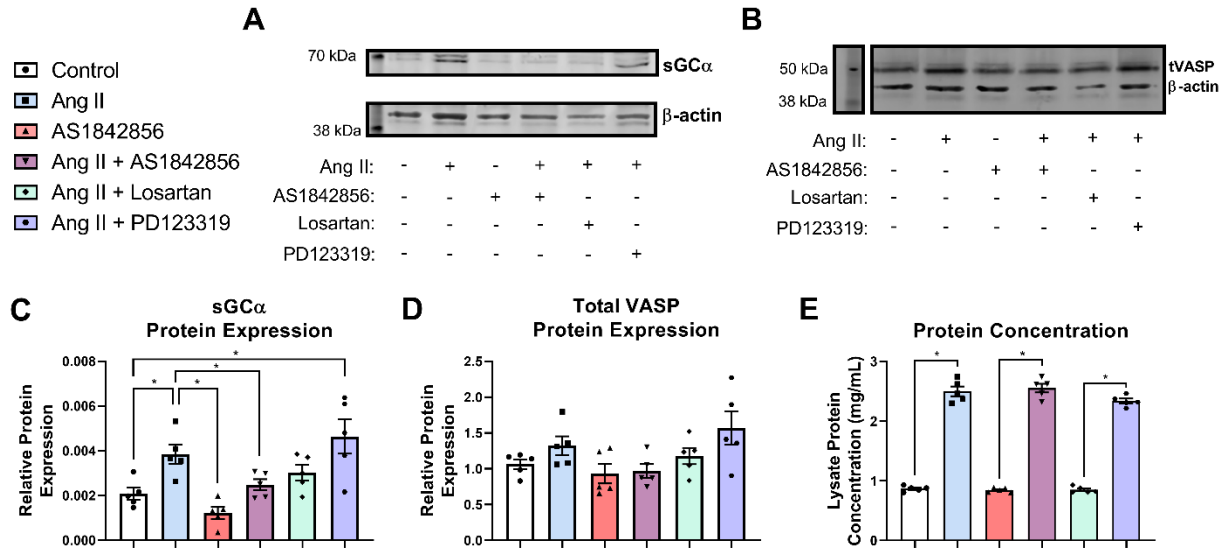


Figure 16

sGC α protein expression is AT₁R and FoxO-dependent, hypertrophy only requires AT₁R agonism, and tVASP expression remains unaffected in renal smooth muscle.

Western blot analysis and total protein expression in RPSMCs following treatment with Control, Ang II (10^{-6} M), AS1842856 (10^{-6} M), Losartan (10^{-7} M), and/or PD123319 (10^{-7} M). **A, C**) Representative western blot and quantification of sGC α protein expression relative to β -actin expression (n=5 samples per group). **B, D**) Representative western blot and quantification of total vasodilator stimulated protein (tVASP) protein expression relative to β -actin expression (n=5 samples per group). **E**) Total protein quantified using a bicinchoninic acid protein assay (n=5 samples per group). The * indicates a $P < 0.05$ statistically significant difference between indicated groups by unpaired two-tailed t -test with or without Welch's correction. Error bars are \pm SEM.

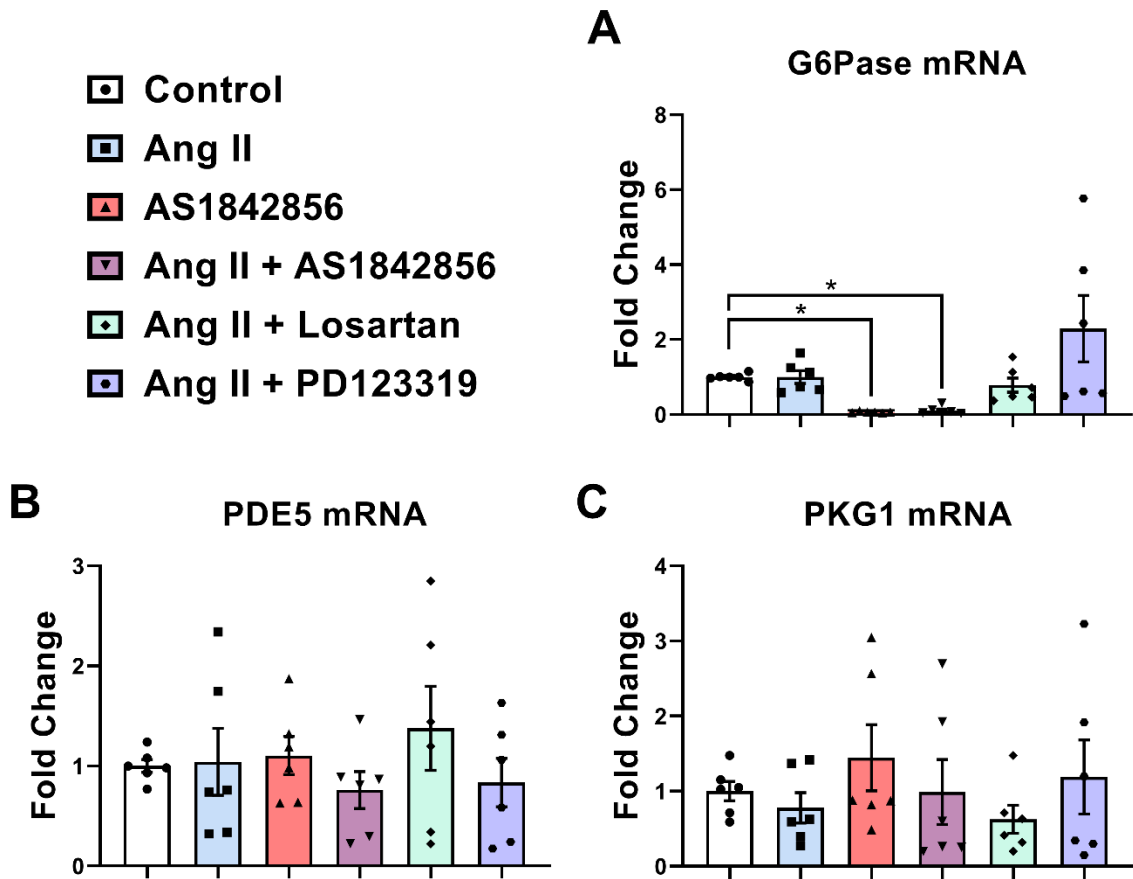


Figure 17

mRNA expression of sGC pathway and FoxO pathway-related genes.

qRT-PCR of genes expressed by RPGSMCs following treatment with Control, Ang II (10^{-6} M), AS1842856 (10^{-6} M), Losartan (10^{-7} M), and/or PD123319 (10^{-7} M). Graphs represent mRNA expression of **A**) glucose-6-phosphatase (G6Pase), **B**) cGMP-specific phosphodiesterase type 5 (PDE5), and **C**) cGMP-activated protein kinase 1 (PKG1). For each group there are n=6 samples. The * indicates a $P < 0.05$ statistically significant difference between control and treated groups by unpaired two-tailed t -test with Welch's correction or Mann-Whitney U -test. Error bars are \pm SEM.

Table 5: Calculations for vasodilatory responses of renal arteries to ACh and SNP

| Vasodilator Drug | Treatment Group | E_{max} (%) | SEM (%) | P-value | EC₅₀ (M) | SEM (M) | P-value |
|-----------------------------|----------------------------|----------------------------|--------------------|----------------|-----------------------------|------------------------------|----------------|
| ACh | Sham | 66.1 | 4.06 | 0.2951 | 1.04x10⁻⁷ | ±3.94x10⁻⁸ | 0.2881 |
| | Clip | 73.4 | 5.37 | | 5.63x10⁻⁸ | ±1.45x10⁻⁸ | |
| SNP | Sham | 44.2 | 6.16 | 0.0592 | 7.77x10⁻⁷ | ±3.12x10⁻⁷ | 0.1943 |
| | Clip | 63.0 | 5.90 | | 2.70x10⁻⁷ | ±1.52x10⁻⁷ | |

Vasodilator drugs acetylcholine (ACh) and sodium nitroprusside (SNP) were used to induce vasorelaxation of contralateral renal arteries for animals receiving 2K1C (renal clip) or sham surgery. Effective maximum dilation (E_{max}), standard error of the mean (SEM), and effective concentration to produce 50% of maximal response (EC₅₀) are shown above. P-values are calculated from unpaired *t*-test or unpaired *t*-test with Welch's correction to account for unequal variances.

Table 6: Catalogue of primary and secondary antibodies.

| Antibody | Species | Application | Concentration | Company | Cat. Number |
|---|----------------|--------------------|----------------------|----------------------|--------------------|
| sGCα | rabbit | WB, IHC | 1:200, 1:80 | Cayman | 160895 |
| sGCβ | rabbit | WB, ICC, | 1:1000, 1:200, | Cayman | 160897 |
| sGCβ | rabbit | IHC | 1:100 | Abcam | ab154841 |
| β-actin | mouse | WB | 1:500 | Santa Cruz | sc-47778 |
| α-tubulin | mouse | WB | 1:10,000 | Sigma | T6074 |
| Anti-rabbit Alexafluor- 594 | donkey | IHC, ICC | 1:250, 1:250 | Life Technologies | A21207 |
| Anti-goat Alexafluor- 647 | donkey | IHC | 1:250 | Life Technologies | A21447 |
| ACTA2 conjugated Alexafluor- 488 | mouse | IHC | 1:500 | Sigma | F3777 |
| Von Willebrand Factor | sheep | IHC | 1:250 | Abcam | ab11713 |
| AlexaFluor 488 Phalloidin | N/A | ICC | 1:100 | ThermoFisher | A12379 |

Table 6 Continued

| | | | | | |
|----------------------------|--------|-----------|--------------------------|------------------------|--------------|
| Phospho-VASP (S239) | rabbit | WB | 1:1000 | Cell Signaling | 3114S |
| VASP | rabbit | WB | 1:500 | Proteintech | 13472-1-AP |
| Rabbit IgG | rabbit | IHC | concentration matched | Vector Laboratories | I-1000 |

Soluble guanylyl cyclase α -subunit (sGC α), soluble guanylyl cyclase β -subunit (sGC β), smooth muscle α -actin (ACTA2), vasodilator-stimulated protein (VASP), and immunoglobulin (IgG) antibodies which were used for western blots (WB), immunohistochemistry (IHC), and/or immunocytochemistry (ICC).

Table 7: Catalogue of PCR primer sequences used.

| Primer | Sequence (5'→3') |
|---------------------------------------|-------------------------------|
| Rat sGCα_1 F | CTC CCG TGA CCG CAT CAT |
| Rat sGCα_1 R | CCG GTG TTG ATG TTG ACT GA |
| Rat sGCβ_1 F | AAT TAC GGT CCC GAG GTG TG |
| Rat sGCβ_1 R | GCA GCA GCC ACC AAG TCA TA |
| Mammalian 18S F | ACG GAC AGG ATT GAC AGA TTG |
| Mammalian 18S R | TTA GCA TGC CAG AGT CTC GTT |
| Rat PDE5 F | GCC GAT CTG GGC TGA ACT AAC |
| Rat PDE5 R | GCT CAC GGT TCC CTC AGA AT |
| Rat PKG1 F | ATG AGC GAA CTG GAG GAA GAC |
| Rat PKG1 R | GTC GAT CAA TGG CCC AGA GT |
| Rat G6Pase F | GGC TCA CTT TCC CCA TCA GG |
| Rat G6Pase R | ATC CAA GTG CGA AAC CAA ACA G |

Primers for soluble guanylyl cyclase α -subunit type 1 (sGC α_1), soluble guanylyl cyclase β -subunit type 1 (sGC β_1), 18S small subunit ribosomal RNA (18S), cGMP-specific phosphodiesterase type 5 (PDE5), cGMP-activated protein kinase type 1 (PKG1) and glucose-6-phosphatase (G6Pase), listed here were used in our analyses. For primers, F denotes forward primer and R denotes reverse primer with sequences reported in 5' – 3' direction.

Acknowledgements: We would like to acknowledge the Center for Biological Imaging at the University of Pittsburgh for its support and confocal microscope usage. In addition, we would like to thank Dr. Delphine Gomez for use of her fluorescent light microscope at the University of Pittsburgh. Financial support for this work was provided by the following National Institutes of Health (NIH) and American Heart Association (AHA) grants: NIH R01 HL 133864 and R01 HL 128304, AHA Grant-in-Aid [16GRNT27250146], and AHA Established Investigator Award [19EIA34770095] (A.C.S.); NIH F31 Pre-Doctoral Fellowship Award [HL 151173], Louis J. Ignarro Cardiovascular T32 Fellowship [5T32GM008424], and NIH T32 Division of Geriatrics Aging Institute Fellowship [AG021885] (J.C.G.); NIH Post-Doctoral Fellowship Awards [T32 DK007052 and 1F32HL152498] (B.G.D.); NIH [DK091190, HL109002, HL069846, and DK079307] (E.K.J.); and NIH [R01 HL152680] (S.D.S.). We would also like to acknowledge the support of Dr. Katherine C. Wood for her help editing and reviewing the manuscript for publication.

Author Contributions: Participated in research design: Galley, Durgin, Miller, Hahn, Stocker, Straub. Conducted experiments: Galley, Miller, Durgin, Hahn, Stocker. Contributed new reagents or analytic tools: Galley, Hahn, Durgin, Jackson, Stocker. Performed data analysis: Galley, Miller, Hahn. Wrote or contributed to the writing of the manuscript: Galley, Durgin, Straub.

4.0 FoxO4 Regulates sGC β Transcription in Vascular Smooth Muscle

Joseph C. Galley, B.A.^{1,2}, Megan P. Miller, B.S.¹, Subramaniam Sanker, Ph.D.², Mingjun Liu, M.S.^{1,3}, Iraida Sharina, Ph.D.,⁴ Emil Martin, Ph.D.,⁴ Delphine H. Gomez, Ph.D.^{1,3}, and Adam C. Straub, Ph.D.^{1,2,5}

¹Heart, Lung, Blood and Vascular Medicine Institute, University of Pittsburgh, Pittsburgh, Pennsylvania;

²Department of Pharmacology and Chemical Biology, University of Pittsburgh, Pittsburgh, Pennsylvania;

³Department of Pathology, University of Pittsburgh, Pittsburgh, Pennsylvania;

⁴Department of Cardiovascular Medicine, McGovern Medical School, Houston, Texas;

⁵Center for Microvascular Research, University of Pittsburgh, Pittsburgh, Pennsylvania;

4.1 Summary:

The nitric oxide (NO) receptor, soluble guanylyl cyclase (sGC), produces cyclic guanosine 3', 5' – monophosphate (cGMP) primarily to cause rapid dilation of smooth muscle cells (SMC). Because of the importance of sGC for proper SMC function, many new sGC activity modulator drugs have been approved for the treatment of cardiovascular diseases,⁵⁸⁻⁶⁰ however, transcriptional regulation of sGC remains incompletely understood. We recently showed that functional Forkhead box subclass O (FoxO) transcription factor activity is required for expression of sGC within SMC.¹⁴⁷⁻¹⁴⁸ We sought to investigate which FoxO transcription factor is responsible for gene expression of the heme-containing sGC β subunit, as loss of this subunit is necessary and sufficient to cause severe hypertension and lethal gut dysmotility.²⁶⁻²⁷ FoxO shRNA knockdown adenoviruses show FoxO1 or FoxO3 knockdown causes greater than

2-fold increases in sGC α and sGC β mRNA expression, with no change in NO-dependent cGMP production or cGMP-dependent phosphorylation. FoxO4 knockdown produced 50% loss of sGC α and sGC β mRNA and sGC β protein expression. Loss of FoxO4 expression decreased cGMP production and cGMP-dependent phosphorylation by more than 50%. Triple FoxO knockdown exacerbated the loss of sGC-dependent function, phenocopying our previous findings with FoxO inhibition. Transfection of sGC β promoter – luciferase constructs showed that the 0.5kb upstream of the transcriptional start site are key for its gene expression, and that inhibition of the FoxO transcription factors abolishes luciferase activity. Chromatin immunoprecipitation experiments confirm that FoxO4 binds the sGC β promoter at several locations. Taken together, our data show FoxO4 is the indispensable regulator of sGC β expression in SMC.

4.2 Introduction:

Soluble guanylyl cyclase (sGC) is the nitric oxide (NO) receptor within smooth muscle cells (SMC) responsible for initiating one of the key dilatory mechanisms for arterial blood vessels through the enzymatic formation of 3',5'-cyclic guanosine monophosphate (cGMP).^{23,149} The critical function of sGC within this dilatory cascade makes this enzyme a promising potential medicinal target, though many challenges still remain. Therapeutic strategies using sGC-stimulating drugs have recently been approved for the treatment of heart failure,⁵⁸ chronic thromboembolic pulmonary hypertension,⁵⁹ and pulmonary arterial hypertension,⁶⁰ however the regulation of sGC gene mechanisms which govern the resistance to various stressful stimuli. expression in smooth muscle remains largely unknown.

Studies show that the sGC protein functions as an obligate heterodimer, requiring both a functional α and β subunit in order to form cGMP. While there are multiple sGC genes, heterodimer pools have been shown to commonly form out of $\alpha 1\beta 1$ or $\alpha 2\beta 1$ dimers, as the $\beta 2$ subunit is seldom found in SMC.²⁸ Loss of the heme-containing $\beta 1$ subunit has been shown to be sufficient to cause lethal gut dysmotility in mice at 3-4 weeks of age,²³¹ which can be prevented with diets lacking fiber. These mice develop severe hypertension, with the aorta demonstrating a lack of dilation to NO-stimulation and a lack of NO-dependent platelet aggregation inhibition, both of which were rescuable with non-hydrolyzable cGMP analog treatment. Additionally, SMC-specific knockout of sGC $\beta 1$ causes severe NO-insensitive hypertension as well,²⁶ demonstrating the importance of the sGC $\beta 1$ protein that is uniquely important to the SMC for the proper maintenance of blood pressure. Together, these studies highlight the significance of sGC $\beta 1$ for proper SMC function and serve as the basis for our targeting of the sGC $\beta 1$ gene.

We have recently identified that inhibition of the Forkhead box subclass O (FoxO) family of transcription factors in vascular smooth muscle cells results in the loss of sGC expression and downstream function in multiple cell types.¹⁴⁷⁻¹⁴⁸ This family of transcription factors is known for its control over resistance to oxidative stress,¹¹¹⁻¹¹² cell cycle progression,¹¹³⁻¹¹⁴ governance of the progression through the cell cycle,¹¹³⁻¹¹⁴ and apoptosis in circumstances where these cellular mitigation strategies prove disadvantageous survival.¹²⁴⁻¹²⁸ Previous studies have identified significant regulation of function by post-translational modifications, primarily through the insulin signaling pathway to abolish transcriptional activity and alter DNA binding affinity.⁹⁹⁻¹⁰² Developmental research indicates functionally diverse roles for the FoxO transcription factors found in mammalian tissues, suggesting that there may be differing contributions of each FoxO transcription factor in the regulation of sGC expression.¹³⁹ The highly conserved DNA-binding

domain (DBD) of the FoxO transcription factors has been well-characterized to identify the consensus sequences commonly recognized by this family of transcription factors, however, recent studies have sought to identify the changes that may govern the structural differences that adjust observed changes in transcription.¹⁷⁶ This study sought to identify which transcription factors were important for the regulation of sGC and the regulatory loci within the human sGC β 1 promoter within SMC.

4.3 Methods:

Cell culture:

Rat aortic SMC (RASMC) and human aortic SMC (HASMC) were cultured as previously described.¹⁴⁷ Cells were cultured at 37°C in SmGm-2 fully supplemented growth medium (Lonza, CC-3181) containing 5% FBS and SmGm-2 SingleQuot (Lonza, CC-3182) reagents and passaged using 1X trypsin-EDTA (Gibco, 10779413) dissolved in 1X PBS. Cells were cultured to approximately 90% confluency. Cos7 cells were cultured in DMEM (Gibco, 11995-065) with 10% FBS (Gibco, 10438-026) and 100 U/mL penicillin/streptomycin (Gibco, 15140-122) to 90% confluency before being passaged using 1X trypsin-EDTA dissolved in 1X PBS for experiments.

Virus and drug treatments:

During drug treatments, RASMCs were washed twice with 1X PBS and cultured in serum and growth factor starved Dulbecco's Modified Eagle Medium/Ham's F12 (DMEM/F12, Sigma, D6421) media containing: 100 U/mL penicillin/streptomycin (Gibco, 15140-122), 1.6 mM L-glutamine (Gibco, 25030-081), 200 μ M L-ascorbic acid, 5 μ g/mL apo-transferrin, and 6.25 ng/mL sodium-selenite. AS18428456 FoxO inhibitor (Cayman, A15871) was dissolved in

dimethyl sulfoxide (DMSO, D8418) prior to treatment. Treatment concentration for AS1842856 was 10^{-6} M. Control treatments involved 0.1% DMSO treatment for 48 hours prior to harvesting. Adenovirus (AV) constructs were designed as previously described.⁴¹ For knockdown experiments, RASMCs were transduced with AV containing non-targeting (NT, 1.95×10^9 copies/mL), rat FoxO1 shRNA (1.38×10^7 copies/mL), rat FoxO3a shRNA (1.18×10^7 copies/mL), or rat FoxO4 shRNA (1.1×10^9 copies/mL) for 24 hours in SmGm-2 fully supplemented growth media before having the media replaced with serum and growth factor starved Dulbecco's Modified Eagle Medium/Ham's F12 media for 48 hours. For NO stimulation experiments measuring cGMP, cells were pretreated with 10 μ M sildenafil citrate (Sigma, PZ0003) for 45 minutes to inhibit cGMP-specific phosphodiesterase 5 activity, and then stimulated with the NO-donor, diethylammonium (Z)-1-(N,N-diethylamino)diazene-1,1,2-diolate (DEA-NONOate, Cayman, 82100) at a concentration of 10^{-6} M, for 15 minutes prior to lysis. NO-dependent VASP phosphorylation was assessed using DEA-NONOate treatment without sildenafil citrate treatment.

For luciferase-reporter experiments, Cos7 cells were cultured in DMEM with 10% FBS to 70% confluency in 6-well dishes. Media was then removed from cells and replaced with Opti-MEM serum-free media (Gibco, 31985-062) and transfected with 2 μ g of the indicated pGL3 luc+ vector using Lipofectamine 3000 reagent mixture according to manufacturer's protocol (Invitrogen, L3000-015) for 8 hours. Opti-MEM media was then removed and replaced with DMEM media and cells were allowed to grow for 40-48 hours.

qRT-PCR:

RASMCs were grown in 6-well plates until approximately 90% confluent before being washed and switched to serum and growth factor starved media. Cells were then subjected to 48-

hour drug and/or peptide treatment before lysis in TRIzol reagent (ThermoFisher, 15596026). The Direct-zol RNA miniprep plus (Zymo, R2051) manufacturer's protocol was used to isolate RNA from cells. For cDNA synthesis, the SuperScript IV First Strand Synthesis (ThermoFisher, 18091050) kit manufacturer's protocol was used. For quantitative real time PCR analysis, the PowerUp SyBr Green (ThermoFisher, A25742) and 1 μ M target primer (Table 8) were mixed according to manufacturer's protocol with settings for 40 PCR cycles, 95°C melting temperature, 58°C annealing temperature, and 72°C extension temperature set on a QuantStudio 5 Real-Time 384-well PCR System (ThermoFisher A28140) for amplification. The Δ - Δ -ct value fold change in expression was used in order to control for cell number and RNA quality with values normalized to an 18S housekeeping gene transcript.

Western blot:

RASMCs were cultured in 12-well culture dishes until approximately 90% confluent before being switched to serum and growth factor starved media for 48 hours. Cells were then washed with PBS and 1X Cell Lysis Buffer (Cell Signaling, 9803) containing: (pH 7.5) 20 mM Tris-HCl, 1 mM Na₂EDTA, 1 mM EGTA, 1% Triton, 1 mM β -glycerophosphate, 1 mM Na₃VO₄, 1 μ g/mL leupeptin, 2.5 mM sodium pyrophosphate, and additional 1X protease (MilliporeSigma P8340) and phosphatase inhibitors (MilliporeSigma, P5726) at 4°C. A bicinchoninic acid kit (ThermoFisher, 23225) was used according to the manufacturer's protocol to quantify lysate protein concentration and approximately 15 μ g of protein was used for each western blot lane. Lysates were boiled at 100°C for 10 minutes and Laemmli buffer was added such that final lysates contained: (pH 6.8) 31.5 mM Tris-HCl, 10% glycerol, 1% SDS, 2.5% β -mercaptoethanol and 0.005% Bromophenol Blue before being loaded onto 4-12% gradient BisTris polyacrylamide gels (Invitrogen Life Technologies, NP0335BOX). Proteins were

transferred from polyacrylamide gels to nitrocellulose membranes (LiCor, 926-31092) and blocked for approximately 30 minutes at room temperature with 1% BSA in PBS. Membranes were incubated in primary antibody (Table 9) solution containing 1% BSA in PBST overnight at 4°C. An Odyssey CLx Imager (LiCor, 9140) was used for fluorescence visualization and semi-quantitative analysis was performed using Image Studio software.

sGC β promoter-luciferase vector generation and luciferase assays:

Human GUCY1B3 promoter DNA was generated as previously described.⁷⁵ Promoter DNA was truncated from a 2396 bp total length GUCY1B3 fragment upstream of the transcription start site (TSS) to generate fragments ranging from 400 bp to 2396 bp upstream of the TSS (Figure 3A). Each DNA sequence was confirmed by Sanger sequencing and GUCY1B3 DNA promoter-luciferase constructs were inserted into a pGL3 luciferase vector (modified Luc+ Firefly luciferase gene, Promega PR-E1761) with NheI and XhoI restriction enzymes.

Luciferase assays were performed using a Veritas luminometer (Turner Biosystems 998-9100) 96-well plate reader system. Cells were washed twice with PBS and lysed in 1X Promega Lysis Buffer (Promega, E1531) according to manufacturer's protocol and 100 μ L of lysates were added to black 96-well clear bottom plates (Corning, 07-200-567). 100 μ L of fresh Promega luciferin reagent (E1501) was added individually to each well using Veritas automated injector system and luminescence was measured 0.1 seconds to 2 seconds after the addition of luciferin substrate and total luminescence was recorded using Veritas software and Luciferase assay system with injector protocol. Adjusted measurements were determined by subtracting the luminescence readings from samples with no luciferin reagent added to remove any potential background.

DNA Cross-Linking and Sonication:

HASMC were grown to 90% confluency before being washed twice in 1X PBS and cultured in serum and growth factor starved Dulbecco's Modified Eagle Medium/Ham's F12 media, as described above,²³² for 48 hours in 15 cm culture dishes. Cells were then washed twice with 1X PBS and removed from culture dishes using a cell scraper and centrifuged at 300 rpm for 5 min in 5 mL 1X PBS. Cells were then resuspended in 10 mL 1X PBS for chromatin immunoprecipitation experiments at approximately 10^6 cells/tube. Cells were spun down at 2000 rpm for 5 min at 4°C and PBS was aspirated. Each group of cells was then resuspended in 500 μ L preparatory solution containing 1X PBS with 20 mM sodium butyrate (MilliporeSigma, 156-54-7), 1 mM phenylmethylsulfonyl fluoride (PMSF, MilliporeSigma, 329-98-6), and 1X protease inhibitors (MilliporeSigma, P8340). To each tube, 25 μ L of 2.5 M glycine (MilliporeSigma, 56-40-6) and 31.25 μ L of 16% paraformaldehyde (Fisher, F75P-20) were added and incubated at room temperature for 10 minutes. Cells were then centrifuged at 2000 rpm for 5 minutes at 4°C and supernatant was removed. Pellets were then resuspended in preparatory solution. Cells were centrifuged and resuspended in preparatory solution two additional times to wash pellets of paraformaldehyde. Cell pellets following third centrifugation were resuspended in 120 μ L of complete lysis buffer containing 50 mM Tris-HCl (pH=8.0; Manufacturer), 10 mM EDTA (Manufacturer), 1% SDS, 20 mM sodium butyrate, 1 mM PMSF, and 1X protease inhibitors in water. These contents were vortexed and placed on ice for 5 min. Contents were then transferred to sonication tubes (Diagenode C300010016) and sonicated in a Picoruptor sonicator (Diagenode B01060010) at 0°C for 11 minutes (alternating 30 seconds sonication/30 seconds rest) and cooled in a water bath at 4°C (Diagenode B02010003). 400 μ L of RIPA ChIP lysis buffer containing 10 mM Tris-HCl (pH=7.5), 140 mM NaCl, 1 mM EDTA, 0.5 mM EGTA, 1% Triton X-100, 0.1%

SDS, 0.1% Na-Deoxycholate, 20 mM sodium butyrate, 1 mM PMSF, and 1X protease inhibitors in water was added to each sample and the solution was mixed by vortex and centrifuged at 11000 RPM for 10 min at 4°C. The supernatant was then carefully transferred to a clean Eppendorf tube. 410 µL RIPA ChIP lysis buffer was then added to the remaining pellet and the mixture was vortexed and centrifuged at 11000 RPM for 10 min at 4°C. The supernatant was then added to the previous 400 µL and vortexed. Each 800 µL solution of cellular material was subdivided into 8 aliquots of 100 µL/each. Aliquots were stored at -80°C until next steps.

Immunoprecipitation Bead Preparation:

For 16 ChIP samples, 180 µL of Protein G Dynabeads (Invitrogen 100040) solution were resuspended and collected in a 1.5 mL Eppendorf tube and placed on a magnetic rack (Invitrogen 12321D). Beads were then captured by the magnetic rack, buffer was removed, and tubes were removed from the rack. 500 µL of RIPA ChIP lysis buffer without sodium butyrate, protease inhibitors or PMSF was added to the Dynabeads for 5 min and the solution was continuously rotated. Dynabead solutions were centrifuged at 200 rpm for 10 seconds, tubes were placed on the magnetic rack, solution was removed from the beads and this washing procedure was repeated two additional times. Beads were then resuspended in 170 µL of ChIP RIPA lysis buffer without sodium butyrate, PMSF or protease inhibitors. 10 µL of washed beads was then added to 90 µL ChIP RIPA buffer without sodium butyrate, PMSF or protease inhibitors. Primary or IgG control antibody was then added to each respective tube at a concentration of 1 µg/immunoprecipitation experiment and rotated at room temperature for 2 hours.

Immunoprecipitation:

One aliquot of chromatin (100 µL) was added to the magnetic bead/antibody mix and rotated overnight at 4°C. Tubes were then centrifuged and placed on a magnetic rack.

Supernatant was then removed and 100 μ L of ice-cold CHIP RIPA buffer was added and used to resuspend beads. This wash step was repeated two additional times. To each tube 100 μ L of Tris-EDTA (TE) buffer containing 10mM Tris-HCl and 1mM EDTA at pH=8.0 was added to the beads. The TE/bead mixture was resuspended in the tube and transferred to a clean PCR tube and rotated for 5 minutes at room temperature. Another 100 μ L CHIP aliquot (this will be the input sample) was then added to a clean PCR tube without being subject to immunoprecipitation. To each immunoprecipitation sample 150 μ L of elution buffer containing 20 mM Tris-HCl (pH=7.5), 5 mM EDTA, 50 mM NaCl, 20 mM sodium butyrate, 1 mM PMSF and 1 X protease inhibitors was added and 200 μ L was added to each input sample before each tube was placed on a heating block at 68°C for 2 hours. Every 30 minutes the samples were mixed by vortexing. Input samples were then removed from heat and centrifuged before being moved to a clean 1.5 mL tube. 200 μ L of elution buffer was then added to the PCR tube, vortexed to mix, centrifuged and then added to the previous 300 μ L in the 1.5 mL tube. Immunoprecipitation samples were then removed from heat, centrifuged, and placed on the magnetic rack to collect the beads. Supernatant was then removed from the tubes and placed in a clean 1.5 mL tube. 150 μ L of elution buffer was then added to the PCR tubes with the beads and incubated at 68°C for 5 minutes. PCR tubes were then placed on the magnetic rack and the supernatant was removed and added to the previous 150 μ L of immunoprecipitated sample in the 1.5 mL tube. 200 μ L of additional elution buffer were added to these tubes to bring the total volume to 500 μ L.

DNA extraction:

500 μ L of phenol-chloroform was added to each sample (immunoprecipitated and input) and samples were vortexed and incubated at room temperature while rotating for 5 minutes. Tubes were then centrifuged at 12000 rpm for 10 minutes at 4°C. The infranatant solution was

then carefully removed and discarded from the tube. 460 μ L of chloroform was added to each tube and then vortexed and incubated at room temperature for 5 minutes while rotated. Mixtures were centrifuged for 10 minutes at 4°C at 12000 rpm and the infranatant was again removed and discarded. A solution of 938 μ L of 96% EtOH at -20°C, 50 μ L of 5 M NaCl, and 12 μ L linear acrylamide (Invitrogen AM9520) was added to each tube and incubated overnight at -80°C. Tubes were then centrifuged at 14000 rpm for 15 minutes at 4°C. Supernatant was carefully removed from the pellet and allowed to completely evaporate at room temperature. DNA was then dissolved in 50 μ L Ultrapure water (Invitrogen 10977023) and then stored at -20°C for qRT-PCR reactions. qRT-PCR reactions were performed as described above following cDNA synthesis. Enrichment % was determined by the amount of IP sample detected by PCR compared to the input amount for each ChIP primer. ChIP primer sequences can be found in Table 8 which designate DNA sequences spanning specific regions of human DNA upstream of the GUCY1B3 gene as shown in Figure 4B.

Statistics:

Statistical analyses were performed using Graphpad Prism Software 8.0d. Based upon normality using a Shapiro-Wilk test, p-values for statistics in qPCR, Western blot, and immunostaining were assessed using an unpaired *t*-test with or without Welch's correction to account for unequal variance following Shapiro-Wilk test results. Symbols were consistent throughout wherein * denotes $p \leq 0.05$, ** denotes $p \leq 0.01$, *** denotes $p \leq 0.001$ and **** denotes $p < 0.0001$.

4.4 Results:

We first sought to identify which FoxO transcription factor was responsible for the regulation of sGC expression in smooth muscle cells (SMC). We began by creating adenoviral shRNA constructs targeting either FoxO1, FoxO3a or FoxO4. Rat aortic SMCs were then treated with each FoxO shRNA construct individually. FoxO1, FoxO3a and FoxO4 RNA were measured by RT-qPCR to validate knockdown of expression, respectively, showing a 56% decrease in FoxO1 mRNA expression (Figure 22A), 67% decrease in FoxO3a mRNA expression (Figure 22D), and a 58% decrease in FoxO4 mRNA expression (Figure 22G), respectively. Somewhat surprisingly, we observed a 2.9-fold increase in sGC α and sGC β mRNA expression following FoxO1 shRNA treatment (Figure 18A), and a 2.3-fold increase in sGC α mRNA and 2.1-fold increase in sGC β mRNA expression following FoxO3a shRNA treatment by RT-qPCR (Figure 18B). Conversely, following FoxO4 shRNA treatment we observed a 54% decrease in sGC α mRNA and 56% decrease in sGC β mRNA expression (Figure 18C), indicating antagonistic regulatory roles for FoxO1 and FoxO3a as compared to FoxO4. Likewise, western blot analyses validated knockdown of targets showing 78% knockdown of FoxO1 (Figure 22B-C), 43% knockdown of FoxO3a (Figure 22E-F), and 85% knockdown of FoxO4 (Figure 22H-I). FoxO1 or FoxO3a shRNA knockdown both resulted in elevated sGC β protein expression (Figure 18D, F), while FoxO4 shRNA caused a 49% decrease in sGC β protein expression (Figure 18E, G), consistent with both the loss of FoxO4 mRNA (Figure 22G) and protein expression (Figure 22H-I), and the loss of sGC α and sGC β mRNA (Figure 18C) expression following FoxO4 shRNA treatment. We observed no off-target knockdown of FoxO genes from each specific FoxO shRNA (Figure 23A-C), and each FoxO shRNA showed significant knockdown of the known gene target, glucose-6-phosphatase (Figure 22A, D, G).¹¹⁶ These data indicate the effects on

FoxO expression were specific to each gene and suggest a complex interaction for the regulation of sGC.

Additionally, we treated rat aortic SMC and measured cGMP production and phosphorylation of the protein kinase G specific-serine 239 residue of vasodilator stimulator protein (VASP) as indicators of direct and downstream sGC function following treatment with FoxO shRNAs or the FoxO inhibitor, AS1842856,¹⁶⁸ (Figure 19A). Whereas FoxO1 or FoxO3a shRNA treatment showed no significant differences in cGMP production from controls, FoxO4 shRNA, triple FoxO shRNA treatment, and FoxO inhibition all showed significant decreases in NO-stimulated cGMP production (Figure 19B). Similarly, cGMP production causes phosphorylation of the cGMP-activated protein kinase target, vasodilator stimulated phosphoprotein (VASP) at serine 239.¹⁹⁹ When we measured the phosphorylation of this residue by western blot, we observed no significant change at baseline following FoxO1 or FoxO3a shRNA treatment and likewise observed no significant change after stimulation with the nitric oxide (NO) donor molecule, 2-(N,N-Diethylamino)-diazene-2-oxide, diethylammonium (DEA-NONOate). After treatment with FoxO4 shRNA, triple FoxO shRNA or FoxO inhibition, we observed significant decreases in baseline phosphorylated VASP and significant decreases in phosphorylated VASP following DEA-NONOate stimulation (Figure 19C).

Based upon our data, we sought to identify where FoxO4 was capable of regulating the expression of sGC. To do this, we transfected a pGL3 Luciferase – reporter vectors containing various lengths of sGC promoter DNA upstream to the reported transcription start site into Cos7 cells, which do not express any sGC, thereby avoiding confounding influences of endogenous expression (Figure 20A). Upon transfection of these vectors, we observed the highest luciferase activity in vectors containing promoter lengths of 1400-1800 bp upstream of the sGC β

transcription start site with no significant differences between these vectors, an intermediary (85% of maximum) luciferase activity in the vector containing 900 bp of DNA upstream of the sGC β transcription start site, and the least amount of luciferase activity (62% of maximum) was observed in the vectors containing between 400 and 500 bp of DNA upstream to the sGC β transcription start site (Figure 20B). Cos7 cells were then transfected with both pGL3 Luciferase – reporter vectors and treated with either DMSO or AS1842856, as previously reported to have pleiotropic efficacy to inhibit multiple FoxO proteins.¹⁶⁸ Treatment of SMC has also been shown to dramatically decrease sGC expression.¹⁴⁷⁻¹⁴⁸ Following FoxO inhibitor treatment, luciferase activity was significantly blunted by 70% – 93%, as compared to the controls (Figure 20C).

We next cultured human aortic smooth muscle cells and performed chromatin immunoprecipitation (ChIP) experiments with primers designed to span 2400 bp upstream of the human GUCY1B3 gene transcription start site (Figure 21A). These experiments reveal multiple sites of FoxO4 binding to the human sGC β promoter (Figure 21B), as 3 primer regions show significantly enriched DNA pulldown by FoxO4 immunoprecipitation over the IgG control pulldowns (Figure 21C). These sites suggest that FoxO4 is present at the predicted FoxO4 DNA binding locations found within Primer 2, Primer 4 and Primer 5.

These data show that FoxO4 plays a crucial role in the maintenance of smooth muscle expression of sGC at the transcriptional and protein level. This loss of sGC precipitated by FoxO4 loss causes deficits in cGMP production and PKG-dependent phosphorylation. Additionally, sGC β luciferase-reporter experiments indicate that sGC transactivation requires FoxO transcription factor activity, and ChIP experiments indicate that FoxO4 binds at multiple locations within the sGC β promoter near the TSS. Together, this indicates that FoxO4 is a

critical transcription factor for sGC expression and downstream function due to the binding which occurs on the promoter.

4.5 Discussion:

In this study we identify FoxO4 as the key regulatory FoxO transcription factor for sGC β in vascular smooth muscle. We also demonstrate that FoxO4 is necessary for the proper transcriptional and protein expression of sGC β and function of downstream signaling in the NO-sGC-cGMP pathway. Additionally, we show that sGC β promoter-luciferase activity requires FoxO transcription factor activity and that FoxO4 binding occurs within the promoter region examined by promoter-luciferase experiments. Together, these data show that FoxO4 is an important transcription factor necessary for the regulation of sGC β in vascular smooth muscle in humans as well as animal models.

Our study shows that the loss of FoxO4 results in impaired expression of sGC at the mRNA and protein level, while showing a surprising increase in sGC mRNA and protein following FoxO1 or FoxO3a knockdown. These data are in line with the disparate functions that have been observed between the FoxO transcription factors during development,¹³⁹ and these findings may be indicative of the structural differences that have been observed.¹⁷⁶ Because the loss of FoxO1 and FoxO3a caused elevations in expression of sGC, these FoxO transcription factors may act to prevent excess sGC expression in smooth muscle via competitive sGC regulation. Indeed, crystal structures of the DBD of the FoxO transcription factors demonstrate almost identical DNA recognition sequences with most variation in affinity stemming from the surrounding bases.^{88,233-234}

Analysis of downstream sGC function also demonstrated the importance of FoxO4 in the NO-sGC-cGMP signaling pathway. These data showed that loss of FoxO4 significantly impairs the amount of cGMP produced and PKG-dependent phosphorylation of VASP. Notably, triple FoxO shRNA further decreased cGMP production and VASP phosphorylation over FoxO4 shRNA treatment alone and phenocopied our previous data showing loss of sGC expression and function following FoxO inhibition.¹⁴⁷⁻¹⁴⁸ These data allude to diminished, but not absent, roles for FoxO1 and FoxO3a in the regulation of sGC expression and downstream function in vascular SMC.¹³⁴⁻¹³⁶

Experimental analysis of the sGC β promoter further reinforces the importance of the FoxO transcription factors in the regulation of the human sGC β gene. Transfection with sGC β -luciferase causes effective luciferase activity, however, inhibition of the FoxO transcription factors in transfected cells abolishes this luciferase activity. Previous study of the sGC β promoter region in a neuroblastoma cell line also identified that the first 0.5kb of DNA upstream of the transcriptional start site were critical to its gene expression.⁷⁵ Additionally, FoxO4 ChIP experiments demonstrate that FoxO4 interacts with the human sGC β promoter at several locations that showed FoxO activity-dependence. Many of these FoxO4-bound sGC β promoter regions align with those identified previously to be necessary for the expression of sGC by promoter-luciferase experiments.⁷⁵ Previous data has demonstrated that the NO-sGC-cGMP pathway is critical to proper nerve cell function,²³⁵ though further study will be necessary to identify whether the regulation of sGC is mediated by FoxO4 across multiple tissue types.

Together, these data are the first to identify FoxO4 as a key regulatory transcription factor for SMC expression and downstream of sGC. Moreover, our findings suggest a competitive interaction between the other FoxO proteins and FoxO4 at regulatory sites. We

identified several important FoxO-regulated regions along the human sGC β promoter where FoxO4 binds to interact with the chromatin. All of this establishes that FoxO4 plays an essential role in the expression and function of sGC in smooth muscle.

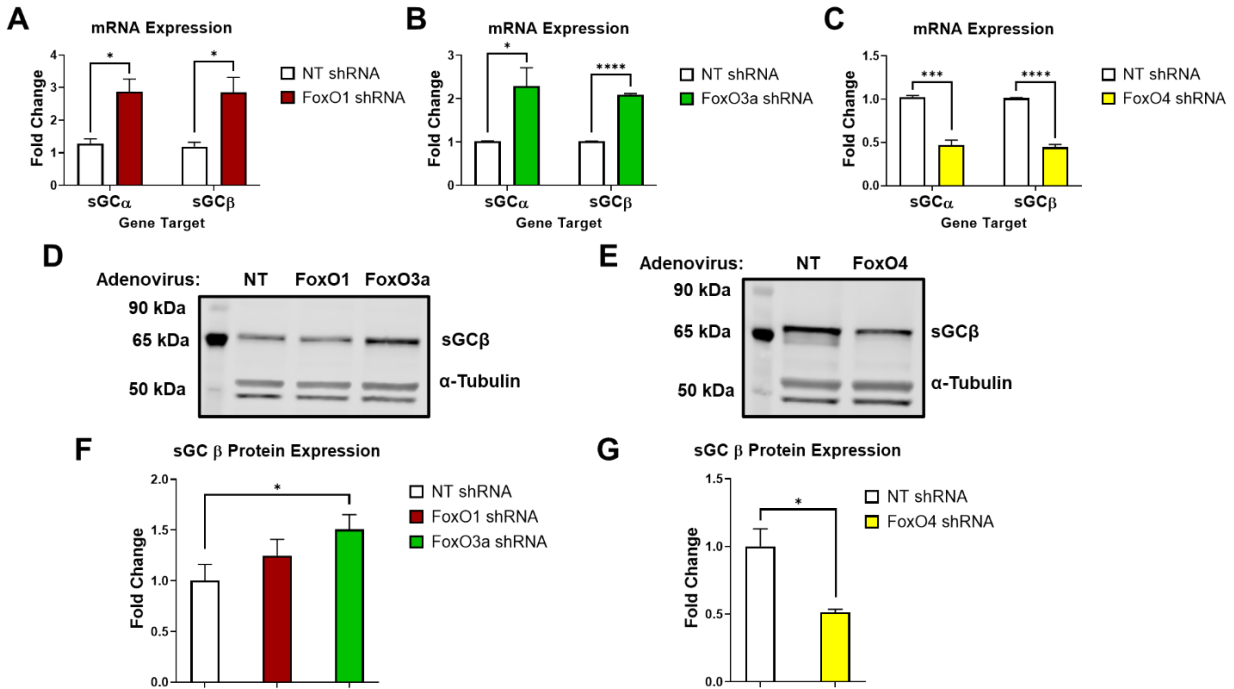


Figure 18

Knockdown of FoxO transcription factors reveal opposing sGC regulation by FoxO1 or FoxO3a and FoxO4.

RT-qPCR experiments from RASMCs showing expression of sGC α or sGC β mRNA following treatment with non-targeting (NT) shRNA control vs. A) FoxO1 shRNA treatment, B) FoxO3a shRNA, or C) FoxO4 shRNA. Western blots for D) sGC β protein expression and F) quantification following NT shRNA vs. FoxO1 FoxO3a shRNA-treatment or E) sGC β protein expression and G) quantification following NT shRNA vs. FoxO4 shRNA. Error bars represent S.E.M.

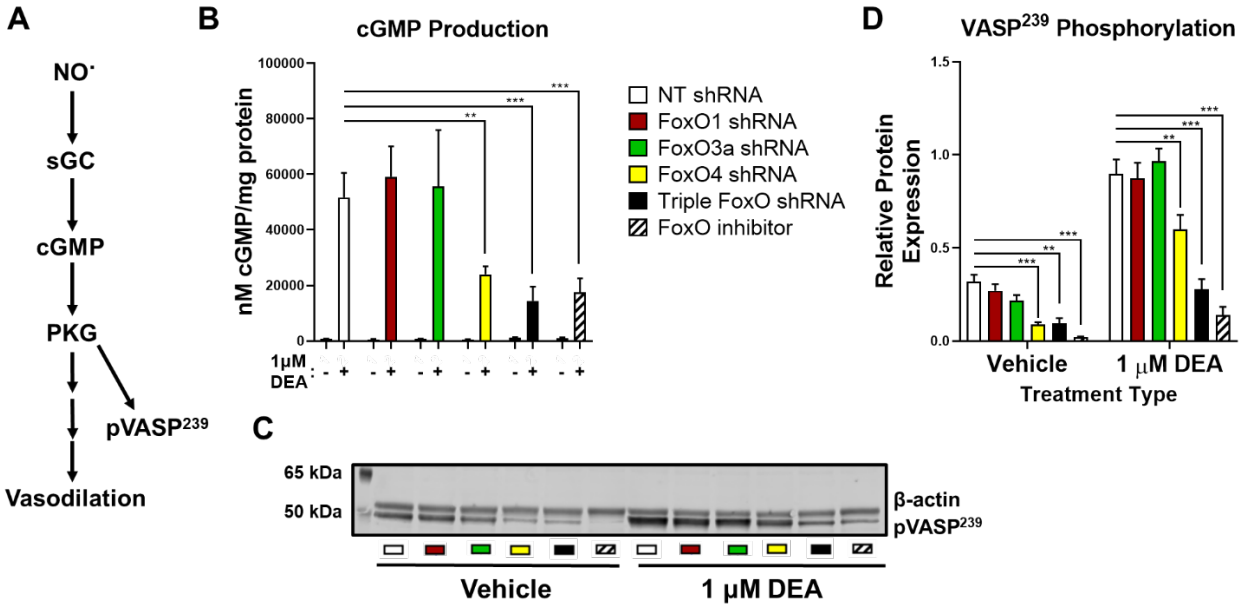


Figure 19

Loss of FoxO4 or all FoxO transcription factor activity blunts downstream sGC function.

A) Vasodilatory signaling contributors and downstream targets in vascular SMC. B) ELISA assay measuring total cGMP production in RASMCs stimulated with vehicle or DEA-NONOate following treatment with shRNA or FoxO inhibitor. Western blot C) and quantification D) of phosphorylated VASP in RASMCs stimulated with vehicle or DEA-NONOate following treatment with shRNA or FoxO inhibitor.

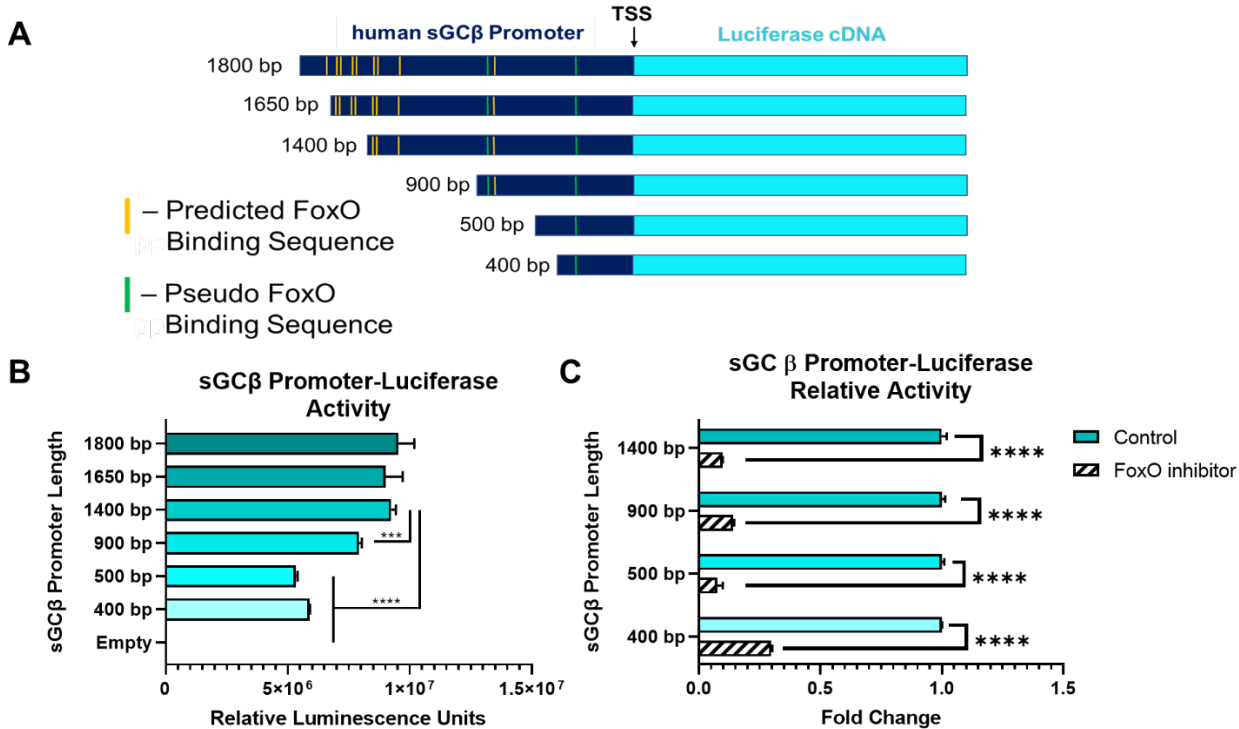


Figure 20

sGC β promoter-luciferase shows that sGC β expression requires FoxO transcriptional activity.

A) Map of human GUCY1B3 (sGC β_1) gene fragments into pGL3 luciferase-reporter vectors used for transfection with putative FoxO and pseudo-FoxO binding sequences labeled in yellow and green, respectively. B) Luciferase activity of cells transfected with different length luciferase-reporter vectors. C) Fold change in luciferase activity of transfected cells treated with vehicle or FoxO inhibitor.

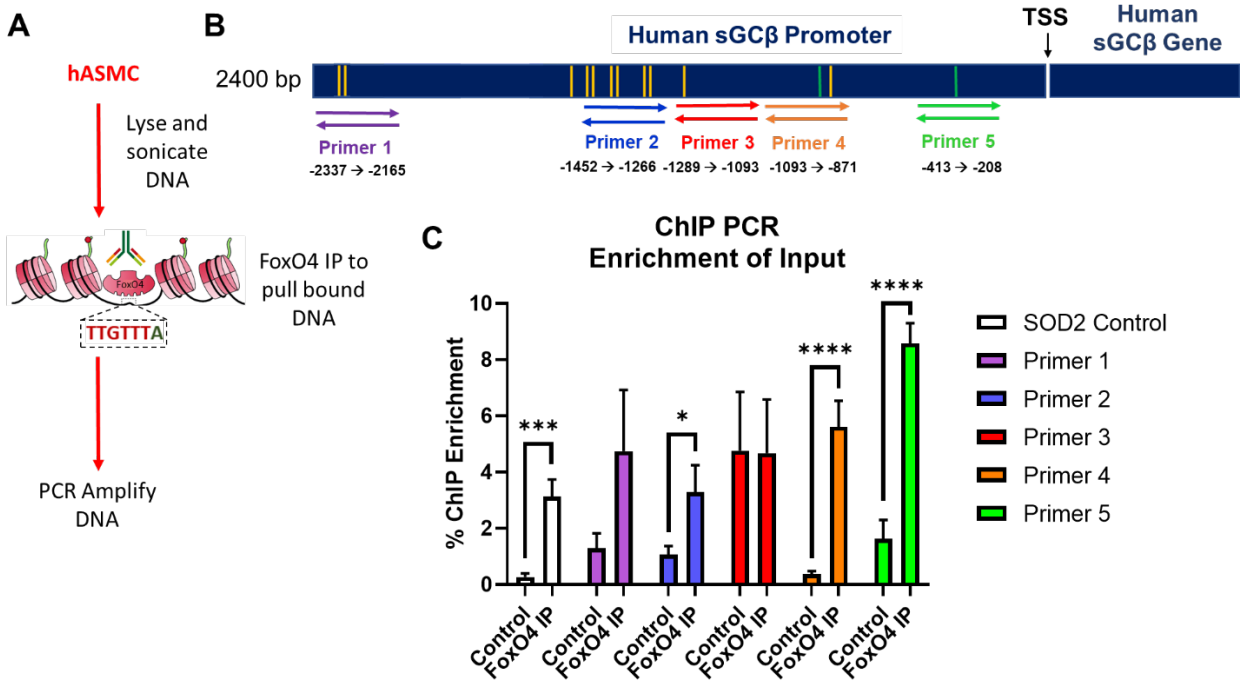


Figure 21

FoxO4 binds the human sGC β promoter at locations of predicted FoxO binding sequences.

A) Protocol for chromatin immunoprecipitation experiments using FoxO4 pulldown to identify interactions on human DNA. B) Map of human sGC β_1 promoter DNA with predicted FoxO and pseudo-FoxO binding sequences and PCR products from the respective labeled primer sets upstream of the transcription start site. C) Chromatin immunoprecipitation experiments from human aortic SMC for five locations on human sGC β_1 promoter region and previously identified FoxO binding location on SOD2 promoter.

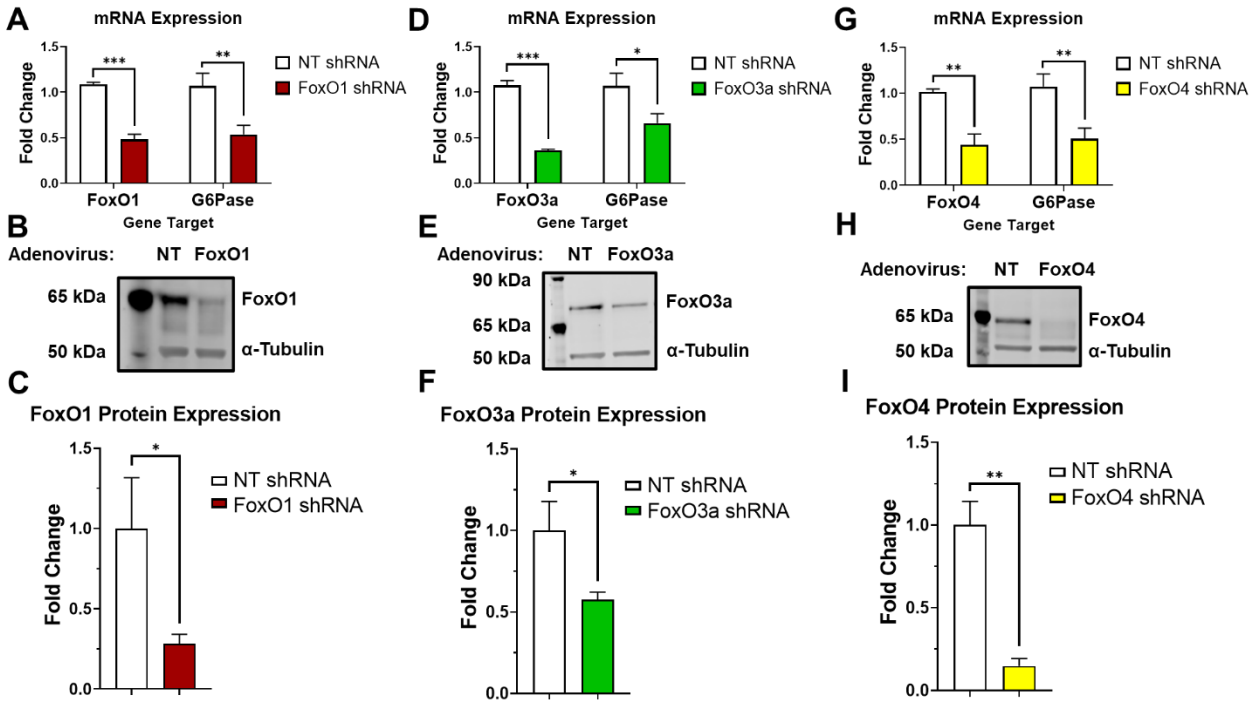


Figure 22

FoxO shRNAs show effective knockdown of target mRNA and protein expression.

RASMCs treated with NT shRNA or FoxO1 shRNA showing RT-qPCR or Western blot analyses from RASMCs. RT-qPCR showing expression of each respective FoxO gene and G6Pase following treatment with non-targeting NT shRNA control vs. A) FoxO1 shRNA treatment, B) FoxO3a shRNA, or C) FoxO4 shRNA. Western blots for D) sGC β protein expression and F) quantification following NT shRNA vs. FoxO1 FoxO3a shRNA-treatment or E) sGC β protein expression and G) quantification following NT shRNA vs. FoxO4 shRNA.

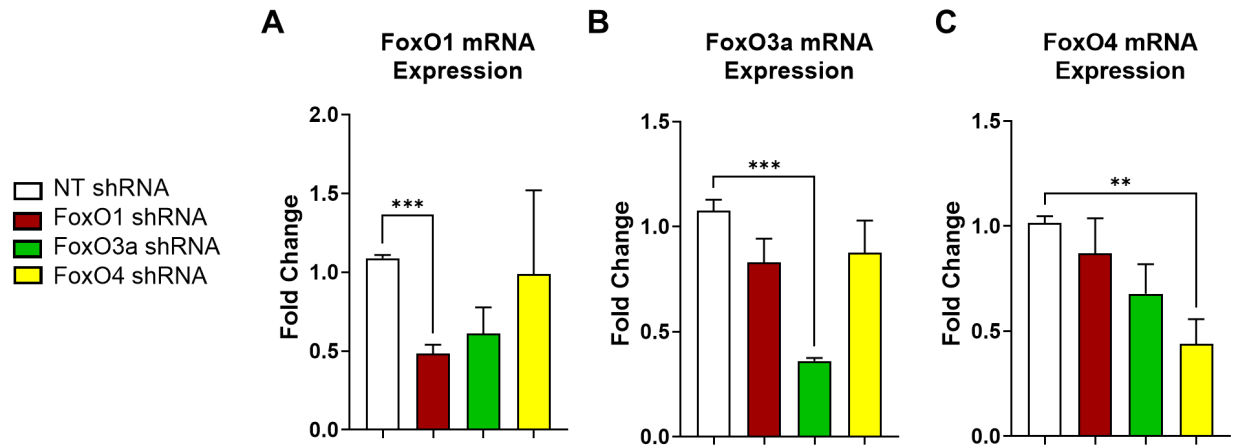


Figure 23

FoxO shRNAs show specific knockdown of the intended target transcription factor.

RT-qPCR following treatment with NT, FoxO1, FoxO3a, or FoxO4 shRNA showing A) FoxO1 mRNA, B) FoxO3a mRNA, or C) FoxO4 mRNA expression.

Table 8: Primer Sequences for RT-qPCR and ChIP

| Primer Usage | Primer Identity | Sequence (5'→3') |
|--------------|---|---------------------------------|
| RT-qPCR | Rat sGC α 1 F | CTC CCG TGA CCG CAT CAT |
| | Rat sGC α 1 R | CCG GTG TTG ATG TTG ACT GA |
| | Rat sGC β 1 F | AAT TAC GGT CCC GAG GTG TG |
| | Rat sGC β 1 R | GCA GCA GCC ACC AAG TCA TA |
| | Mammalian 18S F | ACG GAC AGG ATT GAC AGA TTG |
| | Mammalian 18S R | TTA GCA TGC CAG AGT CTC GTT |
| | Rat G6Pase F | GGC TCA CTT TCC CCA TCA GG |
| | Rat G6Pase R | ATC CAA GTG CGA AAC CAA ACA G |
| | Rat FoxO1 F | CAC CTT GCT ATT CGT TTG C |
| | Rat FoxO1 R | CTG TCC TGA AGT GTC TGC |
| | Rat FoxO3 F | CGG CTC ACT TTG TCC CAG AT |
| | Rat FoxO3 R | TCT TGC CAG TCC CTT CGT TC |
| | Rat FoxO4 F | AGG CTC CTA CAC TTC TGT TAC TGG |
| | Rat FoxO4 R | CTT CAG TAG GAG ATG CAA GCA CAG |
| ChIP | Human SOD2 Promoter Primer F | GTC CCA GCC TGA ATT TCC |
| | Human SOD2 Promoter Primer R | CTA GGC TTC CGG TAA GTG |
| | Human sGC β 1 Promoter Primer 1 F | CGC GTG CTA GCT AGT GCT GG |
| | Human sGC β 1 Promoter Primer 1 R | GCA TGC ATG TGC CTT TAT GG |
| | Human sGC β 1 Promoter Primer 2 F | GCC TGT GTT ATT ACC CAC ATA GC |
| | Human sGC β 1 Promoter Primer 2 R | CAA TTA ACC ACT GAT TTT GAA CC |
| | Human sGC β 1 Promoter Primer 3 F | GGT TCA AAA TCA GTG GTT AAT TG |
| | Human sGC β 1 Promoter Primer 3 R | GCT GAC ATC AGC ACC GAG AG |
| | Human sGC β 1 Promoter Primer 4 F | CTC TCG GTG CTG ATG TCA GC |
| | Human sGC β 1 Promoter Primer 4 R | GAG GAA CAG GAA GTG GCA GC |
| | Human sGC β 1 Promoter Primer 5 F | GCC AGC AAC AGA GGA TAT TCC |
| | Human sGC β 1 Promoter Primer 5 R | GGA GAA GCC CCA GCC GTG C |

Table 9: Catalog of Antibodies for Western Blot and ChIP

| Antibody | Species | Application | Concentration | Company | Cat. Number |
|------------------------------------|----------------|--------------------|-----------------------|----------------|--------------------|
| sGCβ | rabbit | WB | 1:1000 | Cayman | 160897 |
| FoxO1 | rabbit | WB | 1:1000 | Cell Signaling | 2880S |
| FoxO3a | rabbit | WB | 1:1000 | Cell Signaling | 2497S |
| FoxO4 | rabbit | WB, ChIP | 1:1000, 4 μ g | Abcam | ab128908 |
| α-tubulin | mouse | WB | 1:10,000 | Sigma | T6074 |
| β-actin | mouse | WB | 1:500 | Santa Cruz | sc-47778 |
| Phospho-VASP (S239) | rabbit | WB | 1:1000 | Cell Signaling | 3114S |
| Rabbit IgG | rabbit | ChIP | concentration matched | Abcam | ab171870 |

5.0 Conclusions and Future Directions

5.1 Conclusions of Our Work

In this dissertation, my work and that of my colleagues has established several fundamental new findings that have important basic science and clinical implications for our lab and those of others in our field. Our goals were to identify the transcription factors responsible for the regulation of sGC within the SMC. To this end, we analyzed the sGC promoter regions and hypothesized that the FoxO family of transcription factors are capable of governing sGC expression.¹⁴⁷ To this end, we inhibited the FoxO transcription factors in aortic SMC and discovered that loss of their activity abolishes sGC mRNA and protein expression. Furthermore, loss of FoxO transcriptional activity blunted cGMP production and NO-dependent vasorelaxation of isolated mouse aortas. Our next work sought to identify the mechanisms for the elevated renovascular function in contralateral arteries of those with renal hypertension. In a 2K1C model of renal hypertension we showed that renal stenosis causes increased NO-dependent vasorelaxation and expression of sGC within the contralateral renal artery.¹⁴⁸ In cultured renal SMC, we showed that this process occurs through an Ang II-dependent manner, surprisingly via agonism of the AT1R and established that not only is sGC expression increased at the genetic and protein level, but that it also impacts downstream cGMP production as well. This process was also found to require functional FoxO transcription, as their inhibition abolished all increases in expression and downstream function of sGC. Finally, we identified in aortic SMC that loss of FoxO1 or FoxO3 remarkably increase sGC mRNA and protein expression, while only FoxO4 knockdown alone produced loss of sGC expression. These data

suggest that there is a complex regulatory interaction within the sGC promoter for governance of sGC expression. We then show that loss of FoxO4 triggers a loss of downstream sGC-dependent signaling; a process that was exacerbated via concomitant knockdown of FoxO1 and FoxO3 in a manner that phenocopied pharmacological inhibition of the FoxO transcription family.¹⁴⁷⁻¹⁴⁸ Because sGC β is the integral NO-binding subunit and clinical target for many sGC modulator therapies being investigated or approved for treatment of CVD,^{58-60,71,208,217} we sought to identify which, if any, predicted FoxO binding sequences are important for the regulation of sGC β expression. sGC β promoter-luciferase experiments show that the 0.5kb of DNA upstream of the transcription start site represents an essential, FoxO-dependent function. We next used FoxO4 ChIP in human aortic SMC and show that FoxO4 binds several locations predicted by in silico and luciferase-reporter experiments, demonstrating that FoxO4 interacts directly with the human sGC β promoter to regulate its function.

5.2 What are Some of the Additional Non-Transcriptional Mechanisms of sGC?

There are several mechanisms by which sGC is regulated at the post-transcriptional level which govern the functional capacity of the enzyme under various physiological circumstances. Because the FoxO transcription factors are involved in a multitude of different signaling pathways, it is possible that these other regulatory pathways represent indirect methods to alter the expression and function of sGC. Additional regulatory pathways may work to counteract the activity of the FoxO transcription factors, and the scale of this competition may provide future insight for the overall regulation of sGC.

Redox signaling phenomena such as the excess production of hydrogen peroxide,³⁸ superoxide,³⁹ and peroxynitrite have been shown to oxidize sGC heme to “turn off” the production of cGMP by desensitizing the enzyme to NO.⁴⁰ Because of the redox-sensitive cysteine residues and heme iron group within sGC, numerous pathways possess the potential to affect sGC expression and function in physiologically relevant ways. Rahaman, et al. recently identified Cyb5R3 activity as necessary for the maintenance of the reduced (NO-sensitive) redox state of the heme group found within sGC β .⁴¹ Indeed, the loss of Cyb5R3 expression not only leads to blunted cGMP production by sGC, it also leads to loss of sGC protein expression and targeted degradation as a result.

As discussed in Chapter 1, Hsp90 plays an integral role in the proper insertion of a heme moiety into several proteins which require heme for proper function.^{32-34,44,236} The sGC β 1 subunit was first identified to interact with Hsp90 in the early 2000’s where it was presumed only to be a necessary step in the proper formation of the enzyme.⁴⁴ As more research has investigated the interaction between Hsp90 and sGC, it now appears that Hsp90 can keep sGC β 1 stabilized under unfavorable circumstances and may act as a mechanism of keeping additional sGC pools sensitive that do not conform to the conditions which may be found in reducing environments.³² Moreover, the interaction between Hsp90 and sGC β must be interrupted by the presence of NO in order for sGC α to form with sGC β to form a functional cGMP-producing enzyme.³³ This interaction provides an supplementary method for control of sGC in the vasculature, though more research is necessary to elucidate the complete how Hsp90 is regulated and how it, in turn regulates sGC.

Another mechanism shown to affect sGC signaling is the regulatory extracellular protein, thrombospondin-1 (TSP-1), which has been shown to act through the cluster of differentiation 47

(CD47) in multiple vascular cell types.²³⁷⁻²³⁹ Treatment with TSP-1 even at low concentrations was found not only to inhibit the production of NO-dependent sGC activity, but also to inhibit the production of cGMP following treatment with sGC modulator drugs which work independent of NO exposure.²⁴⁰ The mechanism by which this process occurs is not fully elucidated, however, it has been predicted that the TSP-1/CD47 interaction works to elevate Ca²⁺-dependent phosphorylation of sGC.²⁴¹⁻²⁴² While the putative phosphorylation residue(s) have yet to be identified, phosphorylation of SGC has been shown to be capable of inhibiting enzymatic activity,²⁴³ and the importance of these data were confirmed by knockout of CD47, which demonstrated the necessity of CD47 to transduce the inhibitory effect of TSP-1 treatment on sGC.^{240,244} These findings have therapeutically relevant implications, as TSP-1/CD47 have been shown to be upregulated in some pulmonary hypertension,²⁴⁵ presenting a potential barrier for the use of the recently approved sGC modulator therapies for treatment.

Elevated second messenger signaling may also play an important role in sGC gene expression, as some reports have previously reported changes in their transcription following extended treatment with cAMP and cGMP analogs.²⁴⁶ Interestingly, treatment with forskolin for periods less than 24 hours did not inhibit NO-dependent production of cGMP or decrease sGC mRNA while treatment for 1-2 days produced significantly blunted production of sGC mRNA and NO-dependent production of cGMP. Similar results showing significant reduction in sGC mRNA of fetal rat lung fibroblasts were observed with treatment of the non-specific PDE inhibitor, isobutylmethylxanthine (IBMX). Similarly, 6-hour treatment of rat aortic smooth muscle cells with IBMX significantly decreased the NO-dependent accumulation of cGMP, though there is a possibility that this data is confounded by another method of cGMP clearance and depletion of GTP substrate which causes this blunted response. Treatment with protein

kinase A (PKA) inhibitors in cells treated with forskolin rescued the ability of rat aortic SMC to produce cGMP in response to NO, suggesting that PKA is integral in this downregulatory response to elevated cAMP. These data are in line with previous studies which showed that 4-hour pre-treatment with norepinephrine, which decreases the amount of available cAMP, markedly increased the dilatory responses of blood vessels stimulated with SNP.²⁴⁷ Interestingly, there was no difference in dilatory responses between the vessel groups when treated with the non-hydrolyzable cGMP analog, 8-br-cGMP, indicating that the dilatory differences were due to changes in sGC-dependent activity rather than a blockage downstream.²⁴⁶

A recent study identified Cullin-3, a member of E3-ubiquitin ligases, as a significant regulator of sGC expression in smooth muscle.²⁴⁸ This conditional SMC-specific deletion of Cullin-3 caused a significant loss of sGC expression at both the mRNA and protein levels, leading to hypertension and vascular dysfunction in these animals. Interestingly, no other changes in eNOS or PDE5 were observed in these animals, suggesting no additional changes to the NO-sGC-cGMP pathway were found in these animals, and because changes were observed in sGC mRNA expression, changes in transcriptional regulation are heavily implicated. Furthermore, no changes in proteins identified to regulate the stability of sGC mRNA, namely human antigen R (HuR) or AU-rich element RNA-binding protein 1 (AUF1),^{143,161} were observed in this study.²⁴⁸ To date, no connections have been identified between the FoxO transcription factors and Cullin-3, however, due to the many post-translational regulatory sites present on the FoxO proteins, it is possible that Cullin-3 is responsible for mediating the degradation of one of the kinases that restrict FoxO activity. Similar connections have been made with Cullin-1 and the control of the PI3K/Akt pathway, which are well-characterized to act as a brake on FoxO-dependent transcription.²⁴⁹ Finding a potential connection between these two

pathways may provide a solid hypothesis which explains the phenomenon observed following SMC-specific knockout of Cullin-3 and the hypertensive phenotypes that present in patients with mutations in the CUL3 gene.

5.3 What Are the Implications of sGC Activator/Modulator Treatment on RAAS Inhibited Patients?

As was discussed in Chapter 1, sGC modulator therapies represent a promising new therapeutic option for the treatment of several specific cardiovascular pathologies. It is therefore worthwhile to investigate the interactions between many of the common drugs used in the clinic for patients with CVD. Based upon our findings layed out in Chapter 3, we believe that there will be a number of important pharmacological changes in patients treated with drugs that impact the RAAS pathway and those that affect sGC activity.

With the recent FDA approval for sGC stimulator therapy in heart failure patients with preserved ejection fraction,⁵⁸ there is an increasing likelihood that more data will become available concerning potential differences in those with reduced renal blood flow to one or both of the kidneys. While most patients on angiotensin converting enzyme (ACE) inhibitors or Ang II receptor antagonists (aka angiotensin receptor blockers ARBs), will have beneficial inhibition of the Ang II-dependent effects on heart rate, contractility of heart and vascular smooth muscle, and decreased blood pressure,²⁵⁰ our findings may indicate some secondary effects which result from the loss of Ang II-dependent signaling within the renal vasculature in a manner similar to the relief that has been observed for renal fibrosis patients using sGC modulators.²⁰⁸ Because we observed increases in renal SMC expression of sGC as a direct result of Ang II, we believe that

renal blood flow will be augmented in patients that receive sGC stimulator drugs due to increased initial expression of sGC protein. Andreas Friebe's work indicated that sGC protein is highly stable *in vivo*,²⁶ suggesting that Ang II-mediated elevation of renal sGC expression may be capable of remaining long after the signal to boost sGC has been inhibited or suppressed. Future studies should therefore explore the differences between patients treated with sGC stimulators and RAAS blockers and those treated with RAAS blockers alone.

5.4 What are the Implications for Renal Transplant Patients?

For patients facing the prospect of severe kidney malfunction, renal transplantation is often the best chance to improve both quality of life and health outcomes. In such patients, total kidney function is below 10-15% of normal glomerular filtration rate.²⁵¹ The available options make dialysis inevitable unless sufficient glomerular filtration is restored. An interesting component of renal transplantation surgery is that the damaged or diseased kidneys often remain within the patient while the donor kidney is surgically attached below them to one of the iliac arteries.²⁵² This procedure allows the native kidneys to remain intact within the body to assist – insofar as that is possible – while the patient heals, and the donor kidney begins to increase renal function.

The benefits of leaving the native kidneys in place stem primarily from the risks associated with removing them in the short term and the risks associated with rejection. Removal at the time of surgery increases the recovery time by 4-6 weeks, increasing the risk of infection during that period.²⁵³⁻²⁵⁴ This procedure often causes the recipient to need blood transfusions, which can exacerbate the risk of rejection of the newly acquired donor kidney. Finally, this

process forces the patient to begin dialysis treatment immediately,²⁵⁵ which may not be necessary for all patients if some kidney function still remains in the native kidneys. There are, however, certain scenarios like recurring infections,²⁵⁶ cancer,²⁵⁷ severe renal hypertension,²⁵⁵ or pains caused by conditions like polycystic kidney disease where removal may be necessary to help increase the patient's chances of survival or increase quality of life.²⁵⁸

Because most patients will keep the diseased or damaged kidneys following transplantation,²⁵⁹ these organs can perpetuate certain signaling events to occur within the body. As was discussed in Chapter 3, restricted renal blood flow leads to elevated RAAS signaling. Since nearly all kidney transplant patients have reduced blood flow to their native kidneys,²⁵⁹ there is likely elevated RAAS signaling. Based upon the preliminary evidence for efficacy of sGC stimulators and activators in renal diseases and the findings that the AT₁R increases renal smooth muscle expression of sGC, elevated RAAS signaling from native kidneys has the potential to improve renal blood flow to donor kidneys and increase the potency of sGC stimulators or activators on transplant patients that keep their native kidneys.

5.5 Similarities and Differences Between the FoxO Transcription Factors?

Many different structural studies have identified a high degree of similarity between the winged helix Fox transcription factors, which constitute more than 100 proteins found within the animal kingdom.²⁶⁰ Every member of the FoxO family contains a high degree of forkhead homology, at the N-terminal region in particular. This region is generally characterized by the amino acid sequence Arg-X-Arg-Ser-Cys-Thr-Trp-Pro-Leu.²⁶¹ Additionally, all Forkhead proteins generally contain three N-terminal α -helices (symbolized as H1-H3) which help to

coordinate and bind to DNA,^{86,176,262} as well as two flexible loop structures that give the appearance of “wings” (W1-W2) which participate to varying degrees in the stability of DNA-protein interactions.⁸⁶ Importantly, many of these proteins have orthologous transcription factors which have existed for hundreds of millions of years, as is evident from their initial identification in *Drosophila*. The FoxO transcription factors are no exception to this rule, and their orthologs have been identified in *C. elegans* as important regulators of lifespan that have existed for more than half a billion years.^{93,99,103,164} These proteins, despite the recognition of core sequences show differential regulation of genetic targets and demonstrate different interacting partners and post-translational modifications which may affect the differences we observe following knockdown of each FoxO transcription factor in SMC.

One of the first indicators of differential function of the FoxO transcription factors in mammals comes from the knockout studies performed in mice which showed that deletion of individual FoxO transcription factors from birth produce different responses in mouse models.¹³⁹ FoxO1 knockout mice develop severely malformed blood vessels which result in embryonic lethality around E10.5, while FoxO3 and FoxO4 knockout mice survive to birth. Deletion of FoxO3 in female mice causes age-dependent infertility though the male mice appear to be no less fertile than their littermate controls. FoxO4 deletion, interestingly enough, does not appear to have a significant phenotype different from littermate control animals. This may indicate the importance of the different FoxO transcription factors at various stages of development, while also leaving open the possibility that significant compensation may occur when one or possibly multiple transcription factors are absent.

Studies have identified the DNA binding domains of each FoxO protein and the most likely DNA sequences bound by each. Moreover, it appears that FoxO proteins possess two

“core” binding DNA sequences that are recognized by all family members and have been the topic of many studies in the early 2000’s.^{91,134,226} These studies identified a Daf-16 family member binding element (DBE) between all members which demonstrates the highest affinity for the sequence “5’-AACAAATG-3’.” Another binding element has recently been identified as the insulin responsive element (IRE), most well characterized in FoxO1 was identified on the promoter of insulin like growth factor binding protein to recognize a similar “5’-AACAAAAC-3’” DNA sequence.⁸⁶ The H3 of the FoxO proteins and their orthologs has been shown to possess key residues which interact with the major groove of the DNA strand, forming a large number of hydrogen bonds as well as van Der Waals interactions to stabilize the connection.²³³⁻²³⁴ Furthermore, the flexible W2 domain of the FoxO transcription factors have been shown to enhance the interaction of the H3 domain with the DNA structure.¹⁷⁷ In particular, they found that thymine bases flanking these sequences form interactions with the highest affinity due to the hydrogen bonding capabilities capable of forming with the W2 domain. Finally, the H2 domain and the disordered W1 domain also contribute to binding nearby DNA and appear to help stabilize distal interactions between the FoxO protein and DNA, though these contacts undoubtedly require more study due to the flexibility of the W1 domain.⁸⁶

Despite this high degree of similarity between the FoxO family members, there are a number of important differences that likely inform the functional differences we observe. For one, the crystal structure shows that the five amino acid sequence between H2 and H3 is capable of interacting with the DNA via its phosphate backbone.²³³ The Ser142 residue of FoxO4 has been shown through crystal structures to stabilize the protein-DNA interaction, however, the structures from FoxO1 and FoxO3 show that these residues are too far away to allow interaction to occur despite the more similar residues between FoxO1 and FoxO4. This is likely due to the

larger H2 domains and N-termini found within FoxO1 and FoxO3 prevent the same amount of flexion of the residues between H2 and H3 to coordinate with the DNA backbone of the major groove. Additionally, DNA-FoxO4 crystal structures have demonstrated that several residues of its N-terminus, namely Arg94, Asn95 and Ser101 and the hydroxyl group of Tyr102 of the FoxO4 H1 domain form hydrogen bond bridges with water molecules that bring the phosphate backbone into close proximity to enhance the DNA-protein interaction.²³³⁻²³⁴

Post-translational modifications of the FoxO transcription factors have been shown to be diversified from one another leading to altered function and gene targeting following modifications. As has been mentioned before, phosphorylation of the FoxO transcription factors at conserved residues by PKB/Akt is an important negative regulator of FoxO function that affects the DNA binding affinity,^{177,263} cytosolic sequestration due to masking of the conserved NLS,^{90,226,264-265} and targeting for polyubiquitination and degradation.²⁶⁶ Many other phosphorylation sites appear to have a unique phosphorylation profile for different FoxO transcription factors because of non-conserved amino acids that serve as the target for phosphorylation. FoxO1 has been shown to be phosphorylated and inhibited from DNA binding by PKG at a unique cluster of 4 serine residues (Ser152-Ser155) that is absent from FoxO3 and FoxO4 and has also shown to be phosphorylated at Ser184,²⁶⁷ a residue which is also absent from FoxO4.¹⁷⁶ Because these residues are found near the helical regions that interact with DNA, it is plausible that the PKG-dependent phosphorylation could interfere with the ability of the FoxO protein to interact at these locations. FoxO3 contains the Ser181 that corresponds to the Ser184 of FoxO1 and 2 of 4 serine residues at the serine cluster location identified in FoxO1 (Ser151-Ser152), and FoxO4 contains only one serine at this cluster location (Ser96), however no PKG-dependent phosphorylation has been identified in either FoxO3 or FoxO4 to date.

Phosphorylation of FoxO proteins by mammalian Ste-20 like kinase-1 (Mst-1) has shown to increase transcriptional activity in response to oxidative stress stimuli by phosphorylating FoxO3 at the highly conserved Ser209, Ser215, Ser231 and Ser232 residues.^{234,268} The Ser209 and Ser215 residues lie within the H3 domain of the DBD, while Ser231 and Ser232 are part of the W1 domain, suggesting that all four residues can contribute to the transcriptional function of FoxO3. Intriguingly, Brent, et al. showed that phosphorylation of FoxO1 by Mst-1 abolished all DNA-binding interaction, suggesting that there may be a de-phosphorylation of one or multiple residues in order for an increase in transcription to occur.¹⁷⁷ Cyclin-dependent kinase-2 (CDK2), which regulates progression through the cell cycle, phosphorylates FoxO1 at Ser249,²⁶⁹ which is a non-conserved residue within the W2 domain, suggesting that this site is a unique site of regulation that exists for FoxO1. This study revealed that phosphorylation of Ser249 leads to cytosolic shuttling and inactivation of FoxO1 and also showed through electrophoretic mobility shift assay (EMSA) that the phosphomimetic Ser-249-Glu mutant FoxO1 showed no decrease in DNA binding capability. This suggests Ser249 of FoxO1 does not participate in the DNA binding of the W2 domain and that phosphorylation by CDK2 acts as a signal for nuclear export and cytosolic sequestration.

In addition to FoxO transcriptional modulation by phosphorylation of serine or threonine residues, several lysine residues have been identified to play important roles in the function of FoxO transcription factors. Proteolysis and mass spectrometry show that the residues Lys245, Lys248, Lys262, and Lys265 of FoxO1 are acetylated by cAMP-responsive element binding protein (CBP) or p300, while previous research suggested they are de-acetylated by SIRT1.²⁷⁰ Mutation of these lysine residues to alanines showed a decrease in DNA binding affinity, likely because the loss of these positive charges destabilizes the protein-DNA interactions. There is

some controversy regarding the precise role of acetylation of the FoxO proteins, as EMSA assays have shown decreased DNA binding following acetylation of FoxO1.²⁷¹ On the other hand, increased CBP/P300 recruitment by FoxO proteins leads to higher histone acetylation and transcriptional initiation. Additionally, de-acetylation of FoxO proteins have also been shown to be both activating,²³⁰ and inhibitory,²²⁹ depending on the source. These data undoubtedly require more study, as the acetylation/de-acetylation of FoxO proteins and the nearby histones may act as buffers on excessive or deficient transcription at specific regions.

The highly conserved structures of the FoxO proteins allows for in-depth study of differences caused by the minor changes in other domains. Structurally, the FoxO4 protein contains a smaller N-terminal domain and C-terminal transactivation domain than FoxO1 or FoxO3.¹⁷⁶ Changes within these regions affect the DNA binding capability as well as the number and influence of specific regulatory sites that make up the fundamental differences between the FoxO transcription factors. Because the FoxO transcription factors are a highly dynamic group of proteins that act swiftly in response to various stimuli, the ability to modulate activity positively or negatively is essential for their proper function. In addition, because of the broad number of transcriptional targets governed by the FoxO family, rapid post-translational modification, primarily through phosphorylation/dephosphorylation and acetylation/de-acetylation, causes modulation of DNA binding affinity and alters subcellular localization. These small variations in amino acid structures between the FoxO transcription factors represent important modes for signal transduction that promote or inhibit gene expression by FoxO proteins to adjust the production of specific transcripts to modify cellular function.

Bibliography

1. Allen, L. N., et al. (2020). "Implementation of non-communicable disease policies: a geopolitical analysis of 151 countries." Lancet Glob Health **8**(1): e50-e58.
2. Roth, G. A., et al. (2017). "Global, Regional, and National Burden of Cardiovascular Diseases for 10 Causes, 1990 to 2015." J Am Coll Cardiol **70**(1): 1-25.
3. Zhang, D., et al. (2017). "Medical Expenditures Associated With Hypertension in the U.S., 2000-2013." Am J Prev Med **53**(6S2): S164-S171.
4. Heidenreich, P. A., et al. (2011). "Forecasting the future of cardiovascular disease in the United States: a policy statement from the American Heart Association." Circulation **123**(8): 933-944.
5. Collaborators, G. B. D. R. F. (2018). "Global, regional, and national comparative risk assessment of 84 behavioural, environmental and occupational, and metabolic risks or clusters of risks for 195 countries and territories, 1990-2017: a systematic analysis for the Global Burden of Disease Study 2017." Lancet **392**(10159): 1923-1994.
6. Collaborators, G. B. D. C. o. D. (2018). "Global, regional, and national age-sex-specific mortality for 282 causes of death in 195 countries and territories, 1980-2017: a systematic analysis for the Global Burden of Disease Study 2017." Lancet **392**(10159): 1736-1788.
7. Danaei, G., et al. (2009). "The preventable causes of death in the United States: comparative risk assessment of dietary, lifestyle, and metabolic risk factors." PLoS Med **6**(4): e1000058.
8. Kissela, B. M., et al. (2002). "Subarachnoid hemorrhage: a preventable disease with a heritable component." Stroke **33**(5): 1321-1326.
9. Lopez, L., et al. (2009). "Disclosure of hospital adverse events and its association with patients' ratings of the quality of care." Arch Intern Med **169**(20): 1888-1894.
10. Go, A. S., et al. (2013). "Heart disease and stroke statistics--2013 update: a report from the American Heart Association." Circulation **127**(1): e6-e245.
11. Mills, K. T., et al. (2016). "Global Disparities of Hypertension Prevalence and Control: A Systematic Analysis of Population-Based Studies From 90 Countries." Circulation **134**(6): 441-450.
12. Kearney, P. M., et al. (2005). "Global burden of hypertension: analysis of worldwide data." Lancet **365**(9455): 217-223.

13. Whelton, P. K., et al. (2018). "2017 ACC/AHA/AAPA/ABC/ACPM/AGS/APhA/ASH/ASPC/NMA/PCNA Guideline for the Prevention, Detection, Evaluation, and Management of High Blood Pressure in Adults: Executive Summary: A Report of the American College of Cardiology/American Heart Association Task Force on Clinical Practice Guidelines." Hypertension **71**(6): 1269-1324.
14. Lewington, S., et al. (2002). "Age-specific relevance of usual blood pressure to vascular mortality: a meta-analysis of individual data for one million adults in 61 prospective studies." Lancet **360**(9349): 1903-1913.
15. Guo, X., et al. (2013). "Association between pre-hypertension and cardiovascular outcomes: a systematic review and meta-analysis of prospective studies." Curr Hypertens Rep **15**(6): 703-716.
16. Group, S. R., et al. (2015). "A Randomized Trial of Intensive versus Standard Blood-Pressure Control." N Engl J Med **373**(22): 2103-2116.
17. Bundy, J. D., et al. (2017). "Systolic Blood Pressure Reduction and Risk of Cardiovascular Disease and Mortality: A Systematic Review and Network Meta-analysis." JAMA Cardiol **2**(7): 775-781.
18. Bundy, J. D., et al. (2018). "Estimating the Association of the 2017 and 2014 Hypertension Guidelines With Cardiovascular Events and Deaths in US Adults: An Analysis of National Data." JAMA Cardiol **3**(7): 572-581.
19. Wang, Z., et al. (2018). "Status of Hypertension in China: Results From the China Hypertension Survey, 2012-2015." Circulation **137**(22): 2344-2356.
20. Boliko, M. C. (2019). "FAO and the Situation of Food Security and Nutrition in the World." J Nutr Sci Vitaminol (Tokyo) **65**(Supplement): S4-S8.
21. Rees, D. D., et al. (1989). "A specific inhibitor of nitric oxide formation from L-arginine attenuates endothelium-dependent relaxation." Br J Pharmacol **96**(2): 418-424.
22. Rees, D. D., et al. (1989). "Role of endothelium-derived nitric oxide in the regulation of blood pressure." Proc Natl Acad Sci U S A **86**(9): 3375-3378.
23. Furchgott, R. F. and J. V. Zawadzki (1980). "The obligatory role of endothelial cells in the relaxation of arterial smooth muscle by acetylcholine." Nature **288**(5789): 373-376.
24. Huang, P. L., et al. (1995). "Hypertension in mice lacking the gene for endothelial nitric oxide synthase." Nature **377**(6546): 239-242.
25. Zhao, Y., et al. (1999). "A molecular basis for nitric oxide sensing by soluble guanylate cyclase." Proc Natl Acad Sci U S A **96**(26): 14753-14758.

26. Groneberg, D., et al. (2010). "Smooth muscle-specific deletion of nitric oxide-sensitive guanylyl cyclase is sufficient to induce hypertension in mice." Circulation **121**(3): 401-409.
27. Friebe, A., et al. (2007). "Fatal gastrointestinal obstruction and hypertension in mice lacking nitric oxide-sensitive guanylyl cyclase." Proc Natl Acad Sci U S A **104**(18): 7699-7704.
28. Budworth, J., et al. (1999). "Tissue distribution of the human soluble guanylate cyclases." Biochem Biophys Res Commun **263**(3): 696-701.
29. Wedel, B., et al. (1994). "Mutation of His-105 in the beta 1 subunit yields a nitric oxide-insensitive form of soluble guanylyl cyclase." Proc Natl Acad Sci U S A **91**(7): 2592-2596.
30. Ma, X., et al. (2010). "Crystal structure of the signaling helix coiled-coil domain of the beta1 subunit of the soluble guanylyl cyclase." BMC Struct Biol **10**: 2.
31. Khalid, R. R., et al. (2020). "Probing the Structural Dynamics of the Catalytic Domain of Human Soluble Guanylate Cyclase." Sci Rep **10**(1): 9488.
32. Ghosh, A. and D. J. Stuehr (2012). "Soluble guanylyl cyclase requires heat shock protein 90 for heme insertion during maturation of the NO-active enzyme." Proc Natl Acad Sci U S A **109**(32): 12998-13003.
33. Ghosh, A., et al. (2014). "Nitric oxide and heat shock protein 90 activate soluble guanylate cyclase by driving rapid change in its subunit interactions and heme content." J Biol Chem **289**(22): 15259-15271.
34. Nedvetsky, P. I., et al. (2008). "Heat shock protein 90 regulates stabilization rather than activation of soluble guanylate cyclase." FEBS Lett **582**(2): 327-331.
35. Stasch, J. P., et al. (2006). "Targeting the heme-oxidized nitric oxide receptor for selective vasodilatation of diseased blood vessels." J Clin Invest **116**(9): 2552-2561.
36. Schrammel, A., et al. (1996). "Characterization of 1H-[1,2,4]oxadiazolo[4,3-a]quinoxalin-1-one as a heme-site inhibitor of nitric oxide-sensitive guanylyl cyclase." Mol Pharmacol **50**(1): 1-5.
37. Dierks, E. A. and J. N. Burstyn (1996). "Nitric oxide (NO), the only nitrogen monoxide redox form capable of activating soluble guanylyl cyclase." Biochem Pharmacol **51**(12): 1593-1600.
38. Tawa, M., et al. (2015). "Effects of hydrogen peroxide on relaxation through the NO/sGC/cGMP pathway in isolated rat iliac arteries." Free Radic Res **49**(12): 1479-1487.

39. Tawa, M., et al. (2015). "Different influences of extracellular and intracellular superoxide on relaxation through the NO/sGC/cGMP pathway in isolated rat iliac arteries." J Cardiovasc Pharmacol **65**(2): 160-167.
40. Tawa, M., et al. (2014). "Effects of peroxynitrite on relaxation through the NO/sGC/cGMP pathway in isolated rat iliac arteries." J Vasc Res **51**(6): 439-446.
41. Rahaman, M. M., et al. (2017). "Cytochrome b5 Reductase 3 Modulates Soluble Guanylate Cyclase Redox State and cGMP Signaling." Circ Res **121**(2): 137-148.
42. Rahaman, M. M., et al. (2015). "Structure Guided Chemical Modifications of Propylthiouracil Reveal Novel Small Molecule Inhibitors of Cytochrome b5 Reductase 3 That Increase Nitric Oxide Bioavailability." J Biol Chem **290**(27): 16861-16872.
43. Durgin, B. G., et al. (2019). "Loss of smooth muscle CYB5R3 amplifies angiotensin II-induced hypertension by increasing sGC heme oxidation." JCI Insight **4**(19).
44. Venema, R. C., et al. (2003). "Novel complexes of guanylate cyclase with heat shock protein 90 and nitric oxide synthase." Am J Physiol Heart Circ Physiol **285**(2): H669-678.
45. Balashova, N., et al. (2005). "Characterization of a novel type of endogenous activator of soluble guanylyl cyclase." J Biol Chem **280**(3): 2186-2196.
46. Cohen, A. W., et al. (2004). "Role of caveolae and caveolins in health and disease." Physiol Rev **84**(4): 1341-1379.
47. Tsai, E. J., et al. (2012). "Pressure-overload-induced subcellular relocalization/oxidation of soluble guanylyl cyclase in the heart modulates enzyme stimulation." Circ Res **110**(2): 295-303.
48. Trappanese, D. M., et al. (2015). "Chronic beta1-adrenergic blockade enhances myocardial beta3-adrenergic coupling with nitric oxide-cGMP signaling in a canine model of chronic volume overload: new insight into mechanisms of cardiac benefit with selective beta1-blocker therapy." Basic Res Cardiol **110**(1): 456.
49. Sinha, S. C. and S. R. Sprang (2006). "Structures, mechanism, regulation and evolution of class III nucleotidyl cyclases." Rev Physiol Biochem Pharmacol **157**: 105-140.
50. Alapa, M., et al. (2021). "Selective cysteines oxidation in soluble guanylyl cyclase catalytic domain is involved in NO activation." Free Radic Biol Med **162**: 450-460.
51. Craven, P. A. and F. R. DeRubertis (1978). "Restoration of the responsiveness of purified guanylate cyclase to nitrosoguanidine, nitric oxide, and related activators by heme and hemeproteins. Evidence for involvement of the paramagnetic nitrosyl-heme complex in enzyme activation." J Biol Chem **253**(23): 8433-8443.

52. Brandwein, H. J., et al. (1981). "Reversible inactivation of guanylate cyclase by mixed disulfide formation." J Biol Chem **256**(6): 2958-2962.
53. Stamler, J. S., et al. (1992). "S-nitrosylation of proteins with nitric oxide: synthesis and characterization of biologically active compounds." Proc Natl Acad Sci U S A **89**(1): 444-448.
54. Sayed, N., et al. (2007). "Desensitization of soluble guanylyl cyclase, the NO receptor, by S-nitrosylation." Proc Natl Acad Sci U S A **104**(30): 12312-12317.
(Mulsch, 1997 #62) Mulsch, A., et al. (1997). "Effect of YC-1, an NO-independent, superoxide-sensitive stimulator of soluble guanylyl cyclase, on smooth muscle responsiveness to nitrovasodilators." Br J Pharmacol **120**(4): 681-689.
55. Choi, H., et al. (2011). "Thioredoxin reductase inhibition reduces relaxation by increasing oxidative stress and s-nitrosylation in mouse aorta." J Cardiovasc Pharmacol **58**(5): 522-527.
56. Huang, C., et al. (2017). "Guanylyl cyclase sensitivity to nitric oxide is protected by a thiol oxidation-driven interaction with thioredoxin-1." J Biol Chem **292**(35): 14362-14370.
57. Beuve, A., et al. (2016). "Identification of novel S-nitrosation sites in soluble guanylyl cyclase, the nitric oxide receptor." J Proteomics **138**: 40-47.
58. Armstrong, P. W., et al. (2020). "Vericiguat in Patients with Heart Failure and Reduced Ejection Fraction." N Engl J Med **382**(20): 1883-1893.
59. Ghofrani, H. A., et al. (2013). "Riociguat for the treatment of chronic thromboembolic pulmonary hypertension." N Engl J Med **369**(4): 319-329.
60. Ghofrani, H. A., et al. (2013). "Riociguat for the treatment of pulmonary arterial hypertension." N Engl J Med **369**(4): 330-340.
61. Friebe, A., et al. (1996). "Sensitizing soluble guanylyl cyclase to become a highly CO-sensitive enzyme." EMBO J **15**(24): 6863-6868.
62. Mulsch, A., et al. (1997). "Effect of YC-1, an NO-independent, superoxide-sensitive stimulator of soluble guanylyl cyclase, on smooth muscle responsiveness to nitrovasodilators." Br J Pharmacol **120**(4): 681-689.
63. Deruelle, P., et al. (2005). "Pulmonary vascular effects of nitric oxide-cGMP augmentation in a model of chronic pulmonary hypertension in fetal and neonatal sheep." Am J Physiol Lung Cell Mol Physiol **289**(5): L798-806.
64. Deruelle, P., et al. (2006). "BAY 41-2272, a direct activator of soluble guanylate cyclase, reduces right ventricular hypertrophy and prevents pulmonary vascular remodeling during chronic hypoxia in neonatal rats." Biol Neonate **90**(2): 135-144.

65. Evgenov, O. V., et al. (2007). "Inhaled agonists of soluble guanylate cyclase induce selective pulmonary vasodilation." Am J Respir Crit Care Med **176**(11): 1138-1145.
66. Becker, E. M., et al. (2001). "NO-independent regulatory site of direct sGC stimulators like YC-1 and BAY 41-2272." BMC Pharmacol **1**: 13.
67. Stasch, J. P., et al. (2002). "Cardiovascular actions of a novel NO-independent guanylyl cyclase stimulator, BAY 41-8543: in vivo studies." Br J Pharmacol **135**(2): 344-355.
68. Frey, R., et al. (2018). "Clinical Pharmacokinetic and Pharmacodynamic Profile of Riociguat." Clin Pharmacokinet **57**(6): 647-661.
69. Zhou, Z., et al. (2008). "Soluble guanylyl cyclase activation by HMR-1766 (ataciguat) in cells exposed to oxidative stress." Am J Physiol Heart Circ Physiol **295**(4): H1763-1771.
70. Stasch, J. P., et al. (2002). "NO- and haem-independent activation of soluble guanylyl cyclase: molecular basis and cardiovascular implications of a new pharmacological principle." Br J Pharmacol **136**(5): 773-783.
71. Gheorghiane, M., et al. (2012). "Cinaciguat, a soluble guanylate cyclase activator: results from the randomized, controlled, phase IIb COMPOSE programme in acute heart failure syndromes." Eur J Heart Fail **14**(9): 1056-1066.
72. Kumar, V., et al. (2013). "Insights into BAY 60-2770 activation and S-nitrosylation-dependent desensitization of soluble guanylyl cyclase via crystal structures of homologous nostoc H-NOX domain complexes." Biochemistry **52**(20): 3601-3608.
73. Sommer, A., et al. (2018). "BAY 60-2770 activates two isoforms of nitric oxide sensitive guanylyl cyclase: Evidence for stable insertion of activator drugs." Biochem Pharmacol **147**: 10-20.
74. Potoka, K. P., et al. (2018). "Nitric Oxide-Independent Soluble Guanylate Cyclase Activation Improves Vascular Function and Cardiac Remodeling in Sickle Cell Disease." Am J Respir Cell Mol Biol **58**(5): 636-647.
75. Sharina, I. G., et al. (2003). "CCAAT-binding factor regulates expression of the beta1 subunit of soluble guanylyl cyclase gene in the BE2 human neuroblastoma cell line." Proc Natl Acad Sci U S A **100**(20): 11523-11528.
76. Andreopoulos, S. and A. Papapetropoulos (2000). "Molecular aspects of soluble guanylyl cyclase regulation." Gen Pharmacol **34**(3): 147-157.
77. Marro, M. L., et al. (2008). "Characterization of the human alpha1 beta1 soluble guanylyl cyclase promoter: key role for NF-kappaB(p50) and CCAAT-binding factors in regulating expression of the nitric oxide receptor." J Biol Chem **283**(29): 20027-20036.

- (Melichar, 2004 #78) Melichar, V. O., et al. (2004). "Reduced cGMP signaling associated with neointimal proliferation and vascular dysfunction in late-stage atherosclerosis." Proc Natl Acad Sci U S A **101**(47): 16671-16676.
- (Kloss, 2000 #79) Kloss, S., et al. (2000). "Aging and chronic hypertension decrease expression of rat aortic soluble guanylyl cyclase." Hypertension **35**(1 Pt 1): 43-47.
- (Kloss, 2005 #80) Kloss, S., et al. (2005). "Human-antigen R (HuR) expression in hypertension: downregulation of the mRNA stabilizing protein HuR in genetic hypertension." Hypertension **45**(6): 1200-1206.
- (Willcox, 2008 #81) Willcox, B. J., et al. (2008). "FOXO3A genotype is strongly associated with human longevity." Proc Natl Acad Sci U S A **105**(37): 13987-13992.
- (Li, 2009 #82) Li, Y., et al. (2009). "Genetic association of FOXO1A and FOXO3A with longevity trait in Han Chinese populations." Hum Mol Genet **18**(24): 4897-4904.
- (Pawlikowska, 2009 #83) Pawlikowska, L., et al. (2009). "Association of common genetic variation in the insulin/IGF1 signaling pathway with human longevity." Aging Cell **8**(4): 460-472.
- (Galley, 2019 #84) Galley, J. C., et al. (2019). "Antagonism of Forkhead Box Subclass O Transcription Factors Elicits Loss of Soluble Guanylyl Cyclase Expression." Mol Pharmacol **95**(6): 629-637.
- (Galley, 2021 #85) Galley, J. C., et al. (2021). "Angiotensin II augments renal vascular smooth muscle sGC expression via an AT1 R - FoxO transcription factor signaling axis." Br J Pharmacol.
78. Weigel, D., et al. (1989). "The homeotic gene fork head encodes a nuclear protein and is expressed in the terminal regions of the Drosophila embryo." Cell **57**(4): 645-658.
79. Lai, E., et al. (1990). "HNF-3A, a hepatocyte-enriched transcription factor of novel structure is regulated transcriptionally." Genes Dev **4**(8): 1427-1436.
80. Weigel, D. and H. Jackle (1990). "The fork head domain: a novel DNA binding motif of eukaryotic transcription factors?" Cell **63**(3): 455-456.
81. Kaestner, K. H., et al. (2000). "Unified nomenclature for the winged helix/forkhead transcription factors." Genes Dev **14**(2): 142-146.
82. Hannenhalli, S. and K. H. Kaestner (2009). "The evolution of Fox genes and their role in development and disease." Nat Rev Genet **10**(4): 233-240.
(Cirillo, 2007 #93) Cirillo, L. A. and K. S. Zaret (2007). "Specific interactions of the wing domains of FOXA1 transcription factor with DNA." J Mol Biol **366**(3): 720-724.

83. Tuteja, G. and K. H. Kaestner (2007). "SnapShot: forkhead transcription factors I." Cell **130**(6): 1160.
84. Tuteja, G. and K. H. Kaestner (2007). "Forkhead transcription factors II." Cell **131**(1): 192.
85. Cirillo, L. A. and K. S. Zaret (2007). "Specific interactions of the wing domains of FOXA1 transcription factor with DNA." J Mol Biol **366**(3): 720-724.
86. Clark, K. L., et al. (1993). "Co-crystal structure of the HNF-3/fork head DNA-recognition motif resembles histone H5." Nature **364**(6436): 412-420.
87. Jin, C., et al. (1999). "Dynamic DNA contacts observed in the NMR structure of winged helix protein-DNA complex." J Mol Biol **289**(4): 683-690.
88. Tsai, K. L., et al. (2006). "Crystal structure of the human FOXP1a-DNA complex and its implications on the diverse binding specificity of winged helix/forkhead proteins." J Biol Chem **281**(25): 17400-17409.
89. Stroud, J. C., et al. (2006). "Structure of the forkhead domain of FOXP2 bound to DNA." Structure **14**(1): 159-166.
90. Brunet, A., et al. (1999). "Akt promotes cell survival by phosphorylating and inhibiting a Forkhead transcription factor." Cell **96**(6): 857-868.
91. Kops, G. J., et al. (1999). "Direct control of the Forkhead transcription factor AFX by protein kinase B." Nature **398**(6728): 630-634.
(Andreopoulos, 2000 #76) Andreopoulos, S. and A. Papapetropoulos (2000). "Molecular aspects of soluble guanylyl cyclase regulation." Gen Pharmacol **34**(3): 147-157.
92. Cahill, C. M., et al. (2001). "Phosphatidylinositol 3-kinase signaling inhibits DAF-16 DNA binding and function via 14-3-3-dependent and 14-3-3-independent pathways." J Biol Chem **276**(16): 13402-13410.
93. Tissenbaum, H. A. and G. Ruvkun (1998). "An insulin-like signaling pathway affects both longevity and reproduction in *Caenorhabditis elegans*." Genetics **148**(2): 703-717.
94. Lin, K., et al. (1997). "daf-16: An HNF-3/forkhead family member that can function to double the life-span of *Caenorhabditis elegans*." Science **278**(5341): 1319-1322.
95. Guo, S., et al. (1999). "Phosphorylation of serine 256 by protein kinase B disrupts transactivation by FKHR and mediates effects of insulin on insulin-like growth factor-binding protein-1 promoter activity through a conserved insulin response sequence." J Biol Chem **274**(24): 17184-17192.

96. Hall, R. K., et al. (2000). "Regulation of phosphoenolpyruvate carboxykinase and insulin-like growth factor-binding protein-1 gene expression by insulin. The role of winged helix/forkhead proteins." J Biol Chem **275**(39): 30169-30175.
97. Rena, G., et al. (1999). "Phosphorylation of the transcription factor forkhead family member FKHR by protein kinase B." J Biol Chem **274**(24): 17179-17183.
98. Fitch, D. H. (2005). "Introduction to nematode evolution and ecology." WormBook: 1-8.
99. Ogg, S., et al. (1997). "The Fork head transcription factor DAF-16 transduces insulin-like metabolic and longevity signals in *C. elegans*." Nature **389**(6654): 994-999.
100. Paradis, S. and G. Ruvkun (1998). "Caenorhabditis elegans Akt/PKB transduces insulin receptor-like signals from AGE-1 PI3 kinase to the DAF-16 transcription factor." Genes Dev **12**(16): 2488-2498.
101. Gami, M. S. and C. A. Wolkow (2006). "Studies of Caenorhabditis elegans DAF-2/insulin signaling reveal targets for pharmacological manipulation of lifespan." Aging Cell **5**(1): 31-37.
102. Dillin, A., et al. (2002). "Timing requirements for insulin/IGF-1 signaling in *C. elegans*." Science **298**(5594): 830-834.
103. Giannakou, M. E., et al. (2004). "Long-lived *Drosophila* with overexpressed dFOXO in adult fat body." Science **305**(5682): 361.
104. Bluher, M., et al. (2003). "Extended longevity in mice lacking the insulin receptor in adipose tissue." Science **299**(5606): 572-574.
105. Galili, N., et al. (1993). "Fusion of a fork head domain gene to PAX3 in the solid tumour alveolar rhabdomyosarcoma." Nat Genet **5**(3): 230-235.
106. Anderson, M. J., et al. (1998). "Cloning and characterization of three human forkhead genes that comprise an FKHR-like gene subfamily." Genomics **47**(2): 187-199.
107. Parry, P., et al. (1994). "Cloning and characterization of the t(X;11) breakpoint from a leukemic cell line identify a new member of the forkhead gene family." Genes Chromosomes Cancer **11**(2): 79-84.
108. Jacobs, F. M., et al. (2003). "FoxO6, a novel member of the FoxO class of transcription factors with distinct shuttling dynamics." J Biol Chem **278**(38): 35959-35967.
109. Hillion, J., et al. (1997). "AF6q21, a novel partner of the MLL gene in t(6;11)(q21;q23), defines a forkhead transcriptional factor subfamily." Blood **90**(9): 3714-3719.

110. Rudd, M. D., et al. (2003). "Cloning and analysis of a FoxO transcription factor from *Xiphophorus*." Gene **302**(1-2): 31-41.
111. Klotz, L. O., et al. (2015). "Redox regulation of FoxO transcription factors." Redox Biol **6**: 51-72.
112. Essers, M. A., et al. (2004). "FOXO transcription factor activation by oxidative stress mediated by the small GTPase Ral and JNK." EMBO J **23**(24): 4802-4812.
113. Zhang, X., et al. (2011). "FOXO1 is an essential regulator of pluripotency in human embryonic stem cells." Nat Cell Biol **13**(9): 1092-1099.
114. Wang, Y., et al. (2013). "FoxO3a contributes to the reprogramming process and the differentiation of induced pluripotent stem cells." Stem Cells Dev **22**(22): 2954-2963.
115. Salih, D. A. and A. Brunet (2008). "FoxO transcription factors in the maintenance of cellular homeostasis during aging." Curr Opin Cell Biol **20**(2): 126-136.
116. Barthel, A., et al. (2005). "FoxO proteins in insulin action and metabolism." Trends Endocrinol Metab **16**(4): 183-189.
117. Hu, M. C., et al. (2004). "IkappaB kinase promotes tumorigenesis through inhibition of forkhead FOXO3a." Cell **117**(2): 225-237.
118. Zou, Y., et al. (2008). "Forkhead box transcription factor FOXO3a suppresses estrogen-dependent breast cancer cell proliferation and tumorigenesis." Breast Cancer Res **10**(1): R21.
119. Matrone, A., et al. (2010). "p38alpha is required for ovarian cancer cell metabolism and survival." Int J Gynecol Cancer **20**(2): 203-211.
120. Zhang, X., et al. (2017). "Breast cancer suppression by aplysin is associated with inhibition of PI3K/AKT/FOXO3a pathway." Oncotarget **8**(38): 63923-63934.
121. Hong, Z. Y., et al. (2012). "Inhibition of Akt/FOXO3a signaling by constitutively active FOXO3a suppresses growth of follicular thyroid cancer cell lines." Cancer Lett **314**(1): 34-40.
122. Yang, H., et al. (2005). "Constitutively active FOXO4 inhibits Akt activity, regulates p27 Kip1 stability, and suppresses HER2-mediated tumorigenicity." Oncogene **24**(11): 1924-1935.
123. Luo, C. T., et al. (2016). "Graded Foxo1 activity in Treg cells differentiates tumour immunity from spontaneous autoimmunity." Nature **529**(7587): 532-536.

124. Renault, V. M., et al. (2011). "The pro-longevity gene FoxO3 is a direct target of the p53 tumor suppressor." Oncogene **30**(29): 3207-3221.
125. You, H. and T. W. Mak (2005). "Crosstalk between p53 and FOXO transcription factors." Cell Cycle **4**(1): 37-38.
126. Seoane, J., et al. (2004). "Integration of Smad and forkhead pathways in the control of neuroepithelial and glioblastoma cell proliferation." Cell **117**(2): 211-223.
127. Gomis, R. R., et al. (2006). "A FoxO-Smad synexpression group in human keratinocytes." Proc Natl Acad Sci U S A **103**(34): 12747-12752.
128. Vezzali, R., et al. (2016). "The FOXG1/FOXO/SMAD network balances proliferation and differentiation of cortical progenitors and activates Kcnh3 expression in mature neurons." Oncotarget **7**(25): 37436-37455.
129. Brunet, A., et al. (2004). "Stress-dependent regulation of FOXO transcription factors by the SIRT1 deacetylase." Science **303**(5666): 2011-2015.
130. Tran, H., et al. (2002). "DNA repair pathway stimulated by the forkhead transcription factor FOXO3a through the Gadd45 protein." Science **296**(5567): 530-534.
131. Myatt, S. S. and E. W. Lam (2007). "The emerging roles of forkhead box (Fox) proteins in cancer." Nat Rev Cancer **7**(11): 847-859.
(Lapucci, 2002 #169) Lapucci, A., et al. (2002). "AUF1 Is a bcl-2 A + U-rich element-binding protein involved in bcl-2 mRNA destabilization during apoptosis." J Biol Chem **277**(18): 16139-16146.
132. Savai, R., et al. (2014). "Pro-proliferative and inflammatory signaling converge on FoxO1 transcription factor in pulmonary hypertension." Nat Med **20**(11): 1289-1300.
133. Potente, M., et al. (2005). "Involvement of Foxo transcription factors in angiogenesis and postnatal neovascularization." J Clin Invest **115**(9): 2382-2392.
134. Furuyama, T., et al. (2004). "Abnormal angiogenesis in Foxo1 (Fkhr)-deficient mice." J Biol Chem **279**(33): 34741-34749.
135. Greer, E. L. and A. Brunet (2005). "FOXO transcription factors at the interface between longevity and tumor suppression." Oncogene **24**(50): 7410-7425.
136. Schmidt, M., et al. (2002). "Cell cycle inhibition by FoxO forkhead transcription factors involves downregulation of cyclin D." Mol Cell Biol **22**(22): 7842-7852.
137. Yu, S. M., et al. (1997). "cGMP-elevating agents suppress proliferation of vascular smooth muscle cells by inhibiting the activation of epidermal growth factor signaling pathway." Circulation **95**(5): 1269-1277.

138. Cornwell, T. L., et al. (1994). "Inhibition of smooth muscle cell growth by nitric oxide and activation of cAMP-dependent protein kinase by cGMP." Am J Physiol **267**(5 Pt 1): C1405-1413.
139. Hosaka, T., et al. (2004). "Disruption of forkhead transcription factor (FOXO) family members in mice reveals their functional diversification." Proc Natl Acad Sci U S A **101**(9): 2975-2980.
140. Liu, Z. P., et al. (2005). "Phenotypic modulation of smooth muscle cells through interaction of Foxo4 and myocardin." Dev Cell **9**(2): 261-270.
149. Arnold, W. P., et al. (1977). "Nitric oxide activates guanylate cyclase and increases guanosine 3':5'-cyclic monophosphate levels in various tissue preparations." Proc Natl Acad Sci U S A **74**(8): 3203-3207.
150. Kuo, J. F. and P. Greengard (1970). "Cyclic nucleotide-dependent protein kinases. VI. Isolation and partial purification of a protein kinase activated by guanosine 3',5'-monophosphate." J Biol Chem **245**(10): 2493-2498.
151. Ruetten, H., et al. (1999). "Downregulation of soluble guanylyl cyclase in young and aging spontaneously hypertensive rats." Circ Res **85**(6): 534-541.
152. International Consortium for Blood Pressure Genome-Wide Association, S., et al. (2011). "Genetic variants in novel pathways influence blood pressure and cardiovascular disease risk." Nature **478**(7367): 103-109.
153. Wobst, J., et al. (2015). "Molecular variants of soluble guanylyl cyclase affecting cardiovascular risk." Circ J **79**(3): 463-469.
154. Shendre, A., et al. (2017). "Local Ancestry and Clinical Cardiovascular Events Among African Americans From the Atherosclerosis Risk in Communities Study." J Am Heart Assoc **6**(4).
155. Yoshina, S., et al. (1978). "[Studies on heterocyclic compounds. XXXVI. Synthesis of furo[3,2-c]pyrazole derivatives. (4) Synthesis of 1,3-diphenylfuro[3,2-c]pyrazole-5-carboxaldehyde and its derivatives (author's transl)]." Yakugaku Zasshi **98**(3): 272-279.
156. Stasch, J. P., et al. (2001). "NO-independent regulatory site on soluble guanylate cyclase." Nature **410**(6825): 212-215.
157. Frey, R., et al. (2008). "Pharmacokinetics, pharmacodynamics, tolerability, and safety of the soluble guanylate cyclase activator cinaciguat (BAY 58-2667) in healthy male volunteers." J Clin Pharmacol **48**(12): 1400-1410.

158. Meurer, S., et al. (2009). "Nitric oxide-independent vasodilator rescues heme-oxidized soluble guanylate cyclase from proteasomal degradation." Circ Res **105**(1): 33-41.
159. Mittendorf, J., et al. (2009). "Discovery of riociguat (BAY 63-2521): a potent, oral stimulator of soluble guanylate cyclase for the treatment of pulmonary hypertension." ChemMedChem **4**(5): 853-865.
160. Kloss, S., et al. (2004). "Down-regulation of soluble guanylyl cyclase expression by cyclic AMP is mediated by mRNA-stabilizing protein HuR." Mol Pharmacol **65**(6): 1440-1451.
161. Pende, A., et al. (1996). "Regulation of the mRNA-binding protein AUF1 by activation of the beta-adrenergic receptor signal transduction pathway." J Biol Chem **271**(14): 8493-8501.
162. Xu, X., et al. (2012). "Hypoxia induces downregulation of soluble guanylyl cyclase beta1 by miR-34c-5p." J Cell Sci **125**(Pt 24): 6117-6126.
163. Xia, N., et al. (2013). "Role of SIRT1 and FOXO factors in eNOS transcriptional activation by resveratrol." Nitric Oxide **32**: 29-35.
164. Hsu, A. L., et al. (2003). "Regulation of aging and age-related disease by DAF-16 and heat-shock factor." Science **300**(5622): 1142-1145.
165. Hwangbo, D. S., et al. (2004). "Drosophila dFOXO controls lifespan and regulates insulin signalling in brain and fat body." Nature **429**(6991): 562-566.
166. Goubareva, I., et al. (2007). "Age decreases nitric oxide synthesis and responsiveness in human platelets and increases formation of monocyte-platelet aggregates." Cardiovasc Res **75**(4): 793-802.
167. Stice, J. P., et al. (2009). "Role of aging versus the loss of estrogens in the reduction in vascular function in female rats." Endocrinology **150**(1): 212-219.
168. Nagashima, T., et al. (2010). "Discovery of novel forkhead box O1 inhibitors for treating type 2 diabetes: improvement of fasting glycemia in diabetic db/db mice." Mol Pharmacol **78**(5): 961-970.
169. Fogel, G. B., et al. (2005). "A statistical analysis of the TRANSFAC database." Biosystems **81**(2): 137-154.
170. Miga, K. H., et al. (2014). "Centromere reference models for human chromosomes X and Y satellite arrays." Genome Res **24**(4): 697-707.
171. Deng, L., et al. (2015). "Inhibition of FOXO1/3 promotes vascular calcification." Arterioscler Thromb Vasc Biol **35**(1): 175-183.

172. Bachiller, P. R., et al. (2010). "Transforming growth factor-beta modulates the expression of nitric oxide signaling enzymes in the injured developing lung and in vascular smooth muscle cells." Am J Physiol Lung Cell Mol Physiol **298**(3): L324-334.
173. Xia, T., et al. (2007). "Chaperone-dependent E3 ligase CHIP ubiquitinates and mediates proteasomal degradation of soluble guanylyl cyclase." Am J Physiol Heart Circ Physiol **293**(5): H3080-3087.
174. Li, F., et al. (2009). "C terminus of Hsc70-interacting protein promotes smooth muscle cell proliferation and survival through ubiquitin-mediated degradation of FoxO1." J Biol Chem **284**(30): 20090-20098.
175. Damayanti, D. S., et al. (2016). "Revealing the potency of *Annona muricata* leaves extract as FOXO1 inhibitor for diabetes mellitus treatment through computational study." In Silico Pharmacol **5**(1): 3.
176. Obsil, T. and V. Obsilova (2008). "Structure/function relationships underlying regulation of FOXO transcription factors." Oncogene **27**(16): 2263-2275.
177. Brent, M. M., et al. (2008). "Structural basis for DNA recognition by FoxO1 and its regulation by posttranslational modification." Structure **16**(9): 1407-1416.
178. Casper, S. K., et al. (2014). "The solution structure of the forkhead box-O DNA binding domain of *Brugia malayi* DAF-16a." Proteins **82**(12): 3490-3496.
179. Benjamin, M. M., et al. (2014). "Prevalence of and risk factors of renal artery stenosis in patients with resistant hypertension." Am J Cardiol **113**(4): 687-690.
180. Carey, R. M., et al. (2019). "Prevalence of Apparent Treatment-Resistant Hypertension in the United States." Hypertension **73**(2): 424-431.
181. Derkx, F. H. and M. A. Schalekamp (1994). "Renal artery stenosis and hypertension." Lancet **344**(8917): 237-239.
182. Goldfarb, D. A. (2003). "Prevalence of renovascular disease in the elderly: a population-based study." J Urol **170**(3): 1053-1054.
183. Iglesias, J. I., et al. (2000). "The natural history of incidental renal artery stenosis in patients with aortoiliac vascular disease." Am J Med **109**(8): 642-647.
184. Sawicki, P. T., et al. (1991). "Prevalence of renal artery stenosis in diabetes mellitus--an autopsy study." J Intern Med **229**(6): 489-492.
185. Tollefson, D. F. and C. B. Ernst (1991). "Natural history of atherosclerotic renal artery stenosis associated with aortic disease." J Vasc Surg **14**(3): 327-331.

186. Goldblatt, H., et al. (1934). "Studies on Experimental Hypertension : I. The Production of Persistent Elevation of Systolic Blood Pressure by Means of Renal Ischemia." J Exp Med **59**(3): 347-379.
187. Selkurt, E. E. (1951). "Effect of pulse pressure and mean arterial pressure modification on renal hemodynamics and electrolyte and water excretion." Circulation **4**(4): 541-551.
188. Dautzenberg, M., et al. (2011). "Modulation of the myogenic response in renal blood flow autoregulation by NO depends on endothelial nitric oxide synthase (eNOS), but not neuronal or inducible NOS." J Physiol **589**(Pt 19): 4731-4744.
189. Majid, D. S. and L. G. Navar (2001). "Nitric oxide in the control of renal hemodynamics and excretory function." Am J Hypertens **14**(6 Pt 2): 74S-82S.
190. Majid, D. S., et al. (1998). "Intrarenal nitric oxide activity and pressure natriuresis in anesthetized dogs." Hypertension **32**(2): 266-272.
191. O'Connor, P. M. and A. W. Cowley, Jr. (2010). "Modulation of pressure-natriuresis by renal medullary reactive oxygen species and nitric oxide." Curr Hypertens Rep **12**(2): 86-92.
192. Ignarro, L. J., et al. (1987). "Endothelium-derived relaxing factor produced and released from artery and vein is nitric oxide." Proc Natl Acad Sci U S A **84**(24): 9265-9269.
193. Stasch, J. P., et al. (2015). "Renal effects of soluble guanylate cyclase stimulators and activators: a review of the preclinical evidence." Curr Opin Pharmacol **21**: 95-104.
194. Ong, J., et al. (2019). "Renal sensory nerves increase sympathetic nerve activity and blood pressure in 2-kidney 1-clip hypertensive mice." J Neurophysiol **122**(1): 358-367.
195. DeLalio, L. J., et al. (2020). "Excessive dietary salt promotes aortic stiffness in murine renovascular hypertension." Am J Physiol Heart Circ Physiol **318**(5): H1346-H1355.
196. Zhu, X. and E. K. Jackson (2017). "RACK1 regulates angiotensin II-induced contractions of SHR preglomerular vascular smooth muscle cells." Am J Physiol Renal Physiol **312**(4): F565-F576.
197. Murphy, W. R., et al. (1984). "Effects of graded renal artery constriction on blood pressure, renal artery pressure, and plasma renin activity in Goldblatt hypertension." Hypertension **6**(1): 68-74.
198. Sadjadi, J., et al. (2002). "Upregulation of autocrine-paracrine renin-angiotensin systems in chronic renovascular hypertension." J Vasc Surg **36**(2): 386-392.
199. Smolenski, A., et al. (1998). "Analysis and regulation of vasodilator-stimulated phosphoprotein serine 239 phosphorylation in vitro and in intact cells using a phosphospecific monoclonal antibody." J Biol Chem **273**(32): 20029-20035.

200. Timmermans, P. B., et al. (1995). "Discovery of losartan, the first angiotensin II receptor antagonist." J Hum Hypertens **9 Suppl 5**: S3-18.
201. Blankley, C. J., et al. (1991). "Synthesis and structure-activity relationships of a novel series of non-peptide angiotensin II receptor binding inhibitors specific for the AT2 subtype." J Med Chem **34**(11): 3248-3260.
202. Textor, S. C. (2003). "Managing renal arterial disease and hypertension." Curr Opin Cardiol **18**(4): 260-267.
203. Kalra, P. A., et al. (2005). "Atherosclerotic renovascular disease in United States patients aged 67 years or older: risk factors, revascularization, and prognosis." Kidney Int **68**(1): 293-301.
204. de Mast, Q. and J. J. Beutler (2009). "The prevalence of atherosclerotic renal artery stenosis in risk groups: a systematic literature review." J Hypertens **27**(7): 1333-1340.
205. Kalra, P. A., et al. (2010). "Atherosclerotic renovascular disease in the United States." Kidney Int **77**(1): 37-43.
206. Granger, J. P., et al. (2002). "Mechanisms of pressure natriuresis." Curr Hypertens Rep **4**(2): 152-159.
207. Beyer, C., et al. (2015). "Stimulation of the soluble guanylate cyclase (sGC) inhibits fibrosis by blocking non-canonical TGFbeta signalling." Ann Rheum Dis **74**(7): 1408-1416.
208. Sandner, P. and J. P. Stasch (2017). "Anti-fibrotic effects of soluble guanylate cyclase stimulators and activators: A review of the preclinical evidence." Respir Med **122 Suppl 1**: S1-S9.
209. Stasch, J. P., et al. (2011). "Soluble guanylate cyclase as an emerging therapeutic target in cardiopulmonary disease." Circulation **123**(20): 2263-2273.
210. Sigmon, D. H. and W. H. Beierwaltes (1993). "Renal nitric oxide and angiotensin II interaction in renovascular hypertension." Hypertension **22**(2): 237-242.
211. Sigmon, D. H. and W. H. Beierwaltes (1998). "Influence of nitric oxide in the chronic phase of two-kidney, one clip renovascular hypertension." Hypertension **31**(2): 649-656.
212. Griendling, K. K., et al. (1994). "Angiotensin II stimulates NADH and NADPH oxidase activity in cultured vascular smooth muscle cells." Circ Res **74**(6): 1141-1148.
213. Doughan, A. K., et al. (2008). "Molecular mechanisms of angiotensin II-mediated mitochondrial dysfunction: linking mitochondrial oxidative damage and vascular endothelial dysfunction." Circ Res **102**(4): 488-496.

214. Mollnau, H., et al. (2002). "Effects of angiotensin II infusion on the expression and function of NAD(P)H oxidase and components of nitric oxide/cGMP signaling." Circ Res **90**(4): E58-65.
215. Rippe, C., et al. (2017). "Hypertension reduces soluble guanylyl cyclase expression in the mouse aorta via the Notch signaling pathway." Sci Rep **7**(1): 1334.
216. Crassous, P. A., et al. (2012). "Soluble guanylyl cyclase is a target of angiotensin II-induced nitrosative stress in a hypertensive rat model." Am J Physiol Heart Circ Physiol **303**(5): H597-604.
217. Erdmann, E., et al. (2013). "Cinaciguat, a soluble guanylate cyclase activator, unloads the heart but also causes hypotension in acute decompensated heart failure." Eur Heart J **34**(1): 57-67.
218. Geisterfer, A. A., et al. (1988). "Angiotensin II induces hypertrophy, not hyperplasia, of cultured rat aortic smooth muscle cells." Circ Res **62**(4): 749-756.
219. Zhang, Y., et al. (2005). "Vascular hypertrophy in angiotensin II-induced hypertension is mediated by vascular smooth muscle cell-derived H₂O₂." Hypertension **46**(4): 732-737.
220. Harrison-Bernard, L. M., et al. (1997). "Immunohistochemical localization of ANG II AT1 receptor in adult rat kidney using a monoclonal antibody." Am J Physiol **273**(1 Pt 2): F170-177.
221. Jackson, E. K. and W. A. Herzer (2001). "Regional vascular selectivity of angiotensin II." J Pharmacol Exp Ther **297**(2): 736-745.
222. Kaschina, E., et al. (2008). "Angiotensin II type 2 receptor stimulation: a novel option of therapeutic interference with the renin-angiotensin system in myocardial infarction?" Circulation **118**(24): 2523-2532.
223. Savergnini, S. Q., et al. (2010). "Vascular relaxation, antihypertensive effect, and cardioprotection of a novel peptide agonist of the MAS receptor." Hypertension **56**(1): 112-120.
224. Esteban, V., et al. (2005). "Angiotensin IV activates the nuclear transcription factor-kappaB and related proinflammatory genes in vascular smooth muscle cells." Circ Res **96**(9): 965-973.
225. Li, F. and K. U. Malik (2005). "Angiotensin II-induced Akt activation through the epidermal growth factor receptor in vascular smooth muscle cells is mediated by phospholipid metabolites derived by activation of phospholipase D." J Pharmacol Exp Ther **312**(3): 1043-1054.

226. Biggs, W. H., 3rd, et al. (1999). "Protein kinase B/Akt-mediated phosphorylation promotes nuclear exclusion of the winged helix transcription factor FKHR1." Proc Natl Acad Sci U S A **96**(13): 7421-7426.
227. Salminen, A., et al. (2013). "Crosstalk between Oxidative Stress and SIRT1: Impact on the Aging Process." Int J Mol Sci **14**(2): 3834-3859.
228. Ichiki, T., et al. (2003). "Cyclic AMP response element-binding protein mediates reactive oxygen species-induced c-fos expression." Hypertension **42**(2): 177-183.
229. Motta, M. C., et al. (2004). "Mammalian SIRT1 represses forkhead transcription factors." Cell **116**(4): 551-563.
230. van der Horst, A., et al. (2004). "FOXO4 is acetylated upon peroxide stress and deacetylated by the longevity protein hSir2(SIRT1)." J Biol Chem **279**(28): 28873-28879.
231. Friebe, A. and D. Koesling (2003). "Regulation of nitric oxide-sensitive guanylyl cyclase." Circ Res **93**(2): 96-105.
232. Gomez, D., et al. (2013). "Detection of histone modifications at specific gene loci in single cells in histological sections." Nat Methods **10**(2): 171-177.
233. Boura, E., et al. (2010). "Structure of the human FOXO4-DBD-DNA complex at 1.9 Å resolution reveals new details of FOXO binding to the DNA." Acta Crystallogr D Biol Crystallogr **66**(Pt 12): 1351-1357.
234. Tsai, K. L., et al. (2007). "Crystal structure of the human FOXO3a-DBD/DNA complex suggests the effects of post-translational modification." Nucleic Acids Res **35**(20): 6984-6994.
235. Ding, J. D., et al. (2004). "Distribution of soluble guanylyl cyclase in the rat brain." J Comp Neurol **472**(4): 437-448.
236. Ghosh, A. and D. J. Stuehr (2017). "Regulation of sGC via hsp90, Cellular Heme, sGC Agonists, and NO: New Pathways and Clinical Perspectives." Antioxid Redox Signal **26**(4): 182-190.
237. Isenberg, J. S., et al. (2006). "CD47 is necessary for inhibition of nitric oxide-stimulated vascular cell responses by thrombospondin-1." J Biol Chem **281**(36): 26069-26080.
238. Isenberg, J. S., et al. (2007). "Thrombospondin-1 limits ischemic tissue survival by inhibiting nitric oxide-mediated vascular smooth muscle relaxation." Blood **109**(5): 1945-1952.

239. Isenberg, J. S., et al. (2009). "Thrombospondin-1 and CD47 regulate blood pressure and cardiac responses to vasoactive stress." Matrix Biol **28**(2): 110-119.
240. Bauer, E. M., et al. (2010). "Thrombospondin-1 supports blood pressure by limiting eNOS activation and endothelial-dependent vasorelaxation." Cardiovasc Res **88**(3): 471-481.
241. Murthy, K. S. (2008). "Inhibitory phosphorylation of soluble guanylyl cyclase by muscarinic m2 receptors via Gbetagamma-dependent activation of c-Src kinase." J Pharmacol Exp Ther **325**(1): 183-189.
242. Meurer, S., et al. (2005). "Reactive oxygen species induce tyrosine phosphorylation of and Src kinase recruitment to NO-sensitive guanylyl cyclase." J Biol Chem **280**(39): 33149-33156.
243. Zhou, Z., et al. (2008). "Protein kinase G phosphorylates soluble guanylyl cyclase on serine 64 and inhibits its activity." Arterioscler Thromb Vasc Biol **28**(10): 1803-1810.
244. Rogers, N. M., et al. (2012). "Activation of parenchymal CD47 promotes renal ischemia-reperfusion injury." J Am Soc Nephrol **23**(9): 1538-1550.
245. Rogers, N. M., et al. (2013). "Age-associated induction of cell membrane CD47 limits basal and temperature-induced changes in cutaneous blood flow." Ann Surg **258**(1): 184-191.
246. Papapetropoulos, A., et al. (1995). "Regulation of vascular smooth muscle soluble guanylate cyclase activity, mRNA, and protein levels by cAMP-elevating agents." Hypertension **26**(4): 696-704.
247. Hu, Z. W., et al. (1992). "Prolonged exposure to catecholamines enhances sensitivity of smooth muscle relaxation induced by sodium nitroprusside and atriopeptin." J Pharmacol Exp Ther **260**(2): 756-761.
248. Agbor, L. N., et al. (2019). "Conditional deletion of smooth muscle Cullin-3 causes severe progressive hypertension." JCI Insight **5**(14):e129793.
249. Wong, J. J., et al. (2013). "A Cullin1-based SCF E3 ubiquitin ligase targets the InR/PI3K/TOR pathway to regulate neuronal pruning." PLoS Biol **11**(9): e1001657.
250. Matchar, D. B., et al. (2008). "Systematic review: comparative effectiveness of angiotensin-converting enzyme inhibitors and angiotensin II receptor blockers for treating essential hypertension." Ann Intern Med **148**(1): 16-29.
251. "Chapter 1: Definition and classification of CKD." Kidney Int Suppl (2011) **3**(1): 19-62.
252. Abramyan, S. and M. Hanlon (2021). *Kidney Transplantation*. StatPearls. Treasure Island (FL).

253. Roine, E., et al. (2010). "Targeting risk factors for impaired wound healing and wound complications after kidney transplantation." *Transplant Proc* **42**(7): 2542-2546.
254. Tsai, J. L. and S. F. Tsai (2020). "Recovery of Renal Function in a Kidney Transplant Patient After Receiving Hemodialysis for 4 Months." *Exp Clin Transplant* **18**(1): 112-115.
255. Curtis, J. J., et al. (1985). "Benefits of removal of native kidneys in hypertension after renal transplantation." *Lancet* **2**(8458): 739-742.
256. John, U., et al. (2006). "High prevalence of febrile urinary tract infections after paediatric renal transplantation." *Nephrol Dial Transplant* **21**(11): 3269-3274.
257. Suson, K. D., et al. (2011). "Native nephrectomy for renal cell carcinoma in transplant recipients." *Transplantation* **91**(12): 1376-1379.
258. Chebib, F. T., et al. (2015). "Native Nephrectomy in Renal Transplant Recipients with Autosomal Dominant Polycystic Kidney Disease." *Transplant Direct* **1**(10): e43.
259. Mosconi, G., et al. (2010). "Native kidney function after renal transplantation combined with other solid organs in preemptive patients." *Transplant Proc* **42**(4): 1017-1020.
260. Calnan, D. R. and A. Brunet (2008). "The FoxO code." *Oncogene* **27**(16): 2276-2288.
261. Katoh, M., et al. (2013). "Cancer genetics and genomics of human FOX family genes." *Cancer Lett* **328**(2): 198-206.
262. Benayoun, B. A., et al. (2011). "Forkhead transcription factors: key players in health and disease." *Trends Genet* **27**(6): 224-232.
263. Boura, E., et al. (2007). "Both the N-terminal loop and wing W2 of the forkhead domain of transcription factor Foxo4 are important for DNA binding." *J Biol Chem* **282**(11): 8265-8275.
264. Brunet, A., et al. (2002). "14-3-3 transits to the nucleus and participates in dynamic nucleocytoplasmic transport." *J Cell Biol* **156**(5): 817-828.
265. Tang, E. D., et al. (1999). "Negative regulation of the forkhead transcription factor FKHR by Akt." *J Biol Chem* **274**(24): 16741-16746.
266. Vogt, P. K., et al. (2005). "Triple layer control: phosphorylation, acetylation and ubiquitination of FOXO proteins." *Cell Cycle* **4**(7): 908-913.
267. Bois, P. R., et al. (2005). "FoxO1a-cyclic GMP-dependent kinase I interactions orchestrate myoblast fusion." *Mol Cell Biol* **25**(17): 7645-7656.

268. Lehtinen, M. K., et al. (2006). "A conserved MST-FOXO signaling pathway mediates oxidative-stress responses and extends life span." Cell **125**(5): 987-1001.
269. Huang, H., et al. (2006). "CDK2-dependent phosphorylation of FOXO1 as an apoptotic response to DNA damage." Science **314**(5797): 294-297.
270. Daitoku, H., et al. (2004). "Silent information regulator 2 potentiates Foxo1-mediated transcription through its deacetylase activity." Proc Natl Acad Sci U S A **101**(27): 10042-10047.
271. Matsuzaki, H., et al. (2005). "Acetylation of Foxo1 alters its DNA-binding ability and sensitivity to phosphorylation." Proc Natl Acad Sci U S A **102**(32): 11278-11283.